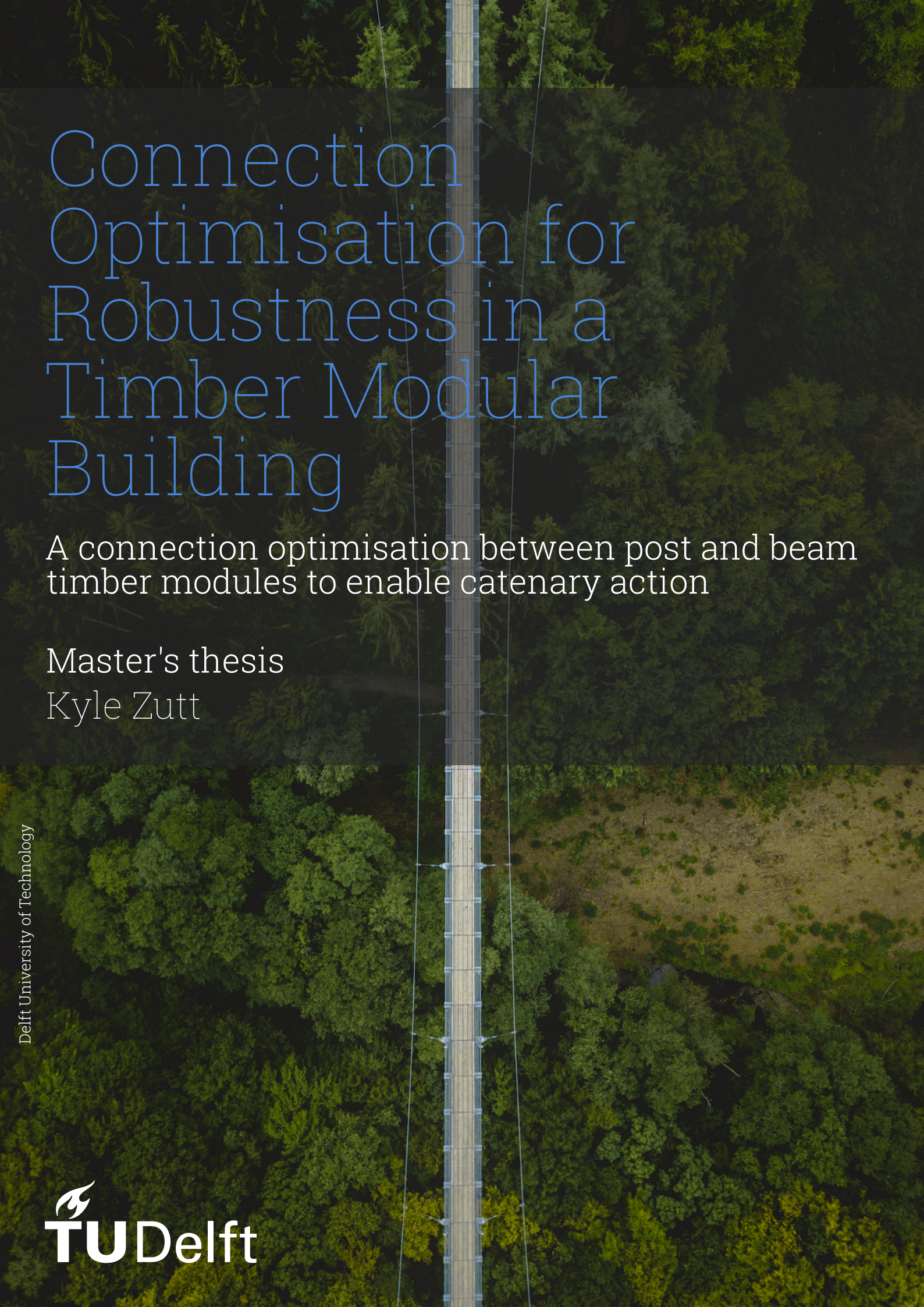

Connection Optimisation for Robustness in a Timber Modular Building

A connection optimisation between post and beam timber modules to enable catenary action

Master's thesis

Kyle Zutt

Delft University of Technology

TU Delft

Connection Optimisation for Robustness in a Timber Modular Building

A connection optimisation between post and beam timber modules to enable catenary action

by

Kyle Zutt

This research study serves as the final step for the completion of a master's degree in structural engineering

Pieters BOUWTECHNIEK

Student number:	4465148	
Thesis committee:	Dr.ir. Geert Ravenshorst	TU Delft, Chair
	Dr.ir. Pierre Hoogenboom	TU Delft, Supervisor
	Dr.ir. Maria Felicita	TU Delft, Supervisor
	ir. Chris Bosveld	Pieters Bouwtechniek, Daily Supervisor
Institution:	Delft University of Technology	
Faculty:	Faculty of Civil Engineering	
Company:	Pieters Bouwtechniek Delft	
Location:	Delft, The Netherlands	
Date:	Thursday 15th February, 2024	

TU Delft

Preface

As a young kid, I always liked to help my father when he was working on a home renovation project. I pretended to help him by trying to saw a piece of timber with an old speed square which in my mind looked exactly like a handsaw. Years later, I collected multiple hand and power tools myself to perform some DIY projects with timber. The workability of the material and the potential to make great structures, despite the lack of strength and stiffness compared to materials such as steel, combined with my fascination for architecture and construction, inspired me to pursue a master's degree in civil engineering with a specialisation in timber structures. A childhood life goal was to someday build the highest timber building in the world.

For my master's thesis, I was looking for an opportunity to work together with a company that has a lot of experience with timber engineering to be able to extend my knowledge on the topic. I quickly found a good connection with engineering firm Pieters Bouwtechniek. They offered me a possibility to continue upon the thesis topic of Joep Knuppe, which analysed the robustness of timber modular buildings. Robustness and modular construction were a completely new topic for me and I saw a great opportunity to learn and add valuable insights in a complex and underdeveloped topic.

Upon doing an initial literature review on robustness of modular building structures, I found that robustness is often assessed for buildings with parameterised module sizes, module layouts, connection properties, element cross-sections, or with the addition of extra building features such as stability frames. Based on the ability of the building to absorb and redistribute additional forces after an element removal scenario, robustness could be guaranteed or not. A reoccurring conclusion was that the inter-module connections are key components in ensuring overall robustness and connections should be designed with adequate mechanical properties. It was herein where I saw a challenge for myself, to come up with a tool to help engineers design connections which can make timber modular buildings robust.

This master thesis report marks the end of my academic journey. I look back at a wonderful time where I got to know a lot of amazing people and learned the foundations for my future career in the field of engineering. It sometimes felt as a never-ending challenge with endless possibilities to learn something new and push my boundaries of knowledge. I think the same goes for the field of engineering, where increasingly more complicated structures and challenges provide endless possibilities to learn something new and push the boundaries of knowledge. Hopefully, this thesis provides a stepping stone in learning something new about connection design for robustness and help others push the topic and timber buildings to further heights.

Kyle Zutt
Delft, February 2024

Acknowledgements

Of course no academic work is done alone and I would like to thank the people that helped me bringing about this thesis.

My appreciation first goes to Pieters Bouwtechniek for providing the opportunity to learn more in one year than I could have imagined. Special thanks goes to Chris Bosveld. Your support and guidance in setting up the topic and throughout the entire thesis kept me on track and helped me persevere. I am genuinely grateful for the time and effort you invested in me. I also want to thank Joep Knuppe for helping me understand the topic of robustness more than I could have on my own and providing me with insight in what you have set up in the field of robustness modelling of timber modular buildings. I appreciate you taking the time to debate specific subjects from my thesis. Also, I want to thank all the other colleagues at Pieters Bouwtechniek for making me feel welcome in the office and making the last ten months an enjoyable time.

Furthermore, I would like to thank my graduation committee, Geert Ravenshors, Pierre Hoogenboom, Maria Felicita, and again Chris Bosveld. Your insightful feedback and thought-provoking questions in our meetings have been instrumental in guiding me on the correct path. Through your support, I have acquired valuable insights into timber construction techniques, design principles, and academic research, for which I am truly thankful.

And finally, I would like to thank my family and friends. Mom and dad, thank you for your unwavering support and encouragement throughout my master thesis and making me the man I am today. Jonne, thank you for always being there for me. Your presence and love has meant the world to me. And thank you to all my friends in and out of the TU Delft and U-BASE. You made my time in Delft unforgettable.

Abstract

To address the increasing housing demand in Europe and simultaneously tackle the challenge of creating a more sustainable construction industry, timber modular buildings present an innovative solution. However, before multi-storey modular buildings become a widespread practice, some engineering challenges need to be overcome. One of these challenges is ensuring the robustness. J. Knuppe conducted a novel study on the ability of a post-and-beam timber modular building to form alternative load paths in scenarios involving notional removal of structural elements [1]. It was determined that for a critical double intermediate façade column removal, robustness could only be assured by relying on flexural action of floor beams spanning the length of the modules. However, alternative load paths through flexural action are not preferred as they may require oversizing to resist the additional gravity loads after the removal of a column. Moreover, they rely heavily on the placement and location of an intermediate supporting column to activate flexural action. Other alternative load paths, such as catenary action, offer a more versatile alternative load path in case of the critical column removal scenario. However, the timber modular building analysed in Knuppe's case study had connections with inadequate tensile resistance and deformation capacity to enable robust catenary action. The objective of this thesis is to develop an optimisation method aimed at determining the required mechanical properties of the inter-module connections in timber modular buildings. This in order to enable catenary action to provide a robust alternative load path.

This study started with a literature review on the state of the art in structural robustness to find any requirements in building codes and reported practical limitations for the formation of catenary action as an alternative load path. The literature review revealed no specific requirements for a structure to comply with regarding the formation of catenary action. It is therefore up to the designer and engineer of a building to create a structure which can prevent progressive collapse to an extend which is disproportionate to the initial damage. Nevertheless, the new working draft of Eurocode 5 does suggest that the robustness of a timber structure can be assessed by performing a dynamic or quasi-static analysis with an appropriate dynamic amplification factor of a sudden element removal scenario. Subsequently, the literature review delved into the numerical models, assumptions, and analysis procedures employed by Knuppe [1] in performing an alternative load path analysis of a timber modular building. Knuppe's alternative load path analysis method dissected a 3D post and beam modular building in 2D frames to determine the presence of different alternative load paths. The 2D frames were analysed with nonlinear quasi-static and nonlinear dynamic numerical methods and the connection properties were determined with spring models. The use of 2D frame models with rigid boundary constraints on the ends of the floors neglected the load distribution and deformation capacity of the discretised modular floor system.

The literature further notes that in a simple catenary, consisting of two spans and a point load in the middle, the tensile force in the catenary required to make equilibrium with the load on a catenary reduces as the vertical displacement increases. Based on this, a so called catenary equation was formulated, which prescribes a catenary requirement boundary. The catenary requirement boundary determines the required tension resistance in the catenary, at a specific total elongation of the catenary, to achieve equilibrium with the point load. This tool can be used to assess how close the force-elongation response in a catenary of a timber modular building is to form robust catenary action.

To optimise the inter-module connections in a timber modular building for the development of robust catenary action in the event of a double intermediate façade column removal, a comprehensive case study was conducted. The timber modular building utilised in the case study consists of twelve consecutive post-an-beam timber modules in length, and five modules in height. To comply with serviceability- and ultimate limit state design scenarios, a steel stability frame is placed after every four modules, and thereby dividing the building into three sections. Figure 1 illustrates the case study building and the original inter-module connection design.

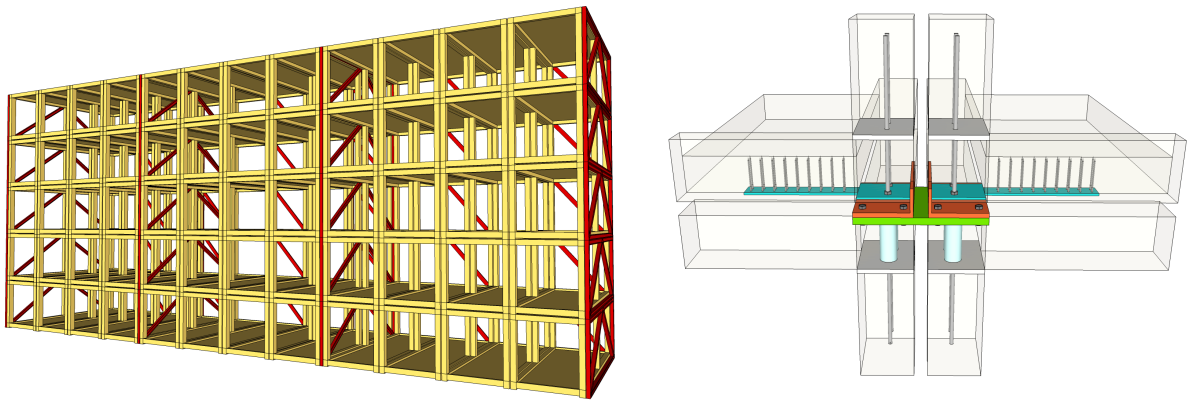

Figure 1: Case study building and original inter-module connection design

The case study was divided into three distinct parts, each building upon the other to form a detailed and accurate optimisation process. The first part analysed the in-plane resistance, load distribution, and load-deformation response of the discrete timber floors exposed to the tensile loads corresponding to catenary action. In the second part, the load-deformation behaviour of the discrete timber floors was included in a 2D frame model of a timber modular building by implementation of spring boundary constraints at the ends of the floors. The spring boundary constraints represent the in-plane behaviour of the discretised timber floor system. Subsequently, the force-elongation response in the catenaries of the building are compared to the catenary requirement boundary. The third part determined how the inter-module connection design should be adjusted in order to ensure that the force-elongation response meets the catenary requirement boundary. If the response does not meet, or overshoots the catenary requirement boundary, the inter-module connection design is either insufficient or conservative and an adjustment to the design is required. The entire process relies on iteration to arrive at an optimised outcome.

In the case study, the three parts of the optimisation process, while contributing to the overall optimisation process, were also treated as an individual sub-study. This approach allows for a broader understanding of the behaviour of timber modular buildings and the effect of certain assumptions on building and connection designs.

The sub-study focusing on the in-plane behaviour of timber modular floor systems, under tensile forces generated by catenary loads, involved numerical analyses of 2D floor models. These models display situations with one, two, three, and six consecutive discrete floor fields on each side of a notional removed façade column. The models with one, two, and three floor fields simulate floor systems of a standalone building section, while the model with six floor fields simulates the floors of the full case study building. Figure 2 presents the two different building types and four distinct floor models. This set of models allowed to study the influence of the location of the removed column in the façade, the influence of having more floor fields consecutive to a removed column, and the influence of having more stability frames. The numerical models are quasi-statically loaded until failure using the finite element software Abaqus. The study reveals that discrete timber floor fields can exhibit substantial in-plane deformations under high catenary loads, contributing to increased ductility in a building system. This phenomenon is particularly noticeable in the stand-alone building section, where catenary forces could only be effectively transferred through diaphragm action once the cavity between the floors above the removed columns was closed. This closure occurred after the floor system displaced 58 mm. The initial unstable response was attributed to the stability frame configuration. Interestingly, models with one, two, and three discrete floor fields exhibited identical behaviours while the model with six discrete floor fields displayed a stiffer response due to a more elaborate stability frame configuration. This imposed a different load path for catenary forces. Consequently, it can be concluded from this sub-study that the stability system configuration significantly influences overall in-plane behaviour.

The second sub-study assessed the effect of incorporating the in-plane floor behaviour into a 2D frame model on the ability of a timber modular building to form robust catenary action. In this sub study, three distinct quasi-static alternative load path analyses are preformed according the methodology as outlined by Knuppe [1]. The three modelling scenarios represented are: a timber modular building with no consideration of in-plane floor behaviour, the three-section case study building with in-plane floor behaviour considered, and the single-section building with in-plane floor behaviour considered. The in-plane behaviours of the floor systems were integrated into the 2D frame models by incorporating their load-deformation responses from the preceding sub-study into spring boundary constraints. The resulting effect on the catenary systems was depicted through the force-elongation behaviour in the catenaries, which was subsequently compared to the catenary requirement boundary corresponding to the building characteristics and loading situation. In order to account for the dynamic effects of a sudden column removal, the quasi-static load was increased with a dynamic amplification factor of 2.0 as suggested by the new working draft of Eurocode 5. Due to the inclusion of the in-plane behaviour of the floors, the analysis indicated that the three section case study building was able to resist 65% more gravity load compared to the same building but without considering the in-plane floor behaviour. For the single section building, an increase of 259% in resistance to gravity load was observed. Despite the improvement, the case study building still demonstrated an inability to achieve robustness through catenary action. This was attributed to the insufficient strength and ductility of the inter-module connections.

Figure 2 presents the full research and analysis procedure of the first and second sub-study, including the different models and results.

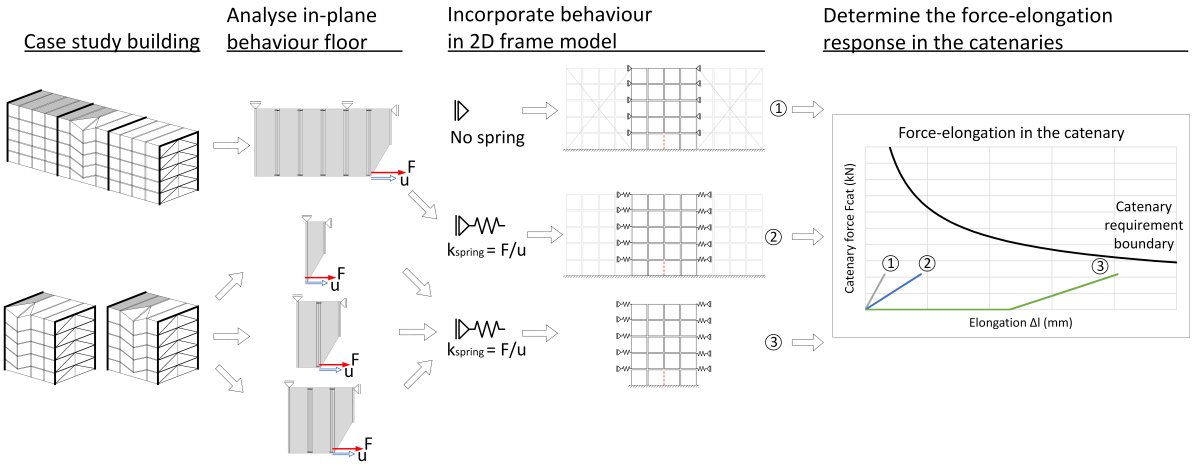

Figure 2: Overview case study

Utilising the revised 2D frame model of the three section case study building, two distinct connection optimisation methods were introduced and implemented in the third sub-study. The goal of the two methods is to create two distinct inter-module connection design options that allow for the force-elongation response of the catenary to meet the catenary requirement boundary and enable robust catenary action. The first optimisation method aimed at creating a high-resistance inter-module connection by increasing the strength of the connection parts. In contrast, the second method focused on developing a ductile inter-module connection by introducing a fuse and relying on the ultimate strain of steel to allow for more elongation capacity. Both optimisation approaches rely on the catenary requirement boundary, derived from the catenary equation and the revised full alternative load path analysis of the floor model and 2D frame model of the building, to iteratively result in an optimised connection design. Application of both methods yielded two new inter-module connection designs, both capable of facilitating a robust catenary response to a double intermediate façade column removal scenario. The optimised high-strength inter-module connection required an increased tension resistance of 143% compared to the original connection design when having a brittle failure mode after 1.99 mm of elastic elongation. The optimised ductile connection required a fuse length of 550 mm to allow the entire catenary to elongate an additional 110 mm when assuming that one fuse in the catenary reaches its potential ultimate strain of 20%. Furthermore, the ductile connection required an increased resistance of 55%. The high-strength

connection and ductile connection design, together with their resulting force-elongation responses are presented in Figure 3.

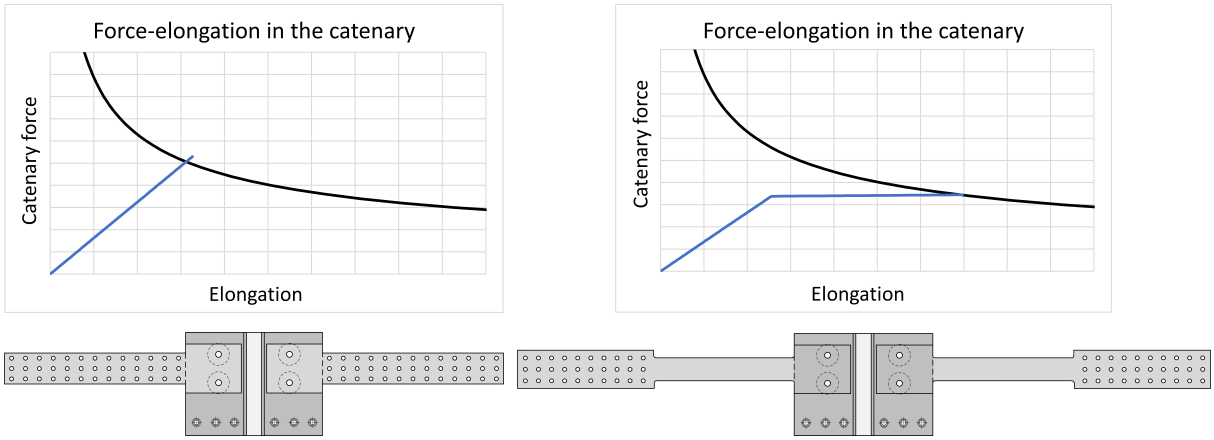

Figure 3: Optimised connection designs with the corresponding force-elongation responses of the catenaries

The optimisation process outlined in this thesis underscores the complexity and critical importance of correct connection design to ensure structural robustness through catenary action. It highlights the need to ensure sufficient strength in connections for the distribution of tie forces, while also maintaining adequate deformation capacity. The methodology presented in this thesis serves as a valuable tool for optimising connections in timber modular buildings to ensure robust catenary action. The catenary equation and the resulting catenary requirement boundary prove to be effective tools for making informed decisions regarding the extent to which resistance or ductility in a connection should be increased to enable a building to form a robust catenary. For further research, it is recommended to include a dynamic analysis in the optimisation process to accurately determine the dynamic amplification factor corresponding to the building structure and associated connection. This is needed to adjust the additional gravity load in the catenary equation and to tailor the catenary requirement boundary to the represented structure. Furthermore, experimental testing of the inter-module connections is recommended because the spring model used to determine the mechanical properties is limited in accurately reflecting the exact resistance and elongation capacity of the connections.

Nomenclature

Abbreviations

Abbreviation	Definition
ALP	Alternative Load Path
ALPA	Alternative Load Path Analysis
ALS	Accidental Limit State
CC	Consequence Class
CLT	Cross Laminated Timber
CRB	Catenary Requirement Boundary
DAF	Dynamic Amplification Factor
DoD	Department of Defence
FEA	Finite Element Analysis
FEM	Finite Element Model
GLT	Glued Laminated Timber
GSA	General Service Administration
ULS	Ultimate Limit State
SLS	Serviceability Limit State

Contents

List of Figures

List of Tables

1 Introduction

1.1. Background

Modular construction is a quickly developing building method in which entire ready to install building sections are prefabricated and installed on site. What makes modular buildings particularly interesting is that modules can be prefabricated in a factory, allowing good access to quality control, little waste, and quick installation capabilities on the building site [2]. Although low rise modular buildings have been built for the past thirty years, new developments have lead countries such as the UK, US, Canada, China, Singapore, and Australia to construct multiple high-rise towers. A great example of the capabilities of modular construction is the J57 Mini Sky City tower in Changsha, China, in which a 57 storey, 2D panelised, building has been built from the ground up in only 19 days [3]. For these reasons, modular construction is often seen as a potential solution in the ongoing housing crisis.

Modular construction can allow up to 95% of a building to be premanufactured [4], allowing for highly efficient production processes. It is believed to be of great importance in the future construction industry [5]. Especially, when combining the efficient construction techniques with timber construction, a good effort can be made towards a sustainable building sector. Manufacturing and transportation of timber modules can save up to 25% of carbon emissions when compared to steel or concrete counterparts [6].

In general three levels of modularity can be distinguished depending on their degree of prefabrication. The lowest level of prefabricated modules are 1D elements such as beams and columns. A higher level of prefabrication is in the form of 2D planer elements for construction of walls, floors, and roofs. The highest level of prefabrication results in 3D volumetric modules [4]. 3D volumetric modules can be further separated in load-bearing modules which transfer loads through the walls of the modules, and corner-supported modules which transfer loads from edge beams to corner posts [2]. Longer corner-supported modules may require intermediate columns in order to limit the dimensions of the edge beams. These volumetric modules are also called post and beam modules [1].

Although modular construction for high rise buildings may at first sound as straightforward as stacking bricks like Lego, the lack of structural design guidelines limits modular construction applications to 1% of all high-rise buildings [7]. More research is required in order to develop a better understanding of the structural performance of horizontal load transfers and structural robustness [8]. Robustness can be described as the capacity of a structure to arrest progressive collapse, disproportionate to the extent of the initial damage [9]. If a column loses its load carrying function, after an unspecified event, and the building can redistribute the loads to other parts of the building without (partially) collapsing, the structure can be called robust.

Traditional monolithic buildings, characterised by continuous floors, are well-suited for horizontal load transfers, caused by wind loads or calamity situations, through diaphragm action and/or membrane action. The challenge for robustness in modular buildings lies in proper connection design. The connections between the modules (inter-module) tie the modules together to create a cohesive building

structure. In the event of a calamity, the loads must be effectively distributed through these connections to the intact sections of the building. Therefore, it is imperative to design connections that are not only sufficiently strong to transfer loads, but also possess the necessary ductility accompany deformations that a partially damaged building may undergo [8].

In order to evaluate how a building's structural integrity reacts when building components are notionally removed, engineers often conduct an analysis known as an Alternative Load Path Analysis (ALPA). The primary aim of an ALPA is to examine how forces are distributed through Alternative Load Paths (ALP) within the structure following the initial damage, and to measure the degree of the ensuing collapse progression [10]. Knuppe conducted a novel computational ALPA as part of a case study focusing on a post-and-beam timber modular building. Since timber column-to-beam connections can hardly be categorised as rigid, and the connection properties are of great importance on the global structural behaviour, a component based spring model was implemented to accurately model the properties of the intra- and inter-module connections. Knuppe's study showed that for some module and beam removal scenarios no proficient robustness could be provided by the structure and its conceptual connections. He concluded that the lack of robustness could be attributed to the lack of rotational resistance, tensile resistance, ductility, and axial stiffness in the proposed connection, which prevented the development of certain ALPs. Particularly, ALPs which depend on large deformations, such as catenary action [1].

1.2. Problem

Connections in modular buildings are critical components because they provide the structural continuation and allow lateral forces to be distributed. Multiple ALPAs of steel modular buildings, and one on a timber modular building, have been performed to study the global structural behaviour after column or module loss scenarios [11][12][13][14][15][1]. Most studies conclude that an increase in connection properties such as rotational and axial stiffness and resistance, and ductility will improve the structural robustness of a building. Some studies even included a parameter study to assess the influence of increased properties on the global structural behaviour. However, the problem has not yet been analysed from the optimisation perspective. What connection properties are actually required for a robust modular construction, and how can they be attained?

Knuppe's in depth ALPA of a timber modular building was done to quantify the inherent robustness of a timber modular reference building. The reference building is developed by engineering firm Pieters Bouwtechniek, in cooperation with project developer Lister Buildings and timber engineering firm CLT-S. The purpose of this collaboration was to innovate and test new ideas and calculation methods specifically tailored for timber modular structures. The connections used in the building were concept connections, specifically designed for ultimate limit state, serviceability limit state, and building phase usage requirementes. Knuppe concluded that multiple ALPs could be activated, but not all had sufficient capacity to withstand progressive collapse with the given conceptual connection. For an intermediate façade column removal scenario, see Figure 1.1, a sufficient ALP could be found in flexural action of the longitudinal floor beams of the modules in the side view. However, an ALP through flexural action is generally not preferred as it may lead to oversizing of the floor beams. Furthermore, flexural action is only possible when an intermediate column is positioned on the longitudinal side of the modules to support the upper floor beam. Moreover, the position of the intermediate column is detrimental to the formation of flexural action. If the intermediate column is moved more towards the remaining column in the side view, the floor beams will fail in bending. A more suiting and wider applicable ALP for a double intermediate façade column removal would be through catenary action. However, in the reference building the mechanical properties of the concept inter-module connections were insufficient to enable a robust ALP through catenary action [1]. Figure 1.2 shows the location and details of the connection responsible for creating the catenary. Knuppe conducted a parameter study on the rotational stiffness and resistance of the connections to evaluate their impact on the formation of catenary action. However, the study did not try to determine the necessary mechanical properties of the connection, leaving room for optimisation considerations. Furthermore, Knuppe used 2D frame analyses of the front and side view of the building to perform ALPAs. This approach neglects the potential contribution of other ALPs such as diaphragm action and in-plane deformation of the modular floor system to the development of catenary action. Additionally, it does not assess whether the modular floors can withstand the

horizontal forces associated with catenary action.

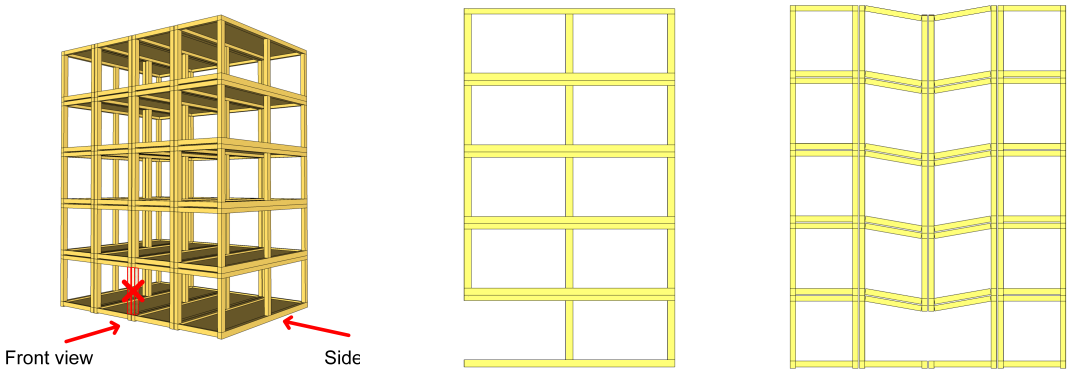

(a) Case study building Knuppe **(b)** Side view **(c)** Front view

Figure 1.1: Double intermediate façade column removal in the case study building of Knuppe [1]

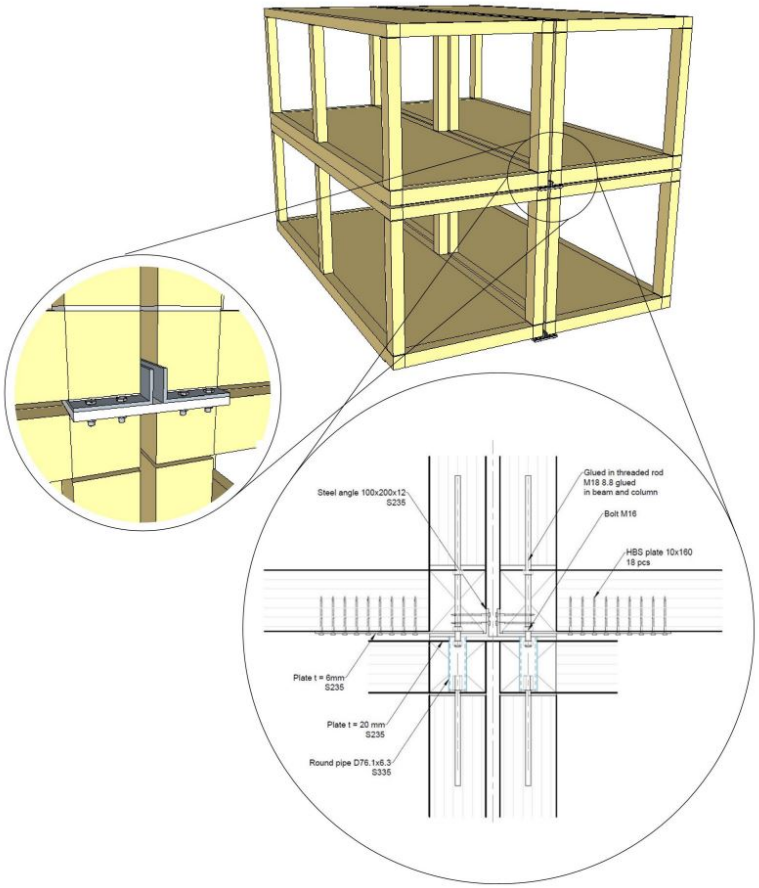

Figure 1.2: Concept connection by CLT-S, designed for ultimate limit state and serviceability limit state [1].

1.3. Goal

This thesis builds upon the research conducted by Knuppe, who identified insufficient mechanical properties of the inter-module connections in a timber modular reference building, for the development of catenary action, in the event of a double intermediate façade column removal. The goal of this thesis is to establish the necessary connection properties through the development of an optimisation method. By developing an optimisation method for connections, a significant contribution is made to ensure robustness and safety in timber modular buildings, stimulating the further development and widespread adoption.

In order to determine the optimal connection properties for catenary action, the following sub goals are formulated.

Sub goals

1. Describe the current guidelines and requirements regarding robustness and catenary action as an alternative load path.
2. Describe the in-plane behaviour of a timber modular floor system, when subjected to large tensile forces generated by catenary loads.
3. Develop an approach to seamlessly integrate the in-plane behaviour of timber modular floor systems into a 2D frame model of a timber modular building.
4. Assess the effect of incorporating the in-plane floor behaviour into a 2D frame model on the global response of a timber modular building.
5. Develop a method to determine the required connection properties in order to develop a sufficient alternative load path through catenary action in timber modular buildings.

1.4. Research questions and outline

The report is structured into three main parts. The first part is a literature review exploring the state of the art in robustness, catenary action, and the methodology for conducting an ALPA on a timber modular building. This section includes a detailed examination of Knuppe's approach, exploring his methodologies and findings. The second part encompasses a case study, incorporating an analysis of the in-plane behaviour of discrete timber modular floors under catenary loads. The case study also explores the incorporation of floor behaviour in a 2D frame analysis and introduces an optimisation method for enhancing the inter-module connections of timber modular buildings to enable robust catenary action. The third part presents and discusses the results. Collectively, these sections address the main research question:

What are the optimal mechanical properties of inter-module connections in timber modular buildings to facilitate structural robustness through catenary action and what method can be used to obtain these optimal properties?

To answer the main research question, sub questions are formulated. The sub questions are addressed according to the outline below.

Part I - Literature review

Chapter 2: Robustness and catenary action

- Where does the concept of catenary action intersect with the concept of robustness?
- What are the most influential design parameters for the formation of catenary action?
- What are regulatory requirements, or prominent guidelines an alternative load path in the form of catenary action should meet?

Chapter 3: Robustness of timber modular buildings

- How can the ability of a modular building system to form catenary action be quantified?

Part II - Case study

Chapter 4: Introduction of the case study

Chapter 5: Discrete timber floors

- What is the in-plane stiffness and resistance of the discretised floor system in the reference building?
- What is the effect of building size on the in-plane load distribution and ability to deform of timber modular floor systems?

Chapter 6: Integration of floor response

- What is the effect of adding the diaphragm action and in-plane deformation of the modular floor system into a 2D frame model of a timber modular building on the global structural response and ability to form catenary action?
- What insights can be gained regarding the significance of in-plane floor behavior in influencing the overall structural behavior of the building?

Chapter 7: Connection optimisation

- How can the optimal mechanical properties for timber modular building connections be determined?
- What is the effect of certain design alterations on the mechanical behaviour of the connections and building structure on the formation of catenary action?
- What are the differences between the optimised connection design and the original connection design?

Part III - Research outcome
Chapter 8: Discussion

- What design alterations are most preferable to establish catenary action in a timber modular building?

Chapter 9: Conclusion and recommendations

1.5. Methodology

The methodology employed in this study can be categorised into multiple distinct sections, each gathering essential information for subsequent sections. A visual representation of the methodology, showing the sequence of the sections and the required flow of information, is depicted in figure 1.3.

Literature review

There is a scarcity of literature specifically addressing the robustness of timber modular buildings. However, literature exists on the robustness of steel modular buildings and on the robustness of structures made from timber, steel, and concrete. To address the sub-question regarding the intersection of catenary action with the concept of robustness, a broader analysis of general literature on robustness is conducted. Additionally, literature review explores influential design parameters for the formation of catenary action and examines potential requirements related to catenary action. This is done by reviewing various design codes and examining (partial) collapsed building cases to determine factors contributing to the occurrence or absence of catenary action. Insights gained from these case studies offer valuable lessons in identifying critical challenges associated with designing for catenary action. Based on the determined requirements for catenary action, an analytical tool is presented which helps in determining the required properties of a catenary system to enable a robust response.

Moreover, the literature review aims to identify a method for quantifying catenary action in a timber modular building. Knuppe's research offers a well-defined approach to conducting an ALPA, enabling a segregated analysis of catenary action. Therefore, the literature review incorporates an examination of Knuppe's approach to provide additional insights into the methodology.

Case study

To establish optimised connection properties for a timber modular building, an ALPA is conducted to evaluate the catenary behavior in a case study building. The optimisation is performed in three steps, corresponding to Chapters 5 to 7. In the first step, the in-plane behaviour of timber modular floor systems will be examined to determine the maximum resistance against catenary forces and to identify the in-plane deformation response of these floor systems. Multiple 2D numerical analyses will be conducted using Abaqus finite element software.

In the second step, a 2D numerical frame model of the case study building is created to analyse the ability to form catenary action. The model will predominantly be constructed following Knuppe's approach, but with an integration of the in-plane response of the floors. This incorporation involves replacing the rigid boundary constraints at the ends of the floors, as per Knuppe's 2D frame model, with spring boundary constraints. These spring constraints portray the in-plane load-deformation characteristics of the respective floor systems.

In the third step, an optimisation method for the connections will be introduced and applied on the case study building. The optimisation method is guided by the optimal engineering practices and the analytical optimisation tool identified through the literature review, and should result in a building which is able to resist a double intermediate façade column removal in a numerical ALPA performed in Abaqus.

To enable a more comprehensive analysis of various building layouts, and to gain a deeper understanding of how timber modular buildings behave in the development of catenary action, each step of the optimisation process will also be conducted as a sub-study. The goals of the sub-studies allign with the sub-goals of the thesis as presented in Section 1.3.

Case study building

The case study utilises a timber modular case study building which is based on the reference building of Pieters Bouwtechniek, Lister Buildings, and CLT-S. As this thesis is performed in cooperation with Pieters Bouwtechniek, sufficient documentation is available on the design, connections, and loads of the reference building to perform a connection optimisation. The reference building and case study building will be introduced in Chapter 3 and 4 respectively.

1.6. Scope

- Determining the required mechanical properties of a connection depends on the characteristics of the structure. Larger spans for example will yield higher moments, and the inclusion of a stability system influences the direction of load distributions. This study is based on the structure and modules as used in a reference building as composed designed Pieters Bouwtechniek. This is similar to the structures Knuppe [1] used in his research.
- To reach the main goal of this study, the ALPA methodology of Knuppe has to be updated by incorporating the in-plane behaviour of the timber modular floors in the 2D frame model. What lies outside the scope of this study is to reinvent the ALPA methodology. Therefore, this study relies on the methodology outlined by Knuppe. This includes the 2D dimensional approach to dissect the building, the spring model of the connections to determine the connection properties, and the loading procedure of the nonlinear quasi-static analysis. Only where required, some changes are made in order to increase its accuracy.
- A dynamic amplification factor determines the dynamic effects on the structural response when a structural element is removed. Studies have shown that the dynamic amplification depends on the stiffness and ductility of structural components, indicating that a higher stiffness generates a larger peak force for the system to resist. Besides, a higher ductility tends to have lower dynamic amplification factors, because ductility allows the structure to deform and absorb energy during dynamic loading. The draft version of Eurocode 5 suggests a dynamic amplification factor of 2.0 in the absence of more accurate information on a befitting value. Knuppe concludes that the dynamic amplification factor for a timber modular building is very close to the suggested 2.0 from the Eurocode. Therefore, this value is applied to all load scenarios in this research. Also, the search for a new dynamic amplification factor, based on the newly proposed connection, falls outside the scope of this thesis.

- A vertical tie between modules for vertical redistribution of forces is not included in the structural design of the reference building and case study building. It is therefore assumed that each floor provides a distinct ALP through catenary action. Still, all floors of the case study building are included in the models, as it cannot be excluded that all connections prevent the vertical flow of forces.

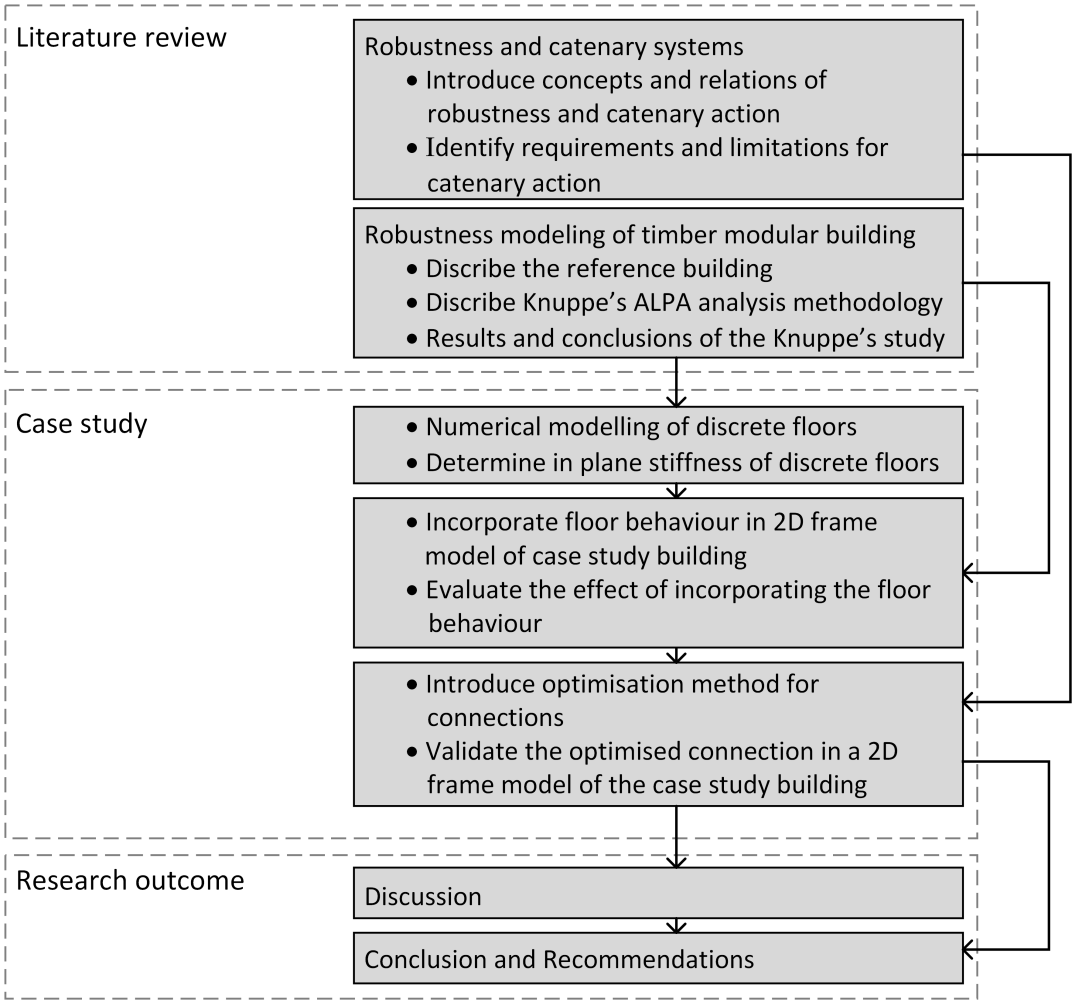

Figure 1.3: Flowchart thesis

Part I

Literature review

2

Robustness and catenary action

2.1. Introduction

In this chapter, the concept of robustness and catenary action in buildings is introduced. The chapter leads with a comprehensive overview, describing the background of the robustness principle, how ALPAs provide a method for assessing robustness, and how catenary action provides a viable way of transferring loads in a damaged building. Following this, the report outlines the principles of catenary action. The emphasis is placed on determining the design parameters that a building design must consider to ensure robust catenary action. Subsequently, an overview is given of the significance of catenary action, and the associated regulations from design codes and construction guidelines. It ends by presenting a tool, useful for assessing the required strength and deformation capacity of structures for the formation of catenary action.

2.2. Robustness

Every structure is susceptible to severe load scenarios. May it be due to foreseen events such as structural alterations, or unforeseen events such as fire, vehicle impacts, explosions, earthquakes etc. Building structures are required to maintain safe to the public, even after the severe load scenarios [16]. The term robustness describes the capacity of a building to mitigate change in structural behaviour disproportionate to the extent of the initial damage. In other words, the loss of a column may not lead to the partial or total collapse of a structure. Eurocode 1 describes robustness as: 'The ability of a structure to withstand events such as fire, explosions, impact or the consequences of human error, without being damaged to an extent disproportionate to the original cause' [9]. For example, if a column loses its load carrying function, and the building can redistribute the additional loads to other parts of the building without (partially) collapsing, the structure can be called robust. Great emphasis was put on incorporating robustness in building designs after a small gas explosion dislodged a load retaining wall of the Ronal Point tower in London in 1968, causing the collapse of an entire corner of the building [17]. Currently, the knowledge on structural robustness is quite comprehensive for concrete and steel structures. The COST action report HELEN [18] describes the state of the art on robustness of tall timber buildings.

2.2.1. Analysis methods

In general, two probabilistic methods and one deterministic method exist for the analysis and quantification of structural robustness [19][20]. The probabilistic analyses use statistical techniques to determine the potential occurrences of future outcomes, taking into account uncertainties in relevant variables. The first probabilistic analyses, risk-based analysis, uses the probability of exposure to risks and quantifies the probability of a certain damage and consequence. The second probabilistic analyses, reliability-based analysis, assumes a specific exposure of damage to a structure. The probability of collapse is than quantified in a reliability index by comparing the structural analyses of the damaged and undamaged state. For a founded robustness index, probabilistic methods need certain data for example the likelihood of a risk or certain exposure event to occur [21]. However, this data is hard to substantiate

as robustness is required for both foreseen and unforeseen events. Moreover, the probability of a certain consequence is often based upon deterministic and quantifiable data such as the structural behaviour, loss of lives, and economic damage [20]. Where probabilistic approaches attain a robustness index for quantification, a deterministic approach calculates the structural response based on a certain damage or exposure. A qualitative evaluation of the collapse progression is provided, simultaneously determining the magnitude of the collapse [19]. Deterministic models based on a particular exposure to for example an explosion blast, fire, or earthquakes are called scenario-dependant, while models based on a particular damage are called scenario-independent [17]. A classical scenario independent approach is through a notational load carrying element removal. Deterministic approaches are the least complex analysis method and the easiest to quantify [20]. The result is often binary valued, comparing the resulting damage to the global structure, after an assumed initial damage, to a certain limit. If the total damage exceeds the limit, the structure is not robust. If the total damage stays under the limit, the structure is called robust [22]. Building codes usually apply the binary deterministic approach to ensure robustness [10].

2.2.2. Design solutions for robustness

Solutions for designing a structure for robustness can result from from direct or indirect design methods. Indirect design methods aim to provide robust designs without accounting for an explicit damage. The goal of indirect design solutions is to incorporate a minimum level of robustness in the design by (I) incorporating minimum tie forces and (II) incorporating a minimum level of redundancy [19]. Tie forces ensure sufficient linkage between building components to form continuous load paths, minimise displacement between components, and facilitate the redistribution of load in the case of damage [17]. Redundancy ensures ALPs without having to do a structural analysis. By for example incorporating two load carrying elements, instead of one, loads are distributed among them. When one of the elements fails, the secondary can transfer the additional load [19]. Direct design solutions are based on structural evaluations and incorporate robustness directly into a design to resist collapse after a certain damage. The most prevalent form of damage is the removal of a load carrying elements such as a column or a load carrying wall. The most common direct design solution is an ALPA. This involves ensuring that if a load bearing element is removed, the remaining structure has sufficient redundancy to redistribute the forces without causing further damage. If providing an ALP is not possible, critical components can be assigned as ‘key elements’. Key elements have to withstand a specific high static load of 34 kPa, corresponding to the pressure of a high explosive blast [23]. Finally, compartmentalisation can be employed to prevent collapse from spreading throughout the entire structure by dividing it into separate compartments [19]. Figure 2.1 illustrates the different indirect and direct solutions.

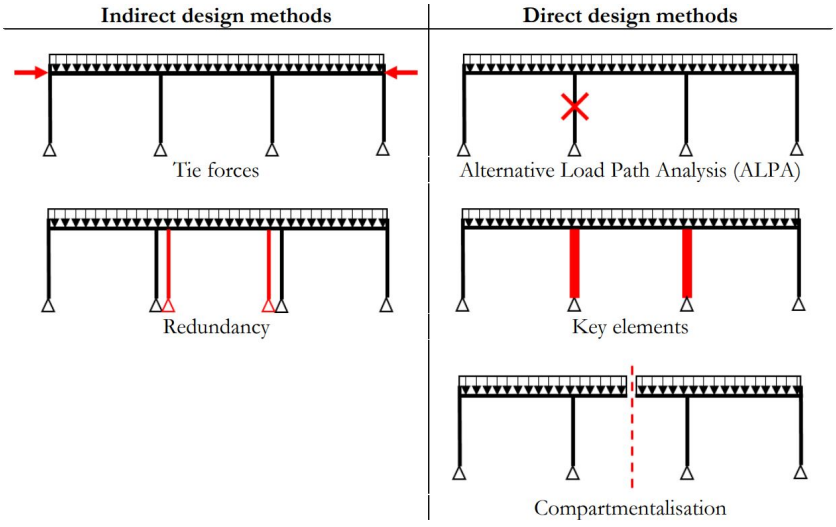

Figure 2.1: Indirect and direct robustness design solutions [20].

2.2.3. Alternative load paths

Alternative load paths are paramount to bridge a damaged component (e.g. a column) of a structure and to transfer loads to alternative load carrying components without causing further damage. If all elements from the ALP have a sufficient capacity to withstand the additional loads, further collapse can be arrested [21]. ALPs pose an economical alternative to direct 'key element' solutions, because it does not require designing every load carrying component to a specific high load requirement [24]. Possible ALPs are catenary action, membrane action, flexural action, arching action, diaphragm action, and compressive strut action. Representations of how these ALPs work are given in Figure 2.2 [17]. Catenary action and membrane action are generally seen as the two key load redistribution mechanisms to arrest progressive collapse as they maintain very high load carrying capacities [20]. For a detailed description of each ALP, the reader is referred to other sources of literature.

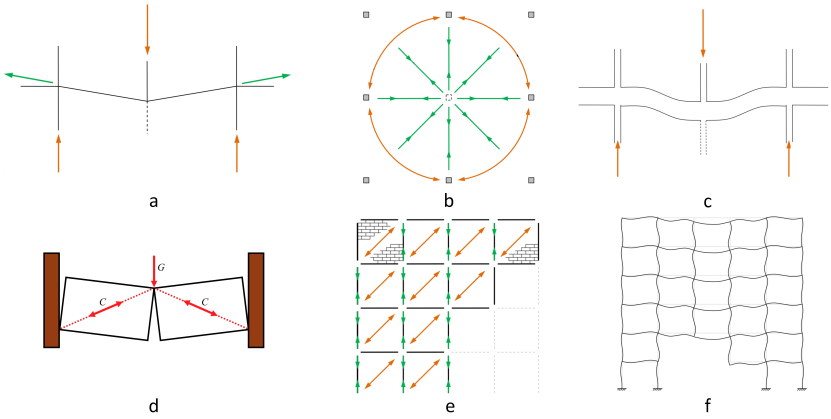

Figure 2.2: Alternative load paths: (a) catenary action, (b) membrane action, (c) flexural action, (d) arching action, (e) Vierendeel action, and (f) compressive strut action [17].

2.3. Catenary action

The term 'catenary' is derived from the Latin word '*catena*,' which translates to 'chain.' A catenary is a chain or cable that, when at rest and hanging between two supports, exhibits pure tensile forces and no flexural forces. Catenaries are shaped by the influence of gravity, assuming a shape with minimal potential energy. When a catenary is subjected to a point load, it undergoes a deformation from its original shape, resulting in the storage of potential energy associated with its strained or displaced state. The deformed shape establishes a new equilibrium in which the stored potential energy balances with the work done by the external load. In the context of structural engineering, the concept of catenary action pertains to a form of structural response that occurs when vertical loads induce significant deformations that exceed the flexural resistance of the system. In such cases, equilibrium is attained between the vertical component of the tensile resistance of the deformed system and the applied vertical loads. This phenomenon, known as catenary action, is characterised by the deformed shape of the system and plays a pivotal role in supporting the vertical loads.

2.3.1. Requirements and opportunities

In order to arrest progressive collapse of a building, after an unforeseen event removes a load carrying column, an alternative equilibrium situation has to be found. In a post and beam modular building without vertical ties, this can either be accomplished through flexural mechanisms, or catenary action [1][25]. ALPs through flexural mechanisms are however not preferred, because they may lead to oversizing of structural elements in order to meet the required capacity. The ideal alternative load path in post and beam timber buildings is developed through catenary action, because it allows for large deformations and high strength capacities through exploitation of the tensile capacity of beams and floors [21][26]. Catenary action occurs when the floors or beams transfer from predominantly flexural load carrying elements to predominantly tensile load carrying elements.

Mpidi Bita described the load-deformation response in a floor system during catenary formation in four

stages [27]. Stage one, directly after column removal, the floors show elastic behaviour, caused by the flexural resistance of the elements. Flexural resistance is only possible for small deformations. Stage two describes the arch thrusting effect of the elements exerting compressive forces against each other. Maximum arching effect is reached when the deformation surpasses the thickness of the floor. With increasing deflections, the compressive forces are replaced by tensile forces. At a deflection of two times the floor thickness, the compressive forces are non-existing and the full resistance is determined by tensile forces. Stage three is characterised as an instable stage with no equilibrium between the vertical load and the vertical component of the tensile force in the catenary. Stage four marks the beginning of an effective catenary where an increase in applied load is met with a linear increase in deflection and resistance. The development is shown in Figure 2.3.

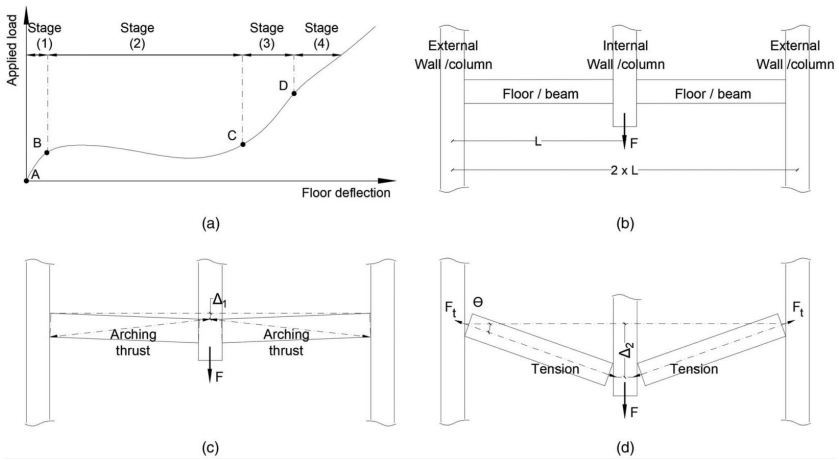

Figure 2.3: Catenary action development in a floor system: (a) load-deformation response, (b) initial condition, (c) thrusting effect, (d) catenary action [27].

A hallmark of a classical catenary is that equilibrium at larger deflections results in reduced tensile forces in the elements forming the catenary. In other words, if a stable catenary equilibrium is created at a small vertical deflection, compared to a large vertical deflection, the catenary- and associated horizontal tie forces are comparably larger. This phenomenon is demonstrated in Figure 2.4, where a 100 kN force is balanced at deflection angles of 0.1 and 0.4 radians. At the former, a normal force of 500 kN is necessary to achieve equilibrium, while at the latter, only 128 kN is required. This characteristic can be advantageous in situations where either the horizontal components or the connections in a catenary have relatively low tensile resistance. Nevertheless, a critical prerequisite for the development of an effective catenary is ensuring that the system possesses sufficient deformability to allow for significant deflections, whilst still retaining sufficient tensile capacity [21][1][25][26]. This is also demonstrated in the example illustrated in Figure 2.4, where the scenario with a high tensile force and low displacement requires a 5‰ elongation of the beams, and the scenario with a low tensile force and large displacement the other scenario requires an 86 ‰ elongation.

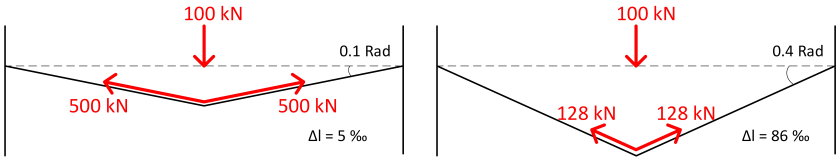

Figure 2.4: Normal forces and elongation in a catenary at different deformation angles.

2.3.2. Significance through examples

Although no examples of partial collapsed, or damage buildings exist, with detailed reports indicating catenary action prevented progressive collapse, the following examples do demonstrate the significance of catenary action in modern buildings and why proper design for catenary action can be of crucial value for ensuring sufficient robustness.

In 2006 Byfield studied the behaviour of nonmilitary buildings subjected to blasts [23]. He conducted his study based on the many reported cases of buildings which were damaged in World War II. During that time many buildings had a comparable building style, being made of masonry or having masonry infill panels as partition walls. From the extensive research Byfield concluded 'While severe localised damage from bombs was routine, disproportionate collapse was rare' [23]. The profound robustness of buildings from that time was attributed to the closely spaced columns and use of masonry panel walling for internal partition walls and cladding. The masonry panels are great at redistributing loads through compressive strut action and provide emergency shear resistance to the building. An example of a multi storey building missing multiple support columns and halting progressive collapse is shown in Figure 2.5.

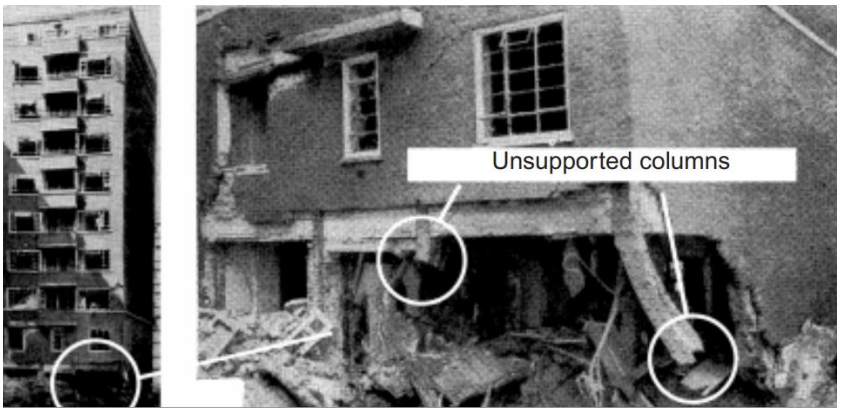

Figure 2.5: Compressive strut action carries additional gravity load after two columns failed during WW2 [28].

Modern buildings have a very different layout compared to buildings from the beginning of the 19th century. Many have large windows or even have entire façades made of glass. Moreover, many designs employ an open-plan architecture with the least amount of strong partition walls. This was determined to be the reason why the Murrah Federal Building in Oaklahoma City partly collapsed after a truck bomb took out three façade columns in 1995 (see Figure 2.6). Although the building was correctly designed according to the building requirements, the fully glazed façade and lack of strong partition walls created a deficit of alternative load paths [23].

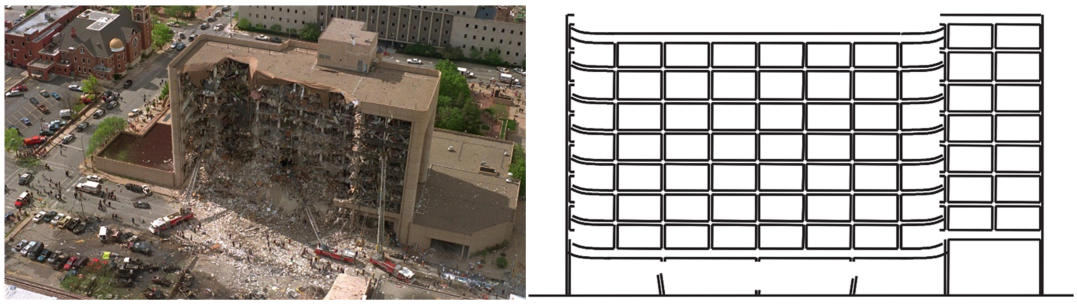

Figure 2.6: Left: Murrah builing in Oaklahoma city after the explosion [29]. Right: Illustrates the failed collumns and shear failure of the floors above [28].

The World Trade Centre towers were designed in a robust manner with multiple ALPs. The towers were designed as a tube-frame structure with load bearing perimeter columns acting as Vierendeel trusses. The perimeter columns were designed to resist all lateral loads and to share the gravity loads with the central core. Moreover, the structures included a hat truss structure to support a tall communication antenna and allow some load distribution from the perimeter columns to the central core.

After the airplane impacts took out multiple perimeter columns, Vierendeel action was activated to distribute the additional gravity loads to the surrounding columns. Also, part of the load of the unsupported columns and floors were distributed to the load carrying central core and façade by the deep outrigger

trusses at the top four floors of the building [30]. In a 2007 paper by Byfield and Paramasivam on catenary action in steel-framed buildings, it was concluded that although Vierendeel action did initially work as an ALP, it is not a commonly preferred ALP in modern buildings. In most cases beams are spaced too far apart and beam-to-column connections are often not fully rigid. Neither do most building incorporate an outrigger truss as a standard design. Its effectiveness is also highly debatable when open-floor spaces require a wide spread of columns. Therefore, the formation of ALPs in modern buildings heavily relies on catenary action [28].

Although the World Trade Centre towers fully collapsed, through thorough investigations by the US National Institude of Standards and Technology, it was concluded that catenary action was activated. Due to the high temperatures from the resulting fire, several long-span floor support trusses lost their flexural capacity and started deflecting. Later finite element analyses showed that some floors reached a deflection of more than 1000 mm. Figure 2.7 shows the resulting deflection in inches of the performed finite element analysis. This phenomenon was what finally caused the towers of to collapse. The large tensile forces, resulting from the catenary, was not met with sufficient ductility. Consequently, the already weakened and overloaded exterior columns were pulled inward, causing them to buckle. This eventually lead to the toppling of the upper part of the towers and the full collapse of the buildings [30].

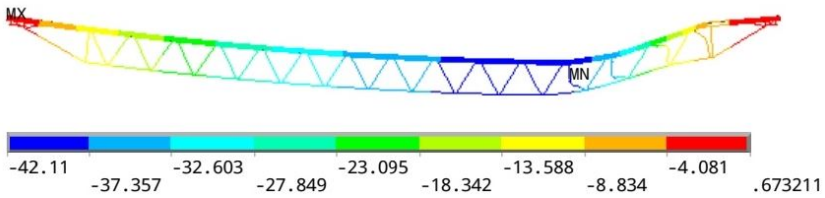

Figure 2.7: Finite Element Model of the steel trusses supporting the floors in the WTC towers while exposed to a temperature of 700 °C [30].

A comparable situation appeared during the collapse of the 16-storey Plasco building in Tehran in 2017 after a fire broke out and spread through the building. The floor system was composed of steel truss girders. Catenary action was activated when the floors started to deflect due to the heat. However, the resulting tensile forces caused excessive bowing of the exterior load carrying columns. The large tensile forces caused premature failure of connections between the trusses and columns. Without the buckling support of the floors, the slenderness ratio of the columns increased. The still attached girders exerted large inward tensile forces on the columns due to catenary action, making the columns instable and causing them to fail due to buckling [31][32][33]. The situation is illustrated in Figure 2.8.

Although the catenaries in the world trade centre and the Plasco building formed due to weakening of steel truss beams under fire exposure, both cases shed light on the important requirements for catenary action. The tensile forces in catenaries can become extensively large. Special care has to be taken during the design stage for possible high tensile stresses that occur in the connections due to catenary action. For catenary action to work, connections must be strong enough to withstand these forces. Besides, the system must possess sufficient deformation capacity to find an equilibrium state where catenary forces remain below the capacity of the catenary components. Failure of connections can result in the detachment of floors from columns, leading to further failure mechanisms, including column buckling and potential progressive collapse.

2.3.3. Research to catenary action in timber floor systems

In the field of timber engineering, there is a growing focus on researching the capacity of timber floors to facilitate catenary action. Experimental work by Lyu et al. [34] examined three types of commercially available post-to-beam connections and one non-commercial novel connection. The findings indicated that standard beam-to-column connections were incapable of forming catenary action under amplified design pressures. Similar limitations were observed in standard joints between Cross-Laminated Timber (CLT) panels, as highlighted by Mpidi Bita and Tannert [35]. Consequently, there is a call for the development of performance-based designs of novel connection types to hold progressive collapse in

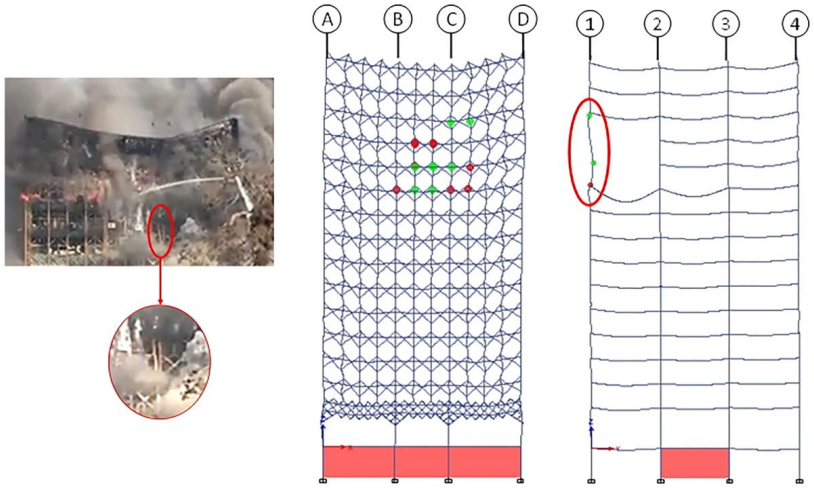

Figure 2.8: The model of Aghakouchak et al. shows that multiple floor trusses had failing connections, causing the façade columns to fail due to buckling [33].

timber structures, as emphasised by Przystup et al. [36] and Voulpiotis et al. [37].

A novel connection design, specifically crafted for enabling catenary action in timber Cross-Laminated Timber (CLT) floors, is the tube connector [38]. In this design, two tubular elements are inserted in two continuous CLT panels and connected to each other with a steel rod. In the event of a supporting column removal under the floor panels, the tubes deform inward, whilst simultaneously creating an anchor. This type of connection exhibits significantly higher resistance and deformation capacity when compared to standard dowel-type connections. A representation of the tube connector and its deformed state in an experimental test is depicted in Figure 2.9.The implementation of these connections in timber modular buildings can potentially pose challenges related to acoustic bridges between modules.

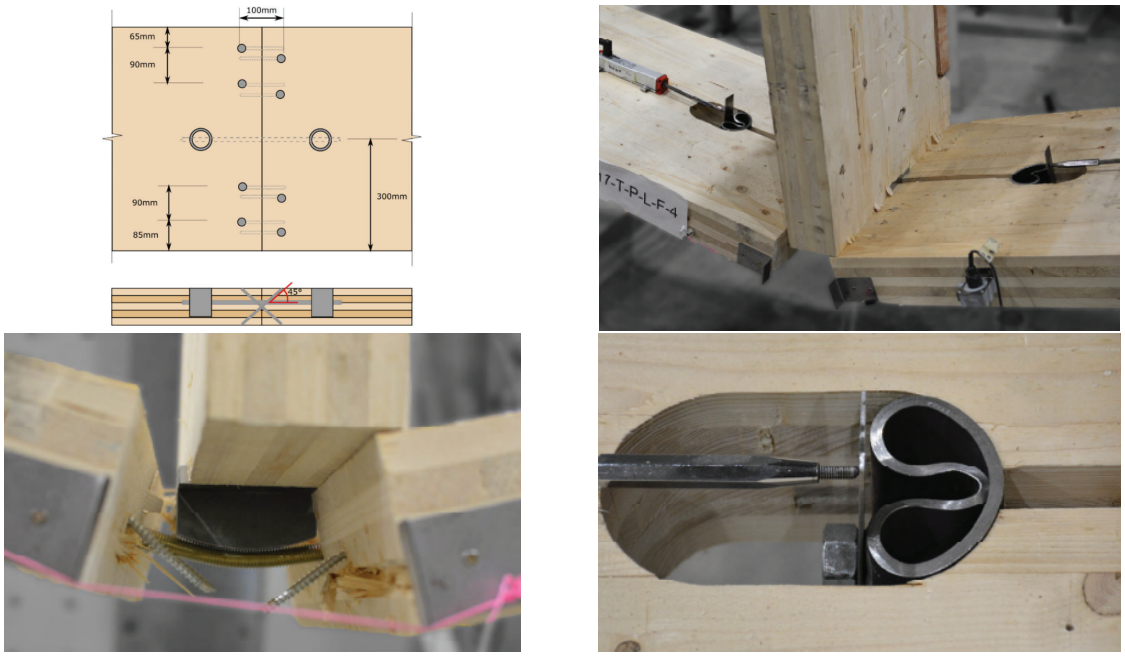

Figure 2.9: Tube connector designed for catenary action between CLT floor panels[38]

2.4. Design codes and guidelines

There are multiple design codes and building regulations throughout the world which touch upon the subject of structural robustness. Three of the most used and most well defined standards are the Eurocode and the American 'Alternate path analysis & design guidelines for progressive collapse resistance' from the General Service Administration (GSA) and the 'Design of buildings to resist progressive collapse' document from the US Department of Defence.

2.4.1. Eurocode

Eurocode 1-7 [9] provides strategies to design for accidental loads and gives guidance to the inclusion of robustness in the Accidental Limit State (ALS). It gives a strategy for design against local collapse by dividing building structures in four consequence classes (CC) (1, 2a, 2b, and 3) depending on size and use of a building structure. For CC1 no specific considerations need to be taken. For CC2a, effective horizontal ties or effective anchorage of floors to walls should be applied. For CC3, in addition to CC2, vertical ties are to be added to all columns and walls. Or alternatively, should the building be reviewed with an ALPA by notational removal of every load carrying column and beam. The total damage after the notational element removal should remain below the recommended limit of 15%, or 100 m^2 of the floor area, in each storey of two adjacent storeys, as illustrated in Figure 2.10. If the total damage is larger than the given limit, the elements have to be designed as a 'key element'. Lastly, for CC3, a probabilistic risk-based assessment should be undertaken, taking into account known and unknown hazards.

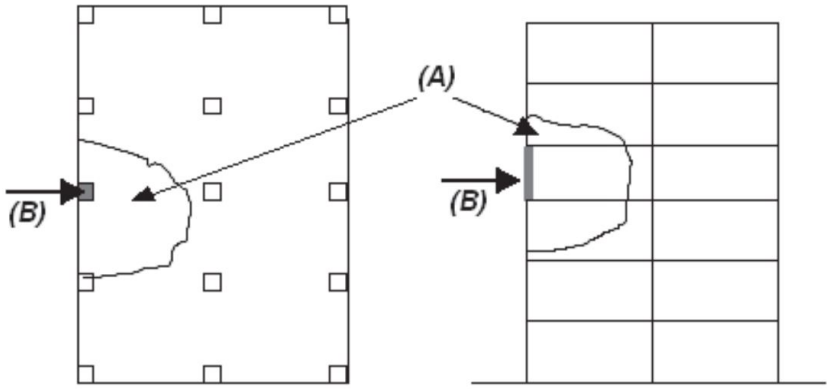

Figure 2.10: Recommended limit of damage after notational element removal with (A) describing the local damaged area, and (B) the removed element [9].

2.4.2. US guidelines

In the United States, the focus of robustness inclusion strategies is primarily aimed at preventing progressive collapse after sudden element failure. The two main guidelines for this purpose are the 'Alternate Path Analysis & Design Guidelines for Progressive Collapse Resistance' from the General Services Administration (GSA) [39] and the 'Design of Buildings to Resist Progressive Collapse' document from the US Department of Defense (DoD) [40]. Similar to the Eurocode, the US guidelines categorise buildings into four risk categories and provide robustness strategies accordingly. Buildings falling into category one do not require specific design considerations. For category two buildings, two distinct approaches are suggested. The structure should either be provided with horizontal and vertical ties, along with an enhanced local resistance of corner columns or walls, or an ALPA should be provided. For category three buildings, a full ALPA is required, and all perimeter elements on the first story require an enhanced local resistance. Category four buildings require the implementation of tie forces, a full ALPA, and an enhanced local resistance of all perimeter elements on the first story. The GSA guidelines focus solely on a direct design approach and provide guidance on performing ALPAs and including redundancy on local elements. Additionally, the DoD also prescribes a direct approach by the implementation of tie forces. Both guidelines provide descriptions on performing linear static, nonlinear static, and nonlinear dynamic calculation procedures for ALPAs.

2.4.3. Minimum tie forces

The prescription of minimum tie forces is an indirect solution strategy to ensure adequate load distribution in the case local damage occurs. By providing continuous tying of all floor edges and by tying all columns and walls in two perpendicular directions to the floors, a coherent construction is created which should provide sufficient ALPs. When a column is removed, the ties in the floor should redistribute the reaction forces from the column. The principle workings of the minimum tie forces are thus comparable to those of the catenary system.

Eurocode 1-7 prescribes different tie forces for the edge ties and internal ties [9].

- For the internal ties, the tie force is prescribed as

$$T_i = 0.8(g_k + \psi q_k)sL \subseteq 75kN \tag{2.1}$$

- For the perimeter ties, the tie force is prescribed as

$$T_p = 0.4(g_k + \psi q_k)sL \subseteq 75kN \tag{2.2}$$

Where:

S Distance between the ties

L Length of the ties

ψ The relevant factor in the expression for combination of action effects for the accidental design situation (i.e. ψ_1, or ψ_2)

The Dutch structural engineering panel, Stufib, has identified an inefficiency in the current configuration of the tie force method, where the perimeter ties are not optimally effective. In a column removal scenario at the facade or edge of a building, compared to a scenario where a column is removed in the middle, the floor fields at the edge of a building require a downward displacement twice as large as the floor fields situated in the building's center. Therefore, Stufib proposes increasing the capacity of the perimeter ties to align with that of the internal ties, which is $0.8(g_k + q_k)sL$ [41].

The UFC document prescribes that unless the structural members (e.g. beams, girders and spandrels), and the connections, can acquire an angular rotation of 0.20 radians (11.3 degrees) while maintaining the tying capacity, tying forces should be carried by the floor and roof systems [40]. This prerequisite is based on the performance of concrete floors. Other floor systems may also be used to carry the tie forces, but it has to be demonstrated that it can maintain the force while undergoing the same rotation of 0.20 radians.

Example tie force method:

A simple frame structure is given with beams and columns which are connected with pinned connections. As part of a column removal scenario, a perimeter column is removed. The tie force method is used to redistribute the additional gravity load resulting from the removed column to the adjacent columns. The goal of this example is to find the required displacement at which the required tie force capacity makes equilibrium with the additional gravity load.

The following parameters are applicable:

$s = 6.0\text{m}$
$L = 6.0\text{m}$
$g_k = 4.0\text{kN/m}^2$
$q_k = 3.0\text{kN/m}^2$
$\psi_1 = 1.0$

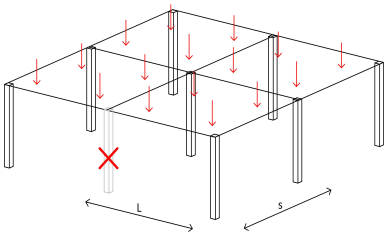

The minimum tie capacity for the perimiter tie, according to the recommendation of Stufib is:

$$T_p = 0.8(g_k + \psi q_k)sL = 0.8(4.0 + 0.5 * 3.0)6 * 6 = 158.4\text{kN}$$

To determine the additional gravity load, the combinations of actions for accidental design situations from Eurocode 0 is used:

$$E_d = g_k + \psi q_k = 4.0 + 0.5 * 3.0 = 5.5\text{kN/m}^2$$

Assuming the load is distributed evenly over the floor area, the reaction force of the removed perimeter column is:

$$R = E_d * L * \frac{s}{2} = 5.5 * 6 * 3 = 99\text{kN}$$

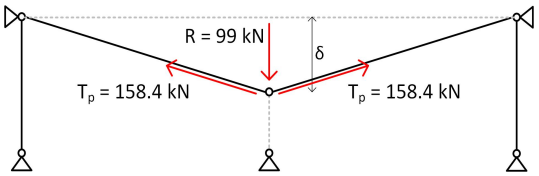

Using geometry, the required deflection to make equilibrium with the tie capacities can be calculated as:

$$\delta = 1.97\text{m}$$

The corresponding angular rotation requirement of the connection is 0.33 rad, and the required elongation of the horizontal elements is 315 mm.

2.4.4. Shortcomings

Tie force method

The tie force method is a cost-effective and convenient way of incorporating robustness in building designs. However, existing literature indicates that relying solely on the inclusion of tie forces may not guarantee success in achieving robustness. The tie force method does not consider the effect of local failure, but rather provides a minimum level of robustness to facilitate load redistribution [42][17]. One major limitation of the tie force method is the lack of attention to the deflected state in which a structure reaches equilibrium in catenary action. The example above presents a structure with a commonly reappearing column spacing and load case for modern residence buildings. It reveals that the required deflection, after a column loss scenario in a frame structure, quickly reaches excessively high values, approaching almost two meters. These deflections must be accompanied by significant rotation and elongation requirements, which most structures are not designed for to accommodate. Moreover, Figure 2.11 demonstrates that significant rotations in steel connections can lead to the generation of prying forces, resulting in a reduction of the effective tying capacity [42]. This further highlights the deficiencies in the tie force method.

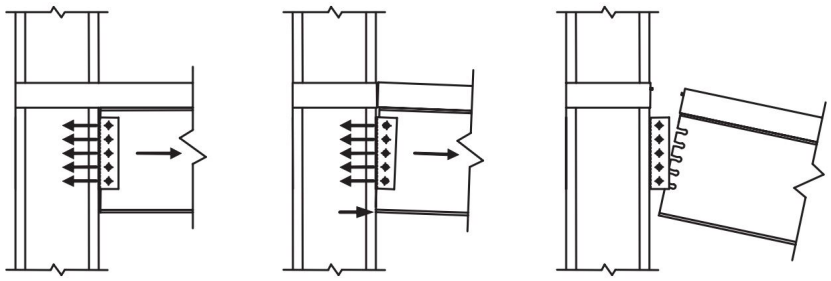

Figure 2.11: Prying effect for large rotational deformation requirements in catenary action for a steel concrete floor [28].

Alternative load path method

The Eurocode proposes an ALPA as means of mitigating the risk of structural failure in the Accidental Limit State. With an ALPA, the performance of a structure is analysed in case of an element removal scenario [9]. However, the Eurocode does not offer any guidance on how to execute an ALPA, nor does it specify which procedures, loads, dynamic amplification factors, or connection modeling procedure to use [19]. Only the new working draft of the Eurocode 5 prescribes a general loading procedure for a quasi-static analysis. It states that if a quasi-static structural analysis is used, the dynamic effect on a structure should be accounted for by increasing the gravity load by a dynamic amplification factor and that in the absence of more accurate information, a dynamic amplification factor of 2.0 may be used for an instantaneous structural element failure scenario. In contrast, the guidelines from the GSA and the DoD describe common ALPA methods for different risk categories and different materials. However, they only offer insight into the execution of the analyses without providing prescriptive rules or requirements for the actual ALPs to comply with [39][40]. The lack of guidance highlights the need for careful consideration by designers to ensure appropriate selection of load paths to mitigate structural failure risks. In the case of designing for catenary action, the designer must determine if an equilibrium state will be created at a large or small deflection. Designing for either attribute can be challenging. If a preference is given towards large deflections to allow for lower tensile forces in the catenary and the connections, the designer must ensure that the horizontal elements and connections can provide the large rotational deformations and contains sufficient ductility. If smaller deflections in the catenary are preferred, more emphasis should be placed on assuring sufficient strength in the horizontal elements and connections. However, this may lead to larger structural elements and a more expensive solution. Therefore, the designer must carefully consider the equilibrium state that best fits the capacities of the structure and materials.

2.5. Catenary equation

As described in Section 2.4.4, there is not a specific method for designing a building system which allows for a robust formation of catenary action. Moreover, robust catenary systems can be formed in multiple equilibrium states. If the assumption is made that rotational capacity in the catenary system is not limited to a certain angle, the most important properties are the tensile load and the required elongation in the catenary system. Or in other words, the tensile capacity and allowable elongation of its constituents. The multiple equilibrium states in a catenary refer to the infinite allowable combinations of catenary load and required elongation.

In Annex A, multiple hand calculations are done on a standard catenary system, to assess the equilibrium situations at different set parameters. The set parameters include the load on the catenary system, deflections of the catenary, the tensile load in the catenary, and the location and magnitude of the elongation in the catenary. From the hand calculations it was concluded that, for small elongations, the location where elongation occurs has an inconsiderable impact on the equilibrium situation. This means that the total elongation throughout the entire catenary can be added up, and as long as the total elongation from all the components in a two span catenary system is the same as in a four span catenary, the equilibrium situations are practically the same.

Taking a two span catenary system in its simplest form as presented in Figure 2.12, the relation between the tensile force in the catenary and the total elongation of the catenary can be described according to a so called 'catenary equation' (Equation 2.3). The full configuration of the catenary equation is also presented in Annex A.

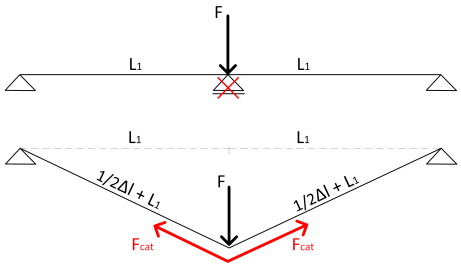

Figure 2.12: A simple catenary system over two floor spans.

$$F_{cat} = \frac{F}{2\sqrt{1 - \left(\frac{L_1}{\frac{1}{2}\Delta l + L_1}\right)^2}} \tag{2.3}$$

Where:

L_1	The original length of the horizontal elements
Δl	The total elongation in the catenary
F	The vertical load in the middle of the catenary
F_{cat}	The tensile force in the catenary

The catenary equation calculates the minimum required tensile resistance of all elements within a catenary when the total elongation in the catenary is known. If the maximum axial resistance of all components is higher than the required tensile load in the catenary (F_{cat}), a robust catenary system can be enabled. Conversely, if the maximum axial resistance is lower than the tensile load in the catenary, robust catenary action cannot be achieved. The catenary equation establishes a theoretical Catenary Requirement Boundary (CRB) for a specific span and point load by determining the requisite tensile resistance of the catenary at any given total elongation. The verification and catenary of the equation are further examined in Chapter 7.

3

Robustness analysis for a timber modular building

3.1. Introduction

This thesis is a continuation of the thesis performed by J. Knuppe in 2022 [1]. In cooperation with engineering and consultancy firm Pieters Bouwtechniek, Knuppe performed a deterministic, scenario independent, ALPA to assess the robustness of a timber modular building. By notionally removing load carrying elements in a finite element model of the building, the structural response was quantified. A robust response and viable alternative load path was identified when the additional gravity loads, following an element removal, could be distributed to other load paths, without the structure progressively collapsing. The same principles concerning the execution of ALPAs, the utilised timber modular building, and the corresponding modeling approach, used in this thesis are derived from Knuppe's research. The ALPA methodology and building modeling have been validated and can be directly employed for the analysis of catenary action. A concise summary of the key principals and assumptions from Knuppe's thesis is the most effective way to describe how this analysis method operates.

3.2. Building design

The timber modular structure, used for Knuppe's case study is based on a fictitious 'reference building'. The reference building is designed in a cooperative effort of project developer Lister Buildings, timber engineering and construction specialist CLT-S, and Pieters Bouwtechniek, to develop a better understanding of viable engineering and building strategies and the structural behaviour of timber modular buildings. It is based on a standard apartment building in the Netherlands, with multiple apartments facing to the front and back of the building, and a corridor in the middle. Due to the open space layout of the post and timber modules, multiple modules can be combined to form an apartment. Figure 3.1 shows the floor layout of the reference building, including the stability systems.

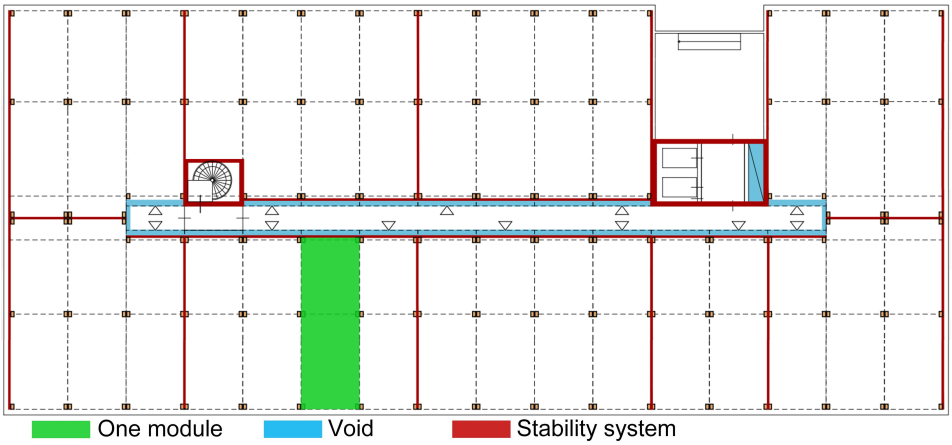

Figure 3.1: Floor plan of the reference building from Pieters Bouwtechniek

Stability frames spanning the short width of the building, divide the building in sections of multiple sections of consecutive modules. The sections generally consists of four consecutive 3D volumetric post and beam modules in horizontal direction, and five vertical layers. The stability frames provide horizontal and lateral support in their perspective longitudinal directions. An assumption was made that the staircase and elevator shaft at either side of the building provide rigid lateral constraints to the building sections. Knuppe's case study therefore focused on the inherent robustness of one of these sections. One standard building section is illustrated in Figure 3.2.

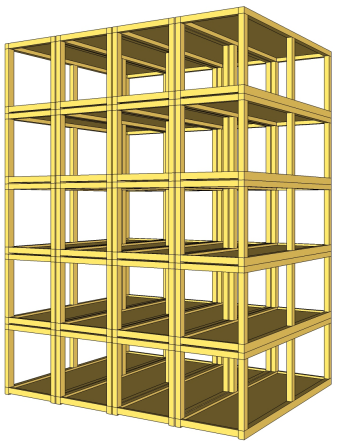

Figure 3.2: Modular system as used in the case study

Module design

Each module is predominantly constructed with glued laminated (GLT) beams and columns and cross laminated (CLT) floor and ceiling panels. Six identical columns are spread out over each corner and halfway the length of the module. Floor and ceiling panels and beams are single continuous elements and span over the entire length of the modules. The CLT panels are connected in between the beams, see Figure 3.3. The dimensions of a module and the elements making up the module are given in Table 3.1. For all timber elements, boards of strength class C24 are used.

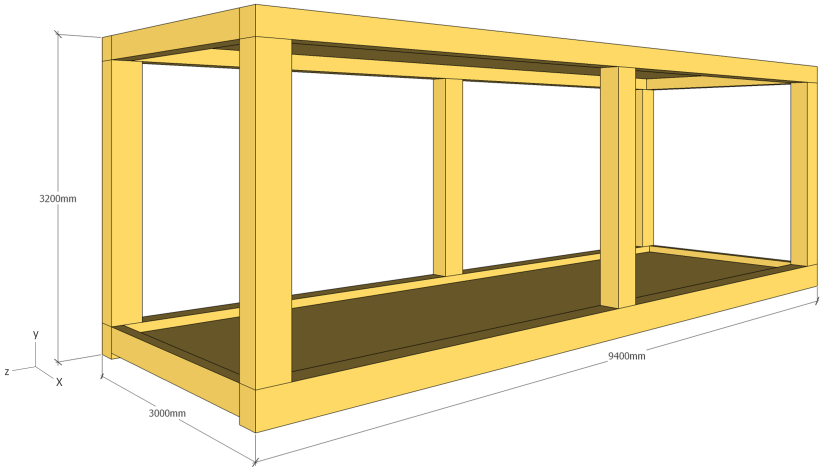

Figure 3.3: Single module

Table 3.1: Dimensions of a single module [1]

Elements	Size	Unit
Module (l x w x h)	9400 x 3000 x 3200	mm
Floor beam (long side) (h x w)	320 x 240	mm
Roof beam (long side) (h x w)	220 x 240	mm
Columns (h x w)	320 x 160	mm
Thickness of floor panel	160	mm
Thickness of roof panel	60	mm

Connections

The modules are connected through connections at each corner, see Figure 3.4. The connections are multipurpose as they are designed to provide horizontal continuity throughout the module floors (inter-module), and to connect the elements which make up the module (intra-module). Figure 3.5 shows the design of the entire connection. In the inter-module connection design, horizontal forces in the floor panels are transferred from the CLT panel to a 6 mm steel plate through 18 10x160 HBS plate screws. The function of this plate is to directly tie the CLT panels of two consecutive modules and it therefore hence called the tie-plate. The tie-plate is vertically positioned between the longitudinal GLT beam and a 12 mm steel angle beam. Two 18 mm steel rods are glued through the longitudinal GLT beams and into the columns. The tie plate and the angle beam are bolted to the module corner at the ends of the rods. The angle beam is subsequently connected to another 30 mm steel plate with two M16 bolts. This 30 mm steel plate is the direct coupling between two modules and is therefore called the coupling plate. After the coupling plate, the connection and load path is inverted to the other module corner and CLT panel. The gap between two modules is 60 mm. Vertical ties are not incorporated in the design, so only compression forces can therefore be transferred vertically.

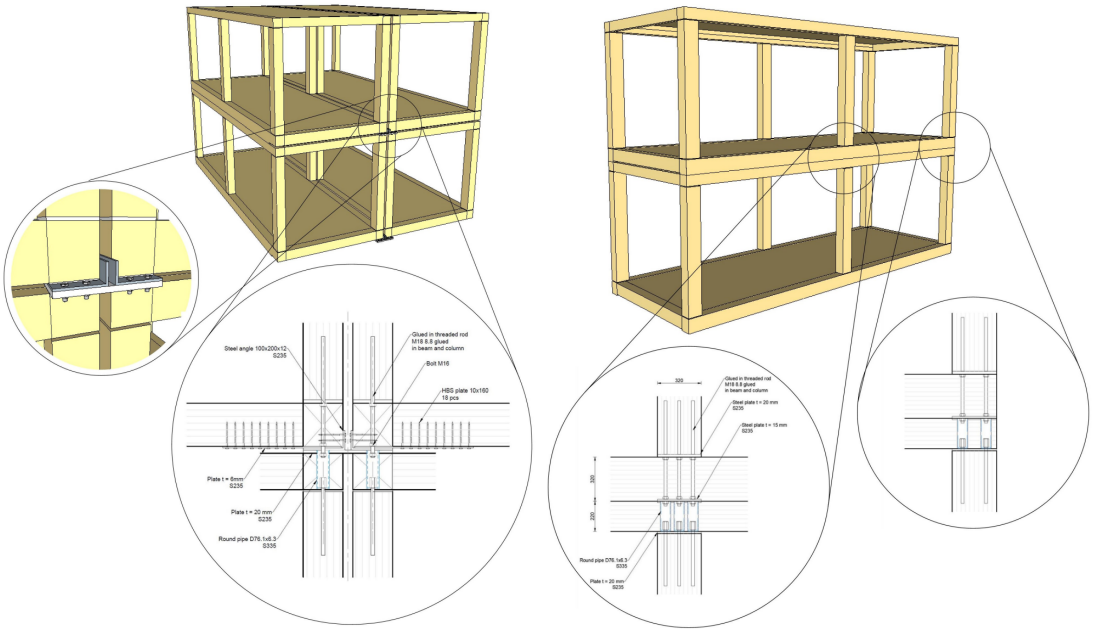

Figure 3.4: connection locations [1]

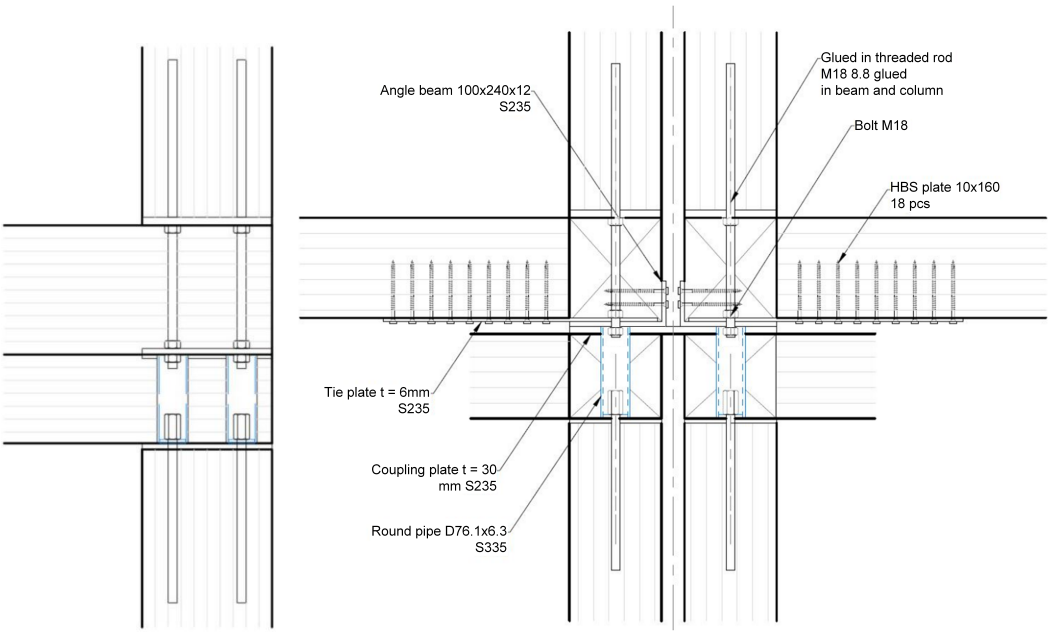

(a) Side view of the connection

(b) Front view connection

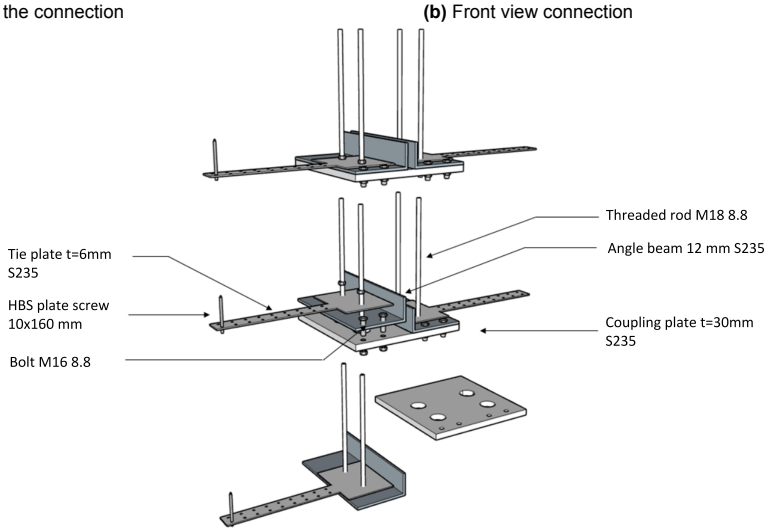

(c) 3D overview of the connection and its components

Figure 3.5: Design of the connection [1]

3.3. Models

The finite element software from Abaqus was used to perform an implicit non-linear static analysis and an implicit non-linear dynamic analysis. By performing both analyses the dynamic amplification effect of the forces in the structure could be assessed.

Analysis models

Determining the individual contribution of multiple ALPs to the overall global response of a 3D structure is a complex task. Consequently, a decision was made to model the timber modular building using 2D frames for simplicity and practicality. The repetitive layout of the beams and columns led to the possibility of representing the building section in only two 2D planar fame models. One frame faces the front plane of the modules, with four modules horizontally and five modules vertically (analysis model 1). The other frame faces the longitudinal plane of the modules, with only one module being represented horizontally and again five modules vertically (analysis model 2). A representation of the analysis model 1 and 2 is given in Figure 3.6. However, only two vertical layers of modules are presented in the Figure. Note that the boundary conditions at the vertical sides of the building section are rigid in translation in x and z direction.

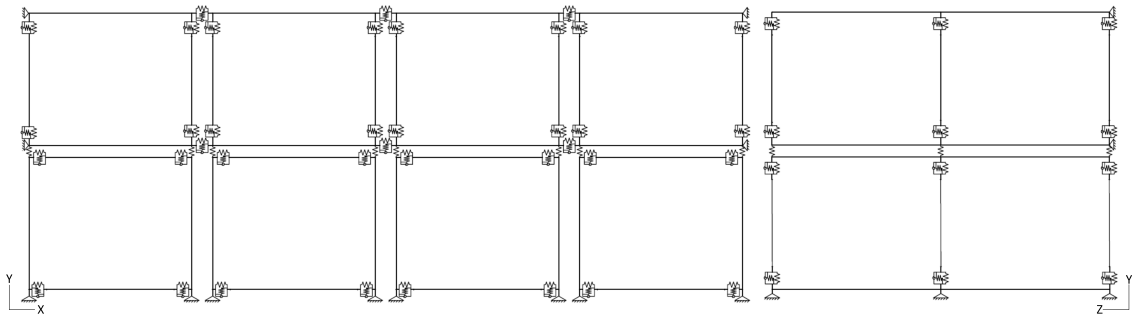

(a) Analysis model 1 **(b)** Analysis model 2

Figure 3.6: Analysis models from Knuppe's case study. Only two of the five vertical module layers are represented [1].

Notional element removal scenarios

For the ALPA three column removal scenarios and two module removal events were considered. The different events are the described in Table 3.2.

Event	Description	Scenario
Event 1	Considers loss of a corner column of the building	a & e
Event 2	Considers loss of a corner module	b
Event 3	Considers loss of two adjacent columns in the front façade simultaneously	c & e
Event 4	Considers loss of an intermediate module	d
Event 5	Considers loss of a middle column on the longitudinal side of a module	f

Table 3.2: Element removal events from Knuppe [1]. The scenarios refer to the corresponding sub figures in Figure 3.6.

Because the 3D building was decomposed in two 2D frames, ALPs could be studied in the short side of the modules and in the long side of the modules. Events 1 and 3 had the possibility of forming ALPs in both directions. For these events an analysis was performed in analysis models 1 and 3. Events 4 and 5 could only form an ALPs in the short side of the modules, so they were analysed with analysis model 1. And event 2 could only be analysed in analysis model 2. In total, six scenarios could be sketched, see Figure 3.7.

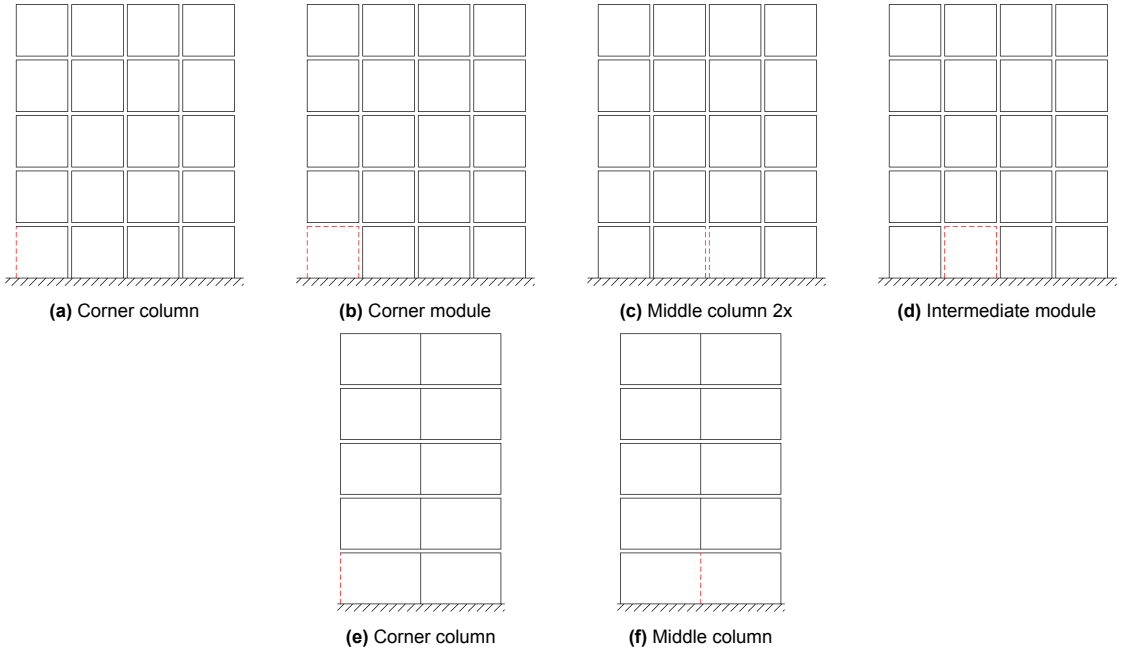

Figure 3.7: All removal scenarios from Knuppe's case study [1]

Accidental limit state

ALPAs are in essence always performed for an ALS design situation. This implies that different load, partial, modification factors are to be applied. New load factors were taken from Eurocode 1990 clause 6.4.3.3 [9]. The partial factors for the material properties γ_M and resistance γ_{Rd} become 1.0, and the modification factor k_{mod} for timber should be taken as 1.1, in the case of service class 1, and an instantaneous load duration [43].

Analysis procedures

For every scenario as presented in Figure 3.6 a nonlinear static and nonlinear dynamic analysis was performed. The loading procedure for the static analysis was based on the push-down method. With the push-down method, the required loads are applied in two steps. In the first step the unamplified gravity loads are applied quasi-statically on the structure. In the second step, the structure directly above the region with localised damage is subjected to additional gravitational forces, equivalent to the difference between the amplified loads and the original unamplified loads. The amplification depends on the recommended dynamic amplification factor (DAF). According to the new draft of Eurocode 5, a DAF of 2.0 may be used.

The dynamic loading procedure, also consisted of two steps. In the first step the reaction forces on the to be removed element are statically determined whilst the structure is still intact. In the second step, the element is removed and the structure is instantaneously loaded with the inverted reaction forces. The behaviour of the structure is subsequently monitored over a specific time period.

Connection properties

In order to include accurate values for the connection properties and create an accurate model of the building, spring models were applied. The overall rotational and translational stiffnesses of the connection were determined by adding the stiffnesses of the individual components and elements of a connection in series or parallel. The resistance of the connection was consequently governed by the weakest link, with the elastic stiffnesses and yield resistances being determined according to the Eurocodes. To include the behaviour of the connections after yielding, and make the load-deformation response bilinear, two distinct theories were applied. For rotational behaviour, zero plastic stiffness and a maximum rotation of 0.15 radian was assumed. The plastic behaviour theory was taken from a review on ductile moment-resisting timber connections from Rebouças et al [44]. Here it was found that for beam-column connections, with glued-in rods, in monotonic tests, a plateau occurs at yielding,

and maximum rotational angles of 0.15 radian can be reached. For translational behaviour, also zero plastic stiffness was assumed. However, the plastic elongation was determined with a ductility ratio of two. This means that the maximum deformation is twice the elongation at the onset of yielding. Tables 3.3 and 3.4 present the rotational and translational properties of the intra- and inter-module connection parts. The translational behaviour of the inter-module connection in x-direction is particularly of interest, as this behaviour is important for the formation of catenary action. The stiffness in translational direction is determined by serial addition of the stiffness of the screw groups (K_{ss}), tie plates ($K_{pt.1}$), coupling plate ($K_{pt.2}$), see Figure 3.8. For more information on how the connection properties are calculated, and how the spring models of the remaining connection parts are determined, the reader is referred to Knuppe's research report.

Property	**Symbol**	**Closing rotation θ_z^-**	**Opening rotation θ_z^+**	**Unit**
Rotational elastic stiffness	K_r	115.20	101.90	kNm/rad
Rotational resistance	M_y	10.97	10.97	kNm
Plastic rotation	θ_p	0.055	0.042	rad
Ultimate rotational resistance	M_u	10.97	10.97	kNm

Table 3.3: Rotational properties of the intra-module connections around the z-axis [1]

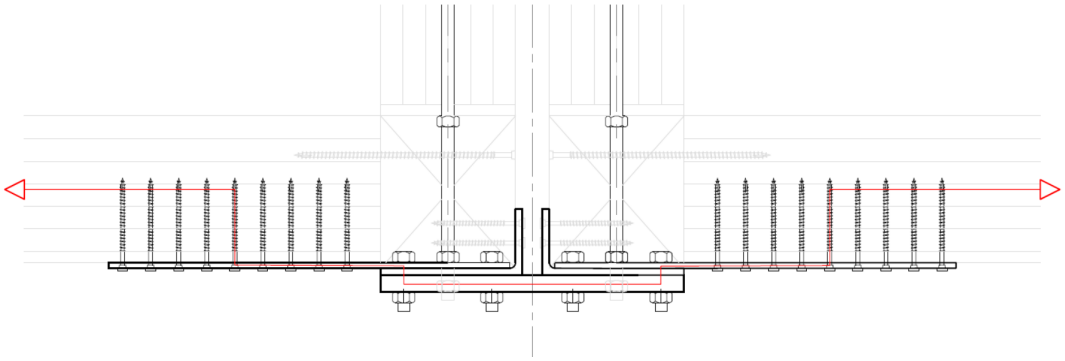

(a) Flow of force in the inter-module connection

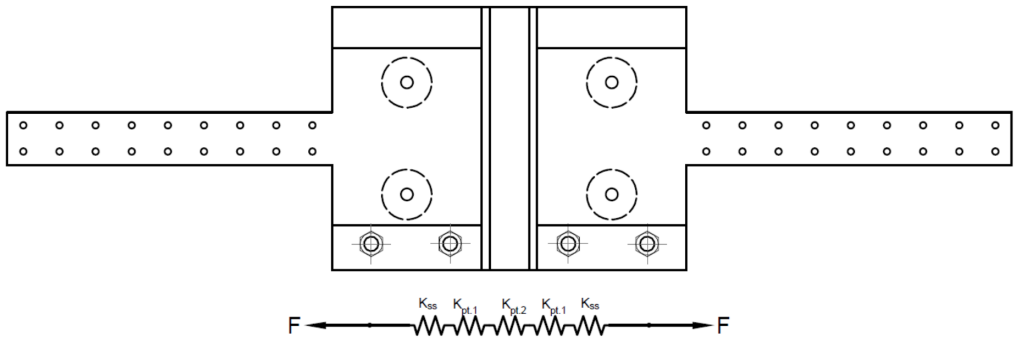

(b) Translational spring model of inter-module connection

Figure 3.8: Force flow and spring model of inter module connection [1]

Property	Value	Unit
Shear resistance threaded rod M18	147.4	kN
Bearing resistance of tie plate with M18 threaded rod	155.5	kN
Shear resistance of bolt M16 with angle beam	120.6	kN
Bearing resistance of angle beam	153.6	kN
Tensile resistance of tie plate	126.9	kN
Tensile resistance of net cross section tie plate	108.9	kN
Shear resistance 10 mm screw (group)	110.2	kN
Shear stiffness screw group K_{ss}	1.25E+05	kN/m
Stiffness tie plate $K_{pt.1}$	1.53E+05	kN/m
Stiffness 30 mm coupling plate $K_{pt.2}$	6.30E+06	kN/m
Elastic stiffness of connection	3.25E+04	kN/m
Yield resistance of connection	108.9	kN
Plastic deformation of connection	3.36	m

Table 3.4: Translational properties of the inter-module connection on the x-axis [1]

Finite elements

The beams and columns in the model are represented by 1D linear beam elements, and the connections are modelled with connector wire elements. Figure 3.9 shows the buildup of the connection in Abaqus. It can be seen that the entire connection is build up by five different wire connectors. Connectors 1 and 3 are the intra-module connections between the columns and the floor and roof beams. These connectors contain the vertical translational properties and the rotational properties for the opening and closing movements given in Table 3.3. Connector 2 represent the inter-module connection as shown in Figure 3.8 and Table 3.4. The models are stacked vertically, without having a vertical inter-module connection. They can only transfer vertical compression loads. No material contact could be accounted for, so connector 4 which only contains a compression stiffness is applied. Connector 5 is a purely rigid connector in every direction and rotation. This is added because only the ends of the connectors with a yellow triangle allow for rotation. By adding the two rigid connectors and confining connector 2 to a small section, the behaviour of the entire connection approaches symmetry. If one large connector, with no rigid connectors, was used, the connection would behave as if only one side could rotate.

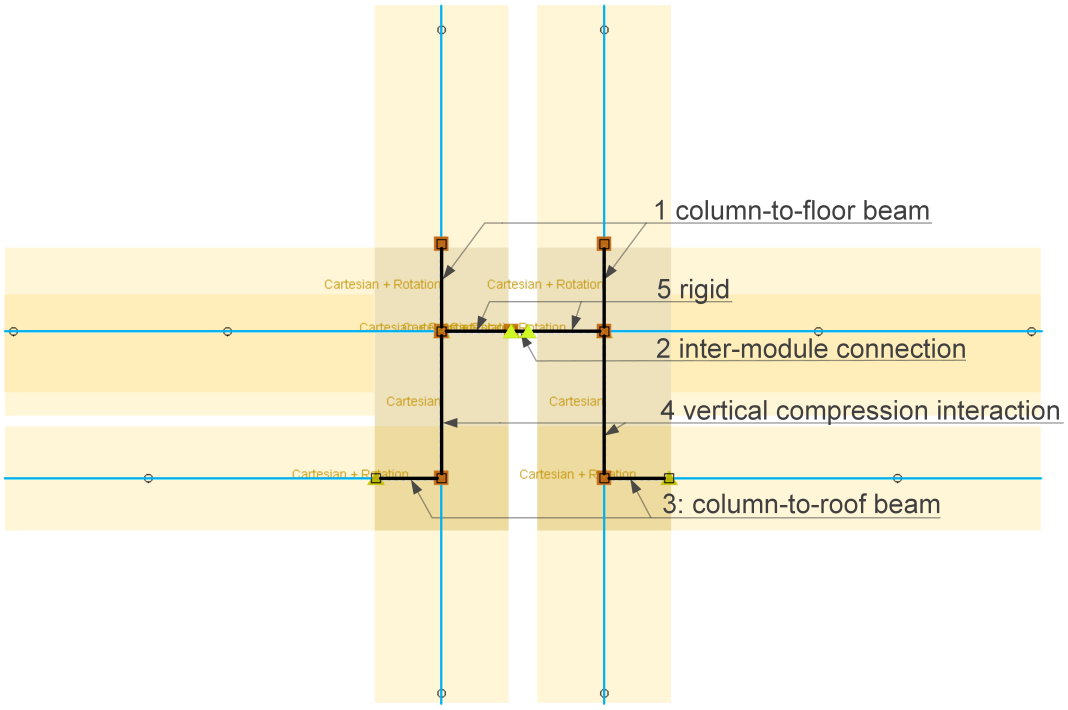

Figure 3.9: Inter-module connection with connector elements in Abaqus model from Knuppe [1].

3.4. Results and conclusions

Results

Results [1] showed that not all removal scenarios in 2D frames could create sufficient alternative load paths. Here the response of all events are shortly described. The events (a to f), correspond to the scenarios from Figure 3.7.

- Scenario a and b (corner column and corner module removal in analysis model 1): The rotation capacity of the intra-module connection around the z-axis is governing for forming an ALP. However, the rotation resistance is insufficient as only 37% of the unamplified design load could be resisted. After the connection rotated 0.15 rad, the analysis is stopped and structure is assumed to have failed.
- Scenario c (double intermediate column in analysis model 1): The translation capacity of the inter-module connection in x-direction is governing. The analysis clearly showed that the system transforms from a stage of bending into a catenary stage due to an increase of stiffness in the vertical load-displacement response. However, the maximum tensile resistance and plastic deformation is reached in the tie plates at 108.9 kN. At this point the catenary had deflected 0.2 meters horizontally. 57% of the unamplified loads could be resisted. The elongation, and with that the vertical deflection, of the catenary system did not reach to a point where the rotation and moment capacity in the connections surpassed its yielding limit. Therefore, a parameter study was performed to analyse the influence of having a larger rotational stiffness and resistance in the intra-module connection. He showed that adding more rotational stiffness contributes most to an increase in resistance of the vertical force-displacement behaviour. However, a sufficient catenary could still not be reached, as by increasing the rotational stiffness and resistance by a factor of two, only 77% of the unamplified design load could be reached.
- Scenario d (intermediate module in analysis model 1): The analysis showed that an ALP could be formed through shear in the 30mm thick coupling plate in the inter-module connection. Through shear the vertical loads could be transferred to a neighbouring column and a sufficient ALP was identified.
- Scenario e (corner column in analysis model 2): Flexural behaviour of the longitudinal beams of the modules was governing. The beam cantilevers over the middle column and transfer the horizontal loads to the remaining columns. The bending capacity of the beam was sufficient to

resist two times the gravity load. This means an ALP was identified, which could also resist the amplified loads.

- Scenario f (middle column in analysis model 2): Flexural behaviour of the longitudinal beams was again the governing ALP. However, the analysis showed that the maximum bending stress in the beams was reached at a load factor of 1.74. Meaning that the unamplified load could be redistributed, but only 74% of the amplified load due to dynamic load effects could be resisted.
- The comparisons between the nonlinear static and nonlinear dynamic analyses indicate that the dynamic amplification factor for this timber structure is close to the upper bound of 2.0 as proposed by the new draft of Eurocode 5.

Conclusions

- Modelling the building in 2D frames allow for using conventional engineering and calculation methods to analyse the behaviour of the building. However, using a 2D setup excludes additional resistance mechanisms in other directions, because loads can only be transferred in one plane. This creates conservative results. Modelling the structure in 3D adds possible ALPs, which can act simultaneously. The gravitational loads can therefore be shared, lowering the capacity demand on either ALP. Moreover, by incorporating the floor structure, additional possible ALP are added, such as diaphragm action or membrane action in the floors.
- An assumption was made to assume structures have failed when the intra-module connection reached a rotation of 0.15 rad. This assumption was based on research on connections with glued in rods. The intra-module connection is not a connection where the glued in rods determine the governing rotational resistance. When a column is removed and the floor beam starts to rotate in analysis model 1, the rotational resistance is determined by the tie plate. As the rotation in a steel plate, after forming a plastic hinge, allows for larger rotations than 0.15 rad, this assumption may be assumed incorrect for this application.
- Although not all removal scenarios provided a sufficient ALP, it does not mean the structure is not robust. The removal of a corner column and intermediate double column could not be resisted by an ALP through the short sides of the modules, but they could be resisted by flexural behaviour in the longitudinal side of the module. However, designing a structure for flexural ALPs can lead to oversized element sizes and is therefore not advised. Finding other ALPs, possibly by catenary of membrane action could be of substantial value when aiming for limiting material use.
- Results showed that catenary action could not develop sufficiently with the current inter-module connection design. Increasing the rotational stiffness and resistance, of the intra-module connection, by a twofold only increased the capacity from 57% to 77% of the unamplified load demand. Improving the rotational capacity alone is therefore insufficient for the formation of catenary action. However, by allowing for more elongation and translational capacity in the inter-module connection the possibility of forming a sufficient catenary can be improved.
- The formation of effective ALPs primarily relies on the rotational resistance, tensile resistance, ductility, and axial stiffness of the connectors. These properties are predominantly influenced by the steel components of the connections.

Part II

Case study

4

Methodology and Framework for the Case Study

This chapter outlines the methodology employed in the current case study to address the limitations identified in Knuppe's ALPA on a timber modular building and optimise the inter-module connections of a comparable case study building to enable the robust formation of catenary action. This multipurpose case study was conducted in collaboration with engineering and consultancy firm Pieters Bouwtechniek and aims for the following three goals:

- Analyse the in-plane resistance, load distribution, and load-deformation response of discrete timber floors exposed to the tensile loads corresponding to catenary action.
- Include the load-deformation behaviour, of the discrete timber floors, in 2D frame models of a timber modular building by implementation of spring boundary constraints at the ends of the floors, and assess its effect on the building model to establish catenary action.
- Introduce and perform an optimisation of the inter-module connections in a timber modular building to efficiently enable the formation of robust catenary action.

Each part of the case study generates results that serve as input for the subsequent part. Simultaneously, each part is also treated as an independent study to gain insights into the effects of various building layouts and modeling assumptions. This allows for a more comprehensive understanding of how timber modular buildings respond in catenary action.

4.1. Building design

This case study is conducted on a building structure based on the same reference building as introduced in Section 3.2 and illustrated in Figure 3.1. As previously described, the reference building is a timber modular building which is divided into multiple building sections. Each building section in turn consist of post and beam modules with a maximum of four modules in width and five modules in height. The building sections are encapsulated by steel stability frames along the long side of the outer modules and on one of the short sides of the modules. Figure 4.1 represents a single building section with the according stability frames.

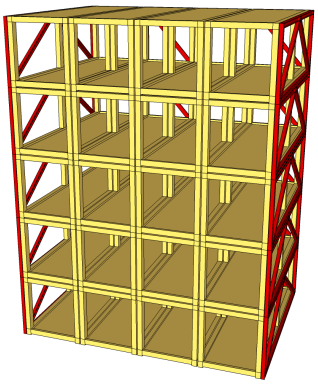

Figure 4.1: Case study building of a timber modular building comprised of a single stand alone building section

The timber modular building in this case study consists of three consecutive building sections. This configuration has been chosen because it provides a more accurate representation of the practical application of this specific building type and its structural layout. Moreover, the three building section layout allows to compare ability to form robust catenary action for two distinct scenarios. The first depicts a scenario where the two outer building sections are considered to form rigid constraints to the middle building section, and where in-plane behaviour of the floor systems does not have to be taken into account when performing a 2D ALPA. The second scenario depicts a situation where the in-plane deformation of all the floors is considered in a 2D ALPA. The timber modular case study building with three consecutive building sections is shown in Figure 4.2.

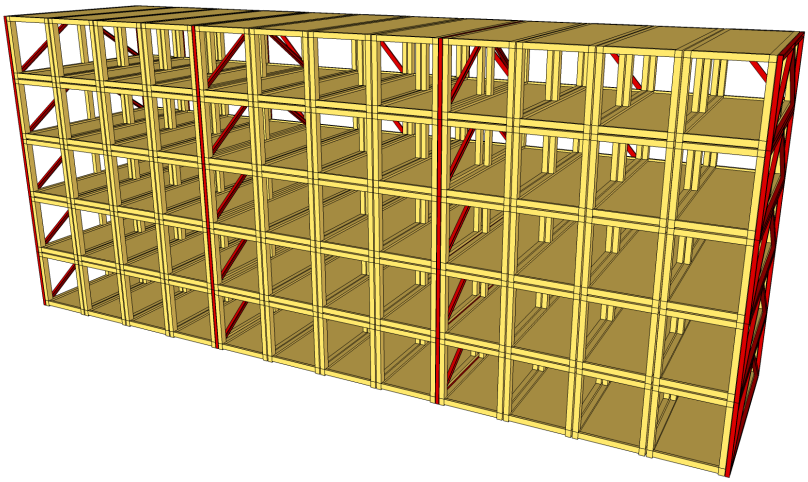

Figure 4.2: Case study building of a timber modular building comprised of three subsequent building sections

The reference building is designed to comply with Eurocode and Dutch design standards for Ultimate Limit State (ULS) and Serviceability Limit State (SLS). The ALS design situation and design for robustness are not taken into account.

The module and connection design of the case study building are the same as described in Chapter 3. However, two aspects in the spring model of the inter-module connection are altered to better approximate the real behaviour of the structure. First, the connector layout of the inter-module connection. In the spring model as proposed by Knuppe, the stiffnesses of all components that make up the inter-module connection are bundled in one connector. This approach results in a non-conservative solution

when accounting for plastic behaviour and a slightly asymmetric deformation. It was also stated that the plastic elongation of the connector is equal to the elastic deformation, because of the assumed ductility ratio of 2.0. This assumes that plasticity occurs in all components in the considered connector. However, in a chain of components, plasticity will occur in the component with the lowest resistance. It is therefore better to divide the bundled connector in smaller connectors, considering smaller groups of components. Moreover, the inter-module connection is symmetric between two modules and the weakest component occurs twice in the series of components. Because both components have the same lowest resistance, theoretically they will both reach a state of plasticity and fail at the same time. However in practice, the probability of the two components having the exact same yield resistance is low. This can for example be due to the impact of micro imperfections in the material or cross section. Again, dividing the bundled connector in multiple connectors allows to separate the two identical components and only allow one to reach its full plastic potential. It is therefore proposed that when modelling the connection, the inter-module connection connector is divided into three components. Two of which are the combined shear stiffness of the screw group and the stiffness of the tie plate (connector 2a in Figure 4.4), and one is the stiffness of the coupling plate (connector 2b in Figure 4.4). Figure 4.3 shows a simplified illustration of the full original connection model and the newly proposed connection model in a deformed state, including the spring model of the inter-module connection. Figure 4.3a is shown in more detail in Figure 3.9 and Figure 4.3b is shown in more detail is Figure 4.4. Table 4.1 contains the new inter-module connection properties for axial translation in tension. The lowest resistance is governed by the net cross section of the tie plate. According to Eurocode 3 for design of steel structures, the resistance of the net cross section at holes for fasteners is determined by the ultimate resistance of the steel [45]. This failure mode can therefore also be described as brittle, meaning no plastic deformation is possible.

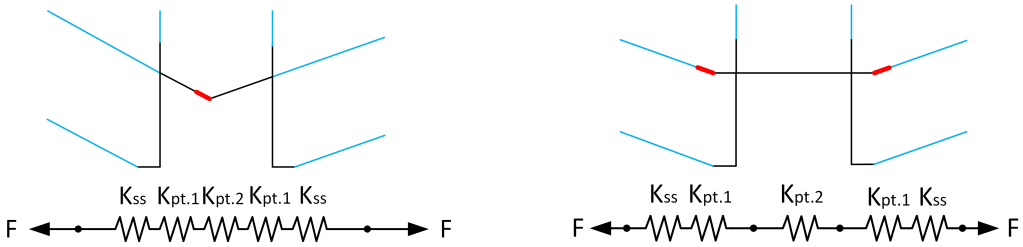

(a) Original connector buildup

(b) New connector buildup

Figure 4.3: Simplified connector layout of the original and new spring models of the full connection. In red indicated the locations where plasticity can occur in the inter-module connection.

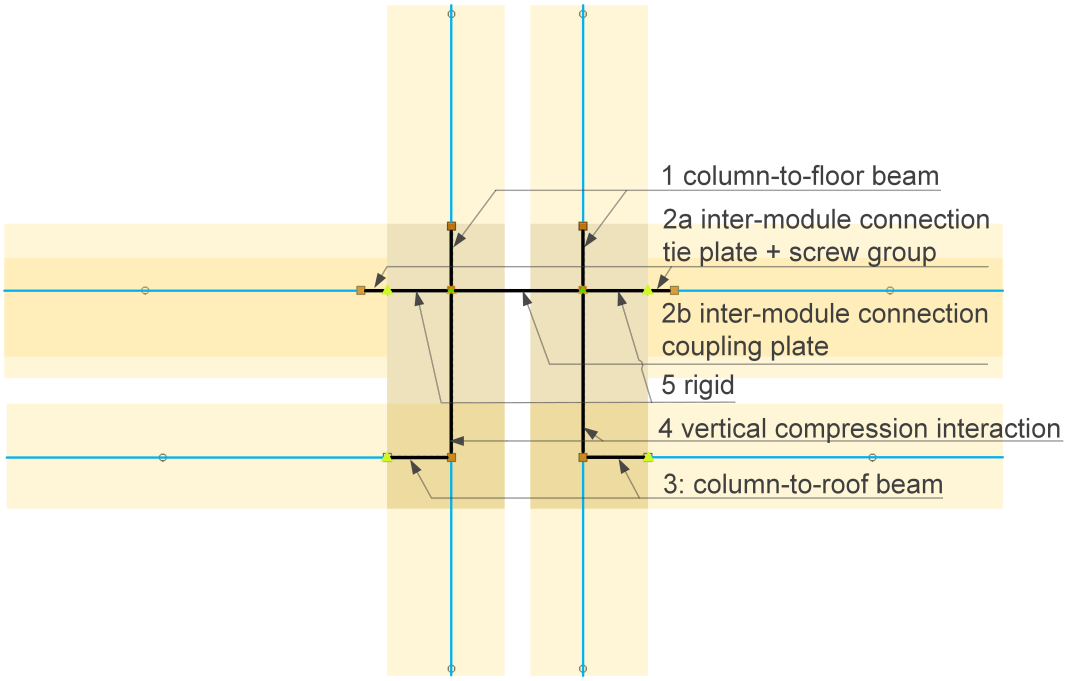

Figure 4.4: New connector buildup of the full connection between four modules. The yellow triangles indicate the rotation points of the connectors. The orange squares indicate rigid connector ends.

Property	Value	Unit
Shear resistance threaded rod M18	147.4	kN
Bearing resistance of tie plate with M18 threaded rod	155.5	kN
Shear resistance of bolt M16 with angle plate	120.6	kN
Bearing resistance of angle plate	153.6	kN
Tensile resistance of tie plate	126.9	kN
Tensile resistance of net cross section tie plate	108.9	kN
Shear resistance 10 mm screw (group)	110.2	kN
Shear stiffness screw group K_{ss}	1.25E+05	kN/m
Stiffness tie plate $K_{pt.1}$	1.53E+05	kN/m
Stiffness coupling plate $K_{pt.2}$	6.30E+06	kN/m
Elastic stiffness of tie plate + screw group	6.88E+04	kN/m
Yield resistance of connection	108.9	kN
Elastic deformation of tie plate + screw group	1.58	m
Plastic deformation of tie plate + screw group	0	m

Table 4.1: Translational properties of the inter-module connection in tension

The second adjustment in the connector model of the inter-module connection addresses the rotation point and the originally proposed maximum rotation. In the original connection, the point of rotation was located in the middle of the connection. See Figure 4.3a. In the new connection two rigid connector elements are positioned on the outside of the vertical connectors, rather than on the inside. This ensures that the rotation point of where the floors actually rotate is be positioned on the correct location. Furthermore, in the original spring model, a maximum rotation of 0.15 radians was adopted. This value originated from a study on the maximum rotation of moment resisting glued-in-rod connections from Rebouças et al. [44]. However, rotation will not occur at the location of the glued-in-rods. The actual

rotation is assumed to occur at the location of the inter-modular connection, in the tie plate which also connects the CLT panel and the longitudinal floor beam. The tie plate and pairs of cross-wise inclined screws between the CLT panel and the floor beam will show immediate plastic deformation in rotation. The relatively thin tie plate will however have a larger plastic rotation than 0.15 rad. Therefore, zero rotational stiffness and no maximum rotation is assigned to the inter-module connectors.

4.2. Case study framework

The three goals from the introduction of this chapter are elaborate in three distinct chapters which build upon each other.

Chapter 5

In chapter 5 the in-plane behaviour of discrete timber floors is analysed. It can be said that all CLT floors consisting of multiple panels are discrete timber floors. However, in this study a discretised timber floor is seen as a floor made up of multiple floor fields from distinct modules. The difference arises from how horizontal shear forces are distributed. In conventional CLT floors this is often done by connecting the floor elements along the full edges. In floor fields from modular buildings, shear forces can only be distributed through the inter-module connections.

In order to further analyse the effect of the location of the removed façade column, as well as the effect of having additional consecutive floor fields adjacent to the removed column and additional stability frames on the in-plane behaviour, the following three situations are considered:

1. Double intermediate façade column removal in a single standalone building section.
2. Double centre-adjacent façade column removal in a single standalone building section.
3. Double intermediate façade column removal in a three section building.

The three situations are analysed in 2D numerical models from a top-down perspective and are illustrated in Figure 4.5. In order to analyse the in-plane behaviour of the three scenarios, four distinct models are used. Analysis scenarios 1 and 3 are modelled using symmetry. They require a model of only two and six floor fields respectively. Analysis scenario 2 requires a model of both one and three floor fields to capture the complete behaviour.

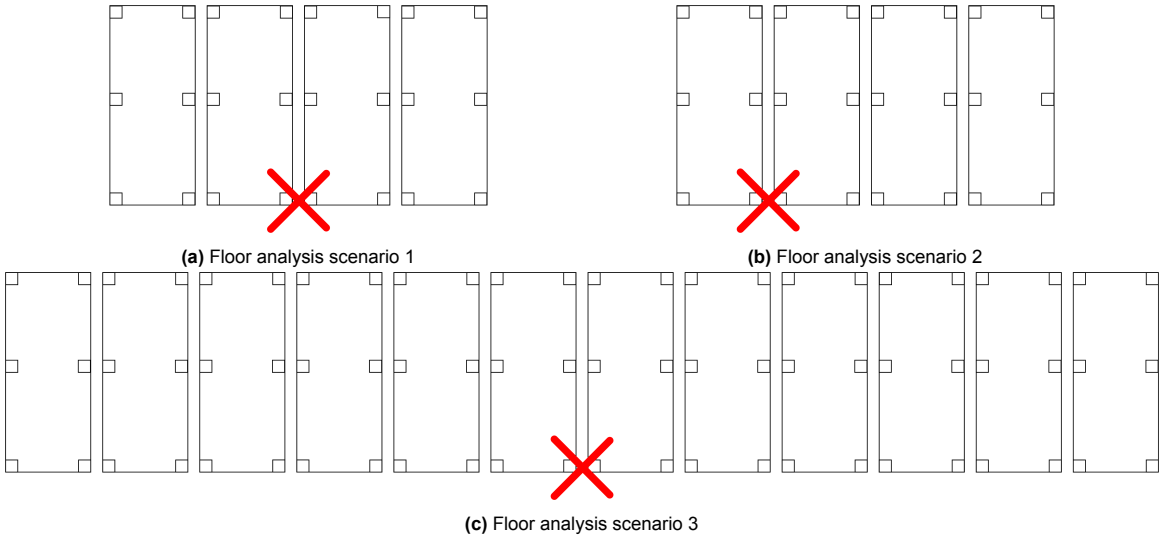

(a) Floor analysis scenario 1

(b) Floor analysis scenario 2

(c) Floor analysis scenario 3

Figure 4.5: Modelling scenarios for analysing the in-plane behaviour of discrete timber floors

Chapter 6

In chapter 6, the influence of incorporating the floor behaviour in the 2D frame model, on the ability to form catenary action is analysed. Three numerical analyses on three distinct models will be performed in order to quantitatively compare the results. The first model relates to the scenario where no in-plane deformation of the floors is considered in the case study building and where the two outer building sections form rigid boundary constraints to the middle building section. The second model relates to the scenario where the in-plane behaviour of the case study building is considered. For this scenario also a single building section is modelled, but with the load-deformation characteristics of floor model with six floor fields from Chapter 5. The load-deformation behaviour is incorporated through spring boundary constraints. A third model depicts a situation where the in-plane floor behaviour is considered in a single standalone building section. For this analysis, the results from the floor models with one, two, and three floor fields is integrated in corresponding spring boundary constraints. The three situations are worked out in 2D numerical models from frontal perspective and are illustrated in Figure 4.6.

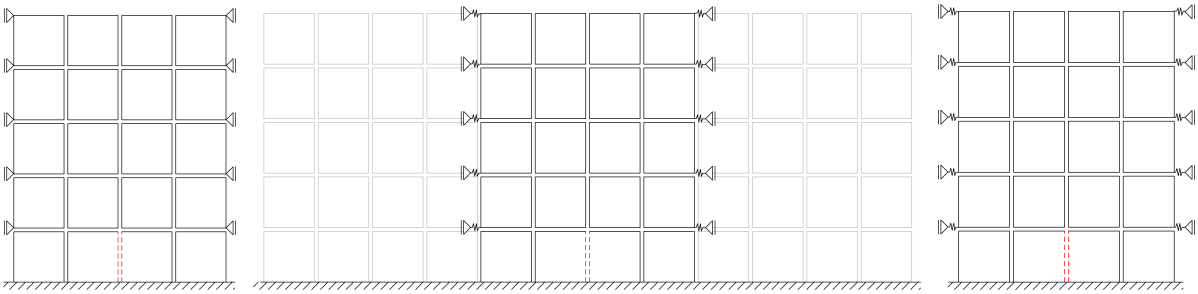

(a) Scenario 1 **(b)** Scenario 2 **(c)** Scenario 3

Figure 4.6: The three models for the boundary constraint analyses

Chapter 7

In chapter 7 an optimisation study is performed on the inter-module connections of the case study building comprised of three building sections. As described in the literature study, a catenary can theoretically find equilibrium at any vertical deflection. This can be either at a relatively small deflection, which requires strong links in the catenary, or at a relatively large deflection, which requires less strength, but more ductility in the links. Therefore, two optimisation methods are proposed and executed. The first method aims to create a strong inter-module connection, and the second method aims to create a ductile inter-module connection. Both methods optimise the connections to the extent that they only permit the minimal requirements for the robust formation of catenary action.

5

Discrete timber floors

5.1. Introduction

When an intermediate facade column is suddenly removed, catenary action emerges as one of the predominant alternative load paths. Catenary action comes hand in hand with high tensile forces and stresses which have to be distributed through diaphragm action in the floors to the stability system of a building. Discrete timber floors from modular buildings require the catenary forces to be distributed through the inter-module connections. This leads to stress concentrations in the floors and a less efficient load transfer compared to continuously connected floor panels. It is therefore important to analyse if the discrete floor systems are able to resist high loads resulting from catenary action. Furthermore, it is important to identify the critical component in the timber module floors in order to determine the maximum catenary load the floors are able to distribute. Another important property to analyse is the in-plane load-deformation response, or the in-plane stiffness. As previously explained in Chapter 2, elongation in a catenary is required to allow for more vertical deflection and a lower required tension resistance in the catenary components at equilibrium. Chapter 6 goes further on how to incorporate the load-deformation and load distributive behaviour of the floors into the 2D frame model of the case study buildings.

In order to determine the resistance and in-plane load-deformation of discrete timber floor systems, numerical analyses are performed with the finite element program Abaqus. This chapter begins with an elaboration of the case study building design, focusing on the floor system of a module. Subsequently, the numerical analysis models, as introduced in Chapter 4, are elaborated, along with its associated input parameters. Moreover, multiple validation tests are performed to verify the model input. Finally, the results of the four different floor models are presented.

5.2. Module floor design

During normal use of the case study building, vertical loads are redistributed from the CLT floor panels to the longitudinal GLT floor beams. The CLT panels act as one-way slabs with the majority of the lamellas in the cross direction over the modules. The panels are build up as a C5s panels [46] with the outer and middle lamellas having a thickness of 40 mm and two intermediate lamellas with a thickness of 20 mm, see Table 5.1 and Figure 5.1. No glue is added to the edges of the lamellas.

Table 5.1: CLT floor panel build-up

Thickness panel [mm]	**Panle type**	**Layers**	**Panel design [mm]**				
			C	L	C	L	C
160	C5s	5	40	20	40	20	40

The longitudinal GLT beams are connected to the ends of the CLT panels and further distribute vertical loads to the three columns of the module below. The short beams on the ends of the modules primar-

ily function as the connecting elements for the façades. They are not connected to the CLT panels and have no further structural or load transferring application. Therefore, they are excluded from the structural analyses.

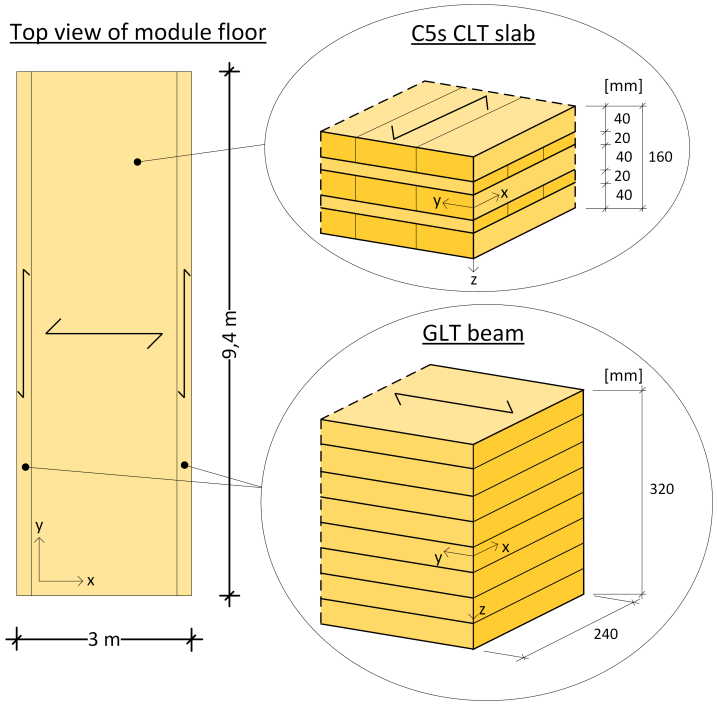

Figure 5.1: Top view of module floor with layups of the CLT panel and GLT beam

Intra-module connection in floor system

The intra-module connections between the CLT panel and the GLT beams are designed with cross-wise inclined screw pairs as illustrated in Figure C.1. The screws are inserted along the full length of the panel to beam interface at a 45 degree angle. Each screw pair has a centre-to-centre distance of 150 mm. The screws have a total length of 260 mm, and a thickness of 7 mm. The connection is designed so that the screw entering from the bottom of the CLT panel provides the shear resistance to the vertical floor loads, while the screw entering from the top of the CLT panel provides a rotational restraint for the beam, relative to the panel.

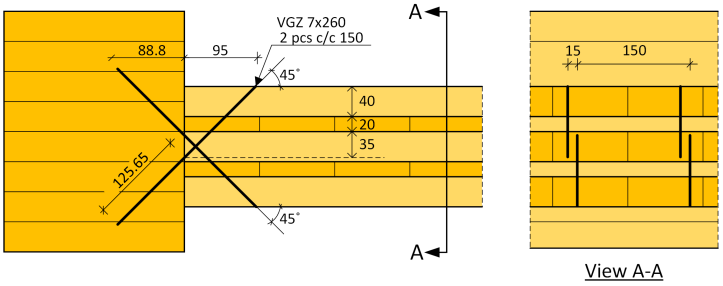

Figure 5.2: Intra module connection between CLT panel and GLT beams

5.3. Analysis models

In section 4.1, the build-up of a single timber modular building section is presented. This section explains how the general design of the discrete floor system models is established and which assumptions are made to be able to determine the in-plane behaviour. It then introduces the four models designed to compare variations in behavior resulting from differences in the number of module floor fields in a building and the configuration of the stability system.

5.3.1. Model assumptions

In the case study building, it is assumed that there is no possibility to add a truss or diagonal struts at the top of the building to facilitate a vertical load redistribution through vertical tying. Adding trusses or large diagonal struts to the top floor would severely impact the liveability of the top apartments. Due to the lack of vertical ties, loads cannot be redistributed vertically to different floors. As there is no sharing of loads between different floors, each floor needs to resist and redistribute the same additional gravity loads, resulting from an exterior column removal scenario. Each floor will therefore have to form the same catenary response. It is assumed that the final deformed state of a single building section, with fully activated catenary action, looks similar to the situation depicted in Figure 5.3.

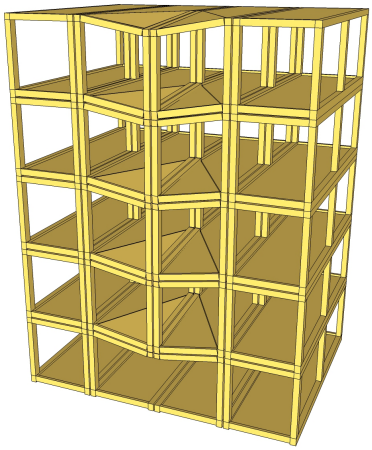

Figure 5.3: The final deformed state of a modular section, after exterior facade column removal scenario. With the lack of vertical ties in a modular building, each floor carries the same load and has the same failure mode.

Hand calculations in Annex A show that when taking a normal load combination with a DAF of 2.0, a maximum catenary resistance of 100 kN, and sufficient ductility of the floor system, the deflection in the catenary reaches 879 mm. This deflection would lead to stresses beyond any reasonable out of plane bending capacity of the CLT panels and GLT beams its presented application. It is therefore assumed that the CLT floors and the longitudinal GLT beams, primarily supported by the removed columns, fail in bending. Failure modes of corner supported CLT panels, with a load on a single unsupported corner is insufficiently researched. Therefore, a straight line is assumed as failure line for this thesis. A further assumption determines that although part of CLT panel and GLT beam fail in bending, they are not fully detached from the rest of the structure, and catenary action is still able to develop due to the tie plate of the inter-module connection being connected to the CLT panel after the failure line.

The inter-module connection at the location of the removed column keeps the two damaged parts of the CLT panels connected together whilst undergoing a vertical deflection. As there is no horizontal movement at that location, no in-plane deformation or force can be attributed a numerical model. The in plane load from the catenary is therefore best attributed to the subsequent connections in the catenary. As the damaged CLT panel at the failure line is not suitable to transfer large in plane loads from the damaged area to the intact area of the panel, it is assumed that the full catenary force is transferred from the removed column to the subsequent inter-module connections. This allows for a model design where the damaged parts, indicated in a lighter colour in Figure 5.4 can be disregarded. The same mechanism is also assumed to occur when a centre-adjacent column is removed.

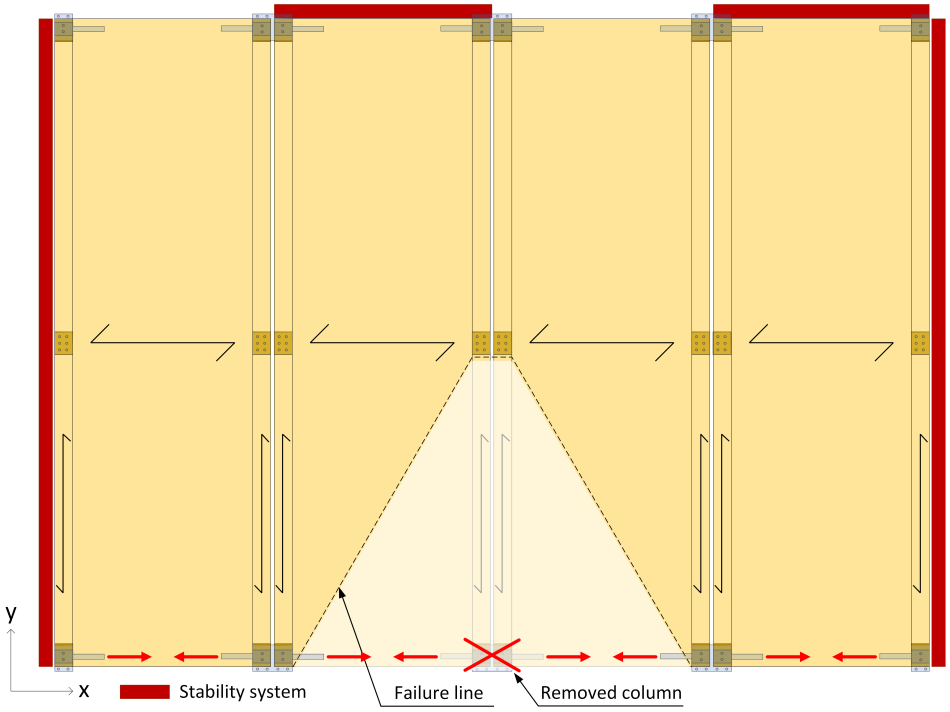

Figure 5.4: Top view of the floor system of the modular building section. The assumed failure line for the CLT panels and GLT beams fail, when the middle facade column is removed, is indicated. Together with the force component in x-direction in the connections forming the catenary.

5.3.2. Models

In this chapter, the response of three different column removal scenarios is analysed. The scenarios are already explained in Chapter 4 and a sketch of the scenarios is given in Figure 4.5. Modelling all floors from the modular floor systems imposes an unnecessarily large computational demand on the numerical analysis. In order to cut the computational demand in half, symmetry is used for scenario 1 and 3 as depicted in Figures 4.5a and 4.5c respectively. Scenario 2, depicted in Figure 4.5b, requires two distinct models to analyse the full in-plane behaviour. In total, the three scenarios are represented in four distinct models of one, tow, three, and six consecutive floor fields consecutively. The models are shown in Figure 5.5.

With the use of symmetry, a great emphasis has to be put on the boundary connections. The boundary connections are mainly determined by the stability systems and the 60 mm cavity between the modules. The steel stability frames (indicated in red in Figure 5.4) are assumed to only providing stability in their longitudinal direction. In other words, the stability frames in y direction restrict movement in the y directions, but allow for movement in x direction. The opposite goes for the stability frames in the x direction, which only restricts movement in x direction. Figure 5.6 shows only one sliding boundary condition for both the stability frames in x and y direction. A second boundary condition in the same direction at the opposite side of the stability frame is excluded, because adding an additional one will create clamping or tensioning of the floor elements, which could lead to ambiguity about where loads are transferred to, and can simulate inaccurate behaviour. The third boundary condition which makes the models with one, two, and three floor fields adequately constrained is established when the longitudinal floor beam of the right module comes into contact with the floor beam of the symmetrical counter side. As a result, all models have a maximum displacement of deformation of 30 mm halfway the longitudinal side of the damaged module. This because after 30 mm deformation of both symmetric sides, the total cavity of 60 mm between the two damaged modules is closed. This is displayed in Figure 5.5 as an offset, fixed, boundary halfway the modules length.

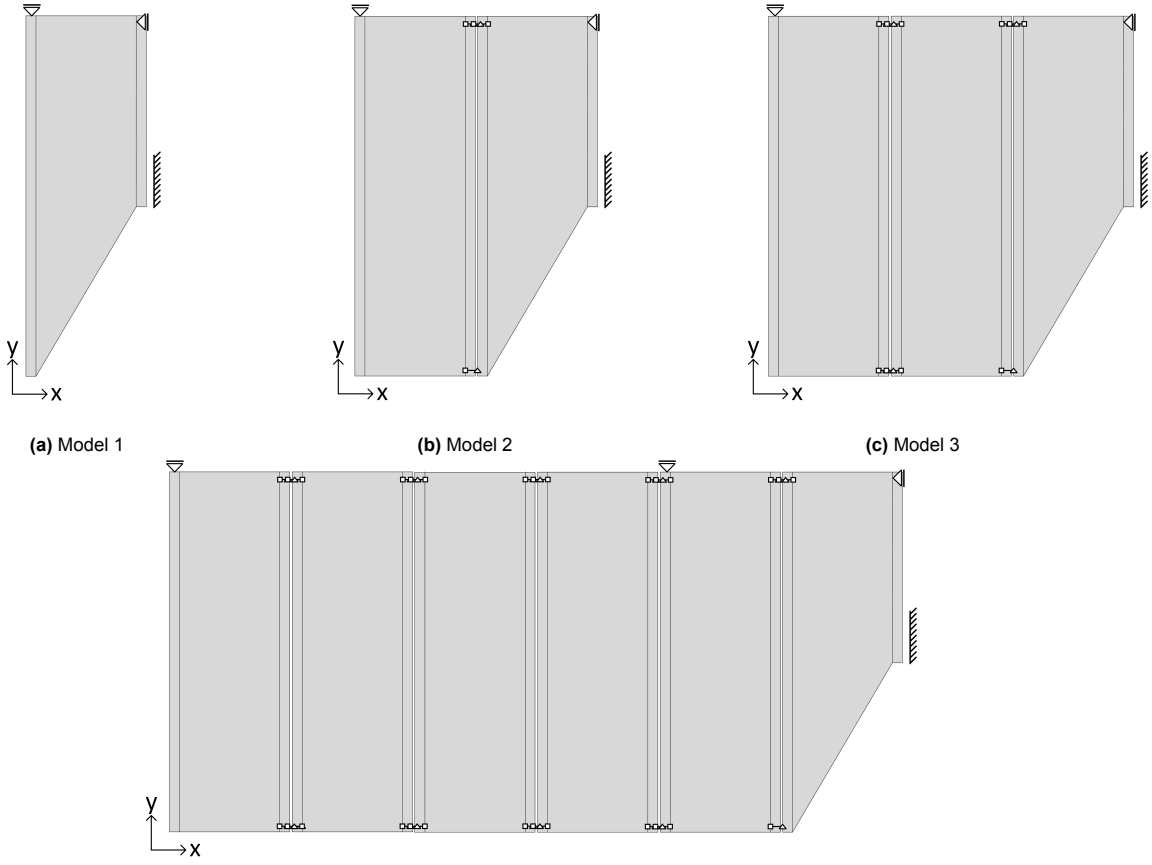

(a) Model 1 **(b)** Model 2 **(c)** Model 3

(d) Model 4

Figure 5.5: Models of floor systems with one, tow, three, and six floor fields

5.4. Analysis procedure

In models 1, 2, and 3, as described in Figure 5.5, the initial movement of the floor system is practically unconstrained until the cavity between the two modules above the failed column is closed. Only when the cavity is closed, the structure becomes stable with a third boundary condition. Until that moment, a force controlled numerical analysis cannot be performed. In order to create a determinate model, the analyses are performed in two load steps. In the first load step, a displacement controlled analysis is performed, with an assigned displacement of 30 mm in x-direction, on the location where the two modules will first make contact. 30 mm is half the cavity opening and assumes the other half of the structure will show a similar initial unconstrained movement. After the 30 mm displacement, the fist load step ends. At the start of second load step, the assigned displacement is converted into a sliding boundary constraint, allowing for movement in y-direction. Also in the second load step, a force controlled load is activated and increases linearly from load factor 0 to 1. An arbitrarily large force is taken which is in excess of the systems total capacity. Figure 5.6 shows the boundary conditions, connectors, interactions and loads in first and second load step.

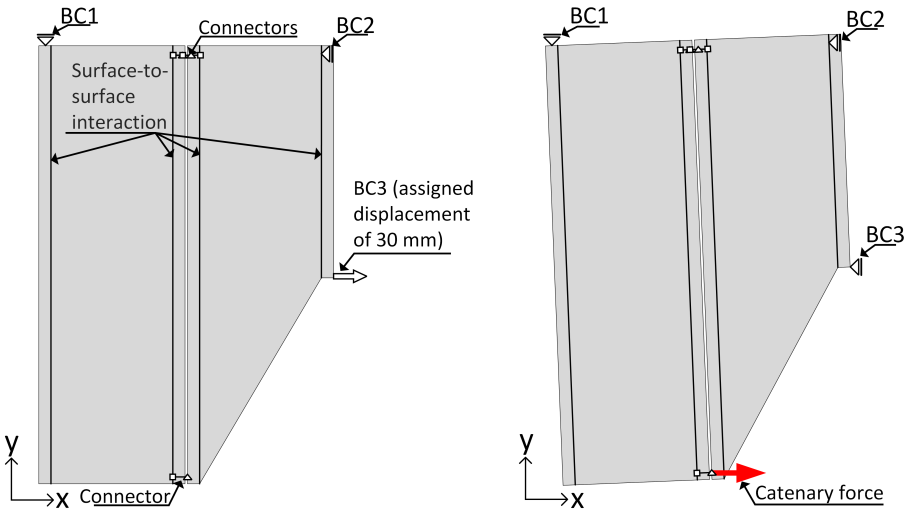

(a) Load step 1 **(b)** Load step 2

Figure 5.6: Abaqus model 2 with (a) depicting the model and boundary conditions at the start of the first load step, and the (b) depicting the model at the start of the second load step.

Model 4, as described in Figure 5.5, contains two stability frames in y-direction. The floor system is therefore constrained from any initial free movement and is statically determined. As a result, only one load step is required in which the catenary force can be excreted on the floors. This can be done in a force controlled manner. To potentially stop further displacement of the contact points between two modules, a row of elements is added to the model at 30 mm offset from the potential contact point. The elements have similar material properties as the GLT beam and are fully clamped in place, so no displacement is possible. Between the additional elements and the GLT beam of the outer module floor, a hard contact interaction property is assigned.

5.5. Material properties

Timber is an orthotropic material with different strengths and stiffnesses in longitudinal and transverse directions. These differences make timber a complex material to model. When using timber in an engineered product such as CLT, the differences are amplified due to the material being stacked in different directions. This section explains the essential aspects of modelling the material properties of CLT and GLT within the context of finite element analyses. And presents the material properties which are used in the current research.

5.5.1. CLT panel

Stiffness

Two main approaches stand out in literature for capturing the behaviour of CLT. The first approach recommends modelling CLT as an orthotropic equivalent plate. The second recommends employing a laminate action model to model each lamella with different material properties[47]. Both approaches are elaborated below.

Orthotropic plate model

CLT's characteristic cross-laminated configuration results in an anisotropic material behaviour, with mechanical properties varying significantly in the principal directions. To effectively represent this anisotropy, CLT is often modelled as an orthotropic plate in finite element simulations. As CLT panels are often considered as thick plates with interactions between shear deformations and rotational effect, the Mindlin-Reissner theory is applied to determine the material's mechanical properties in the longitudinal (L), transverse (T), and through-thickness (Z) directions [48]. By determining the appropriate material constants, including the modulus, Poisson's ratios, and shear moduli, the orthotropic plate model can accurately capture the elastic behaviour of CLT.

Laminate action model
The laminate action model is another widely adopted approach for simulating CLT behaviour, particularly in complex structural analyses. This model treats CLT as a composite laminate, composed of individual layers with distinct material properties determined by the Kirchhoff plate theory. The laminate action model considers the effects of adhesive bonding between the layers, offering a more sophisticated representation of the actual behaviour of CLT and allows for the analysis of behaviour within a plate. Through specifying the orientation and stacking sequence of the layers, the laminate action model enables anisotropic properties to be efficiently captured.

Modelling CLT as an orthotropic plate is a suitable approach for 2D in-plane finite element analysis due to the nature of the analysed problem. In 2D in-plane analyses, the primary focus is on understanding the structural behaviour of CLT within the plane of the panel, deeming the effects of out-of-plane behaviour negligible. Furthermore, this research does not try to analyse the behaviour within laminates such as rolling shear, or the shear interaction between the layers during out op plane bending. The orthotropic plate theory has been widely used and its accuracy and reliability in in-plane analyses has been established by numerous experimental tests and numerical simulations [49][50][51][47][52]. Therefore, this study also adopts the orthotropic plate theory for modelling the CLT panels.

Stiffness matrix
The overall stiffness matrix for orthotropic CLT plates can be described as the following [51]:

$$C_{CLT} = \begin{bmatrix} D_{11} & D_{12} & 0 & 0 & 0 & 0 & 0 & 0 \\ D_{21} & D_{22} & 0 & 0 & 0 & 0 & 0 & 0 \\ 0 & 0 & D_{33} & 0 & 0 & 0 & 0 & 0 \\ 0 & 0 & 0 & D_{44} & 0 & 0 & 0 & 0 \\ 0 & 0 & 0 & 0 & D_{55} & 0 & 0 & 0 \\ 0 & 0 & 0 & 0 & 0 & D_{66} & D_{67} & 0 \\ 0 & 0 & 0 & 0 & 0 & D_{76} & D_{77} & 0 \\ 0 & 0 & 0 & 0 & 0 & 0 & 0 & D_{88} \end{bmatrix} \tag{5.1}$$

Where:

$D_{11} - D_{33}$	Describing the bending and torsional properties
$D_{44} - D_{55}$	Describing the shear stiffness properties of the panel (out of plane)
$D_{66} - D_{88}$	Describing the shear stiffness properties of the panel (in plane)

Abaqus only allows for a more generic orthotropic stiffness matrix to be used as material property input, see Equation 5.2. This stiffness matrix does not take into account the bending and torsional properties and coupling of laminated materials. However, for the intended model assumptions in this research, no out-of-plane load will lead to major bending or torsion behaviour. Therefore, the exclusion of these properties from the stiffness matrix does not lead to considerable different behaviour of the plate in a 2D analysis. The orthotropic stiffness matrix input for Abaqus is as follows:

$$C_{CLT} = \begin{bmatrix} D_{1111} & D_{1122} & D_{1133} & 0 & 0 & 0 \\ D_{2211} & D_{2222} & D_{2233} & 0 & 0 & 0 \\ D_{3311} & D_{3322} & D_{3333} & 0 & 0 & 0 \\ 0 & 0 & 0 & D_{1212} & 0 & 0 \\ 0 & 0 & 0 & 0 & D_{1313} & 0 \\ 0 & 0 & 0 & 0 & 0 & D_{2323} \end{bmatrix} \tag{5.2}$$

Where:

$D_{111} - D_{3333}$	Describing the uni-axial stiffness properties and their interactions
$D_{1212} - D_{2323}$	Describing the shear properties in the xy, xz, and yz planes respectively

As only the in plane behaviour of the CLT panels is of interest, the out of plane stiffness properties, such as shear in the xz and yz plane are not taken into account. The same goes for the transverse stiffness in the z direction of the plane. Excluding the stiffness in z direction of the CLT panel will not cause a difference in the outcome of the analysis, as it is only a 2D analysis. The interaction between the axial stiffness in z direction and the in plane longitudinal and transverse strain (D_{1133}, and D_{2233}) is also excluded from the stiffness matrix because the Poisson's ratios are often assumed to be 0 in engineering practices [51]. The stiffness properties for the input in Abaqus are determined according to the Swedish calculation methods [51]:

$$D_{1111} = E_{0,mean} * h_x \tag{5.3}$$

$$D_{2222} = E_{0,mean} * h_y \tag{5.4}$$

$$D_{1122} = \nu_{xy} * D_{1111} \tag{5.5}$$

$$D_{1133} = \nu_{xz} * D_{1111} \tag{5.6}$$

$$D_{2233} = \nu_{yz} * D_{2222} \tag{5.7}$$

$$D_{3333} = E_{90,mean} * h_{CLT} \tag{5.8}$$

$$D_{1212} = G_{s,mean} * h_{CLT} \tag{5.9}$$

$$D_{1313} = \kappa_x * G_{0,mean} * h_{CLT} \tag{5.10}$$

$$D_{2323} = \kappa_y * G_{0,mean} * h_{CLT} \tag{5.11}$$

Where:

$E_{0,mean}$	Mean value of modulus of elasticity, parallel to the grain
$E_{90,mean}$	Mean value of modulus of elasticity, perpendicular to the grain
$G_{0,mean}$	Mean shear modulus of a timber board
$G_{s,mean}$	Mean shear modulus of the cross section of the CLT panel (See Annex B)
ν_{xy}, ν_{xz}, ν_{yz}	In plane Poisson's ratios of the CLT panel
κ_x, κ_y	Out of plane shear correction factors of the slab
h_x	Total height of lamellas in the x direction of the CLT panel
h_y	Total height of lamellas in the y direction of the CLT panel
h_{CLT}	Total height of the CLT panel

The characteristic stiffness properties of CLT with strength graded timber class C24 are given in Table 5.2, and the stiffness components of the orthotropic stiffness matrix of Equation 5.2 are given in Table 5.3.

Table 5.2: Characteristic properties of a CLT panel with timber strength class C24

Properties	Symbol	Value	Unit
Strength			
Bending strength	$f_{m,k}$	24	N/mm^2
Tension strength along the grain	$f_{t,0,k}$	14.5	N/mm^2
Tensile strength perpendicular to the grain	$f_{t,90,k}$	0.4	N/mm^2
Compressive strength along the grain	$f_{c,0,k}$	21	N/mm^2
Compressive strength perpendicular to the grain	$f_{c,90,k}$	2.5	N/mm^2
Shear strength	$f_{v,k}$	4	N/mm^2
Stiffness			
Mean value of modulus of elasticity, along the grain	$E_{0,mean}$	11000	N/mm^2
Mean value of modulus of elasticity, perpendicular to the grain	$E_{90,mean}$	0	N/mm^2
Mean shear modulus	$G_{0,mean}$	690	N/mm^2
Density			
Fifth percentile volume of density	ρ_k	350	kg/m^3
Mean density	ρ_{mean}	420	kg/m^3

Table 5.3: The stiffness components of the orthotropic stiffness matrix for Abaqus

Stiffness component	Value [N/m]	Stiffness component	Value [N/m]]
D_{1111}	$1.320e+9$	D_{3333}	0
D_{1122} = D_{2211}	$1.320e+9$	D_{1212}	$9.188e+7$
D_{2222}	$4.400e+8$	D_{1313}	$1e+12$
D_{1133} = D_{3311}	0	D_{2323}	$1e+12$
D_{2233} = D_{3322}	0		

Strength capacity and damage evolution

As mentioned before, timber is a predominantly linear elastic material with brittle failure mode in longitudinal direction. In transverse direction timber can be described as having more ductile attributes. However, in this study, boards are not glued on their sides, meaning that no tensile forces can be sustained in the transverse layered lamellas. Moreover, for this analysis, a brittle failure mode is assumed in compression as well. Therefore, only linear material properties for CLT and GLT are assigned with a brittle failure mode. Khorsandnia et al. [53] and Lavrenčič and Brank [54] showed that for modelling of CLT panels, the Hashin failure initiation criteria can be used to describe the point of onset of material damage. The Hashin damage model was initially developed to be used on unidirectional polymeric composite materials. It takes into account the interaction between shear and normal stresses to determine failure modes in tension, compression, and shear in the directions parallel and perpendicular to the fibers. Khorsandnia et al. first proved that the Hashin model could also be used in other non-polymeric composites, such as CLT, under bi-axial stress states [53]. The design values of the strength

properties in the principal directions of the CLT panels are presented in Table 5.4. Because the sides of the timber boards are not connected, the primary tension and compression forces can only transfer through the boards with fibers in the parallel direction. Consequently, the principal strength components are based on the layup of the CLT panel.

The design value of the strength properties are calculated according to Equation 5.12 and Equation 5.13.

$$f_d = k_{mod} * \prod k_i * \frac{f_k}{\gamma_M} \tag{5.12}$$

$$R_d = k_{mod} * \frac{R_k}{\gamma_M} \tag{5.13}$$

Where: f_k and R_k are the characteristic material strength properties, k_{mod} is the modification factor to take into account the effect of the duration of the load and the moisture content, γ_M the partial material factor for timber, and $\prod k_i$ the product of supplementary material factors. For CLT panels in service class 1, subjected to an ALS load situation, with an instantaneous load application, k_{mod} = 1.1 and γ_M = 1.0 [43].

Table 5.4: Design values of strength properties of CLT panel with timber strength class C24

Property	Symbol	Value	Symbol
Tensile stress cross direction (x-axis)	$f_{t,x,d}$	13.76	N/mm^2
Compressive stress cross direction (x-axis)	$f_{c,x,d}$	17.33	N/mm^2
Tensile strength longitudinal direction (y-axis)	$f_{t,y,d}$	4.59	N/mm^2
Compressive strength longitudinal direction (y-axis)	$f_{c,y,d}$	5.78	N/mm^2
Shear strength	$f_{v,xy,d}$	4.40	N/mm^2

In order to model the longitudinal and transverse tensile and compressive brittle failure modes, the respective fracture energy envelopes are assumed to be 0. In other words, the material is assumed to have completely failed when the design values of the strength properties have been reached.

Note: Timber, and CLT, do not have a perfect brittle failure mode in tension, and have a ductile failure mode in compression. For a more accurate model of the CLT plate, continuum damage mechanics can be added to the model to simulate the progressive degradation of the material. However, as wood has many different failure modes, e.i. fiber rupture in tension, fiber buckling in compression, matrix failure due to transverse loads, etc, many different continuum damage mechanics have to be known [55]. This research did not allow for real live testing of the model in a test lab. Moreover, no other test have been done on a similar scale for in plane loading. Therefore, for this research it was only possible to validate the final Abaqus model against simple hand calculations. In order to determine if the model behaves as expected, a relatively simple material model has been used.

5.5.2. GLT beams

Equal to the CLT panels, the GLT beams are modelled as orthotropic linear elastic, with brittle failure modes in tension and compression in longitudinal and transversal directions. However, where CLT panels have wood fibers in longitudinal and cross direction, the wood fibers in GLT beams all orientate in the longitudinal direction only. As the longitudinal and transverse elasticity moduli $E_{0,mean}$ and $E_{90,mean}$ now apply over the entire height, width, and length of the elements, the stiffness matrix can be determined by use of the engineering constants as shown in equation 5.14 [56]. Similar to the stiffness matrix for the 2D CLT panels, the engineering constants related to the z-axis are excluded.

$$C_{GLT} = \begin{bmatrix} \frac{1}{E_1} & \frac{-\nu_{21}}{E_2} & \frac{-\nu_{31}}{E_3} & 0 & 0 & 0 \\ \frac{-\nu_{12}}{E_1} & \frac{1}{E_2} & \frac{-\nu_{32}}{E_3} & 0 & 0 & 0 \\ \frac{-\nu_{13}}{E_1} & \frac{-\nu_{23}}{E_3} & \frac{1}{E_3} & 0 & 0 & 0 \\ 0 & 0 & 0 & \frac{1}{G_{12}} & 0 & 0 \\ 0 & 0 & 0 & 0 & \frac{1}{G_{13}} & 0 \\ 0 & 0 & 0 & 0 & 0 & \frac{1}{G_{23}} \end{bmatrix} \tag{5.14}$$

The characteristic stiffness properties of GLT beams with strength graded timber class C24 are presented in Table 5.5 and the engineering constants for the orthotropic stiffness matrix in Abaqus in Table 5.6. The Hashin failure initiation criterion is again used for the GLT beam. The design values of the strength properties in the different directions are given in Table 5.7. And again, the fracture energy envelopes are assumed to be 0 in order to be able to validate the Abaqus model with hand calculations.

Table 5.5: Characteristic properties of a GLT beam with timber strength class C24 according to EN 14080 [57]

Properties	Symbol	Value	Unit
Strength			
Bending strength	$f_{m,g,k}$	24	N/mm^2
Tension strength along the grain	$f_{t,0,g,k}$	19.2	N/mm^2
Tensile strength perpendicular to the grain	$f_{t,90,g,k}$	0.5	N/mm^2
Compressive strength along the grain	$f_{c,0,g,k}$	24	N/mm^2
Compressive strength perpendicular to the grain	$f_{c,90,g,k}$	2.5	N/mm^2
Shear strength	$f_{v,g,k}$	3.5	N/mm^2
Stiffness			
Mean value of modulus of elasticity, along the grain	$E_{0,g,mean}$	11500	N/mm^2
Mean value of modulus of elasticity, perpendicular to the grain	$E_{90,g,mean}$	300	N/mm^2
Mean shear modulus	$G_{g,mean}$	650	N/mm^2
Density			
Fifth percentile volume of density	$\rho_{g,k}$	350	kg/m^3
Mean density	$\rho_{g,mean}$	420	kg/m^3
Poisson's ratio	ν_{xy}	0.359	

Table 5.6: The engineering constants for the orthotropic stiffness matrix of the GLT beam for Abaqus

Engineering constant	Value	Unit	Engineering constant	Value	Unit
E_1	$1.15e+10$	[N/m]	ν_{23}	0	
E_2	$3.00e+8$	[N/m]	G_{12}	$6.50e+8$	[N/m]
E_3	$1e+12$	[N/m]	E_{13}	$1e+12$	[N/m]
ν_{12}	0.359		G_{23}	$1e+12$	[N/m]
ν_{13}	0				

Table 5.7: Design values of strength properties of GLT beam with timber strength class C24

Property	Symbol	Value	Symbol
Tensile strength longitudinal direction	$f_{t,0,g,d}$	21.12	N/mm^2
Compressive strength longitudinal direction	$f_{c,0,g,d}$	26.40	N/mm^2
Tensile strength cross direction	$f_{t,90,g,d}$	0.55	N/mm^2
Compressive strength cross direction	$f_{c,90,g,d}$	29.70	N/mm^2
Shear strength	$f_{v,090,g,d}$	3.85	N/mm^2

5.6. Inter-module connection properties

The resultant stiffness from the analysis, focusing on the deformation of the floor under catenary loads, will be integrated in a 2D frame model of the case study building in Chapter 6. To prevent double counting of the stiffness of the inter-module connections in the frame models, connectors which are also present in the frame model are assumed to possess infinite axial stiffness. Connectors not included in the frame analysis are given the properties of the proposed connector model outlined in Section 4.1. The axial spring stiffness of the components are given presented in Table 4.1. The stiffness value of the outer inter-module connectors, representing the screw group and tie plate, is 6.88E+04 kN/m. The corresponding maximum resistance is 108.9 kN, and the total deformation is 1.58 mm. The axial spring stiffness of the intermediate connector, representing the coupling plate, is 6.30E+06 kN/m. This connector is not given a maximum resistance as it much larger than the resistance of the tie plate and screw group and failure is excluded.

5.7. Connection properties between CLT panel and GLT beams

The GLT beams are connected to the GLT panels with crosswise inclined screw pairs, evenly distributed over the length of the contact surface. The screw connection is depicted in Figure 5.7. When the displacement and force load are applied on the floor models, the beams and slabs will exert a load on each other in two directions. Due to the beams and panels being pushed together on one side of the panel, and being pulled apart on the other side, pressure and tension stresses are exerted perpendicular to the contact surface between the beams and the panels. Furthermore, due to the cantilever motion of the floor, the beams and panels will try to slide along each other, exerting a shear force parallel to the contact surfaces. An overview of the stresses is given in Figure 5.7. Incorporating the slip and opening stiffnesses included in the intra-module connections results in larger in-plane deformations and presents a more realistic model. Therefore it is important to include the slip- and opening modulus properties of the connections in the model. Moreover, reaching the maximum slip- or opening stress limit in the screw connections is a realistic failure mode, and can dictate the maximum catenary force allowed in the modular floor systems.

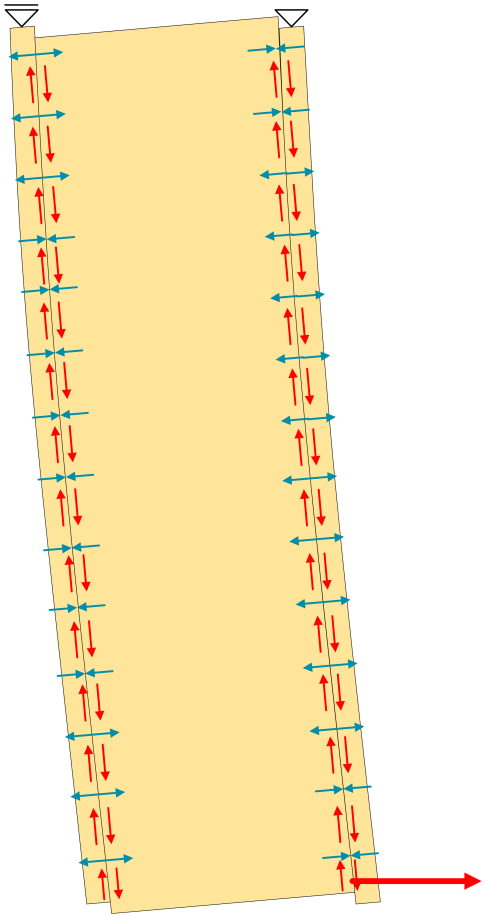

Figure 5.7: Stress distribution parallel and perpendicular to the contact surface between GLT beams and CLT panel.

The shear and normal slip modulus, and the maximum resistances of the intra-module screw connection is given in Table 5.8. Detailed calculations on how these values are obtained are given in C.

Table 5.8: Connection properties per meter of screw connection between GLT beams and CLT panels

Load direction	**Slip modulus** $[N/m * (\frac{1}{m})]$	**Maximum load** $[N * (\frac{1}{m})]$
Parallel to contact surface (Shear)	$8.94e+6$	$8.69e+4$
Perpendicular to contact surface (normal)	$1.09e+8$	$1.84e+5$

5.8. Finite elements

In order to determine the in-plane behaviour of the floor system due to catenary forces, a numerical 2D model is created in Abaqus. The CLT slabs and GLT beams are modelled with linear solid plane stress elements (CPS4R) and linear elastic material properties as given in section 5.5. The size of the elements is approximately 1/10 of the short span of the floors, resulting in elements of 303x315 mm for the CLT panels. This makes the elements twice the size of the load ingress point, eliminating any local deformations due to stress concentrations around the point load. The GLT beams will undergo in-plane bending, resulting in tension and compression stresses being simultaneously present in the cross-section. In order to display both the tension and compression stresses, the beams are modelled with two elements over their widths, resulting in element sizes of 303x120 mm. The inter-module connections are modelled with standard connector elements CONN2D2 for two-dimensional and axisymmetric analyses. Two connectors are displayed in Figure 5.8 by an orange square as the begin point and a yellow triangle the end point of the connector wire. They are rigidly connected to

the CLT slab elements, because the connection transfers loads directly from one CLT slab to the other. At load ingress point, the catenary force acts directly on the outer part of the GLT beam. From there on, a part of the load is directly transferred to the consecutive CLT slab. The interaction between the CLT slabs and the GLT beams is modelled as a surface-to-surface contact interaction with linear elastic cohesive stiffness and brittle failure properties as described in Section 5.7. The elements, inter-module connectors, and translatable boundary conditions are shown in Figure 5.8.

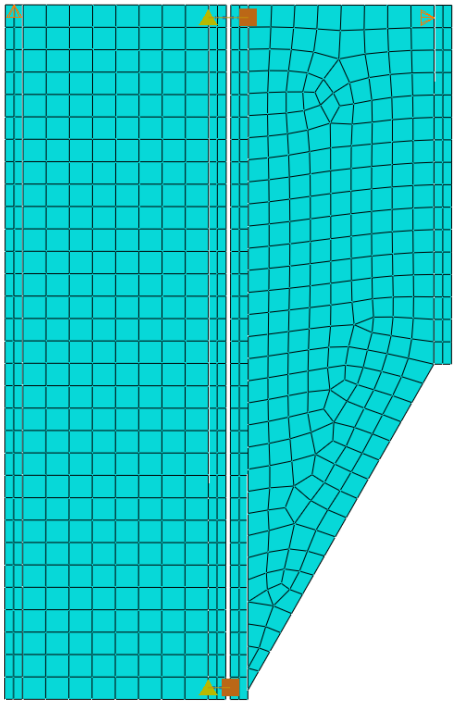

Figure 5.8: Two meshed floor fields, with the connector elements and boundary conditions from the first load step, in the Abaqus environment.

5.9. Validation of the model parameters

The material properties and connection properties, determined in Section 5.5 and section 5.7 will be used as input in the Abaqus model. However, before the model can be ran, and results obtained, first the input parameters in the software have to be validated.

5.9.1. Floor field behaviour and material properties

To validate the material input parameters and the general behavior of the modelled floor fields, a simplified floor is numerically modelled and analytically validated. This simplified floor comprises a CLT panel and two rigidly connected GLT beams. While resembling the floor configurations employed in the case study models, this simplified model excludes the intra-module connection properties between the CLT panel and the GLT beams. This approach is adopted to allow for the use of conventional calculation methods in the analytical assessments. In the validation test, one short side of the floor is fully clamped, and a 100 kN point load is applied on the other short end as illustrated in Figure 5.9. This allows to check if the resulting in-plane deflection from Abaqus align with analytical calculations.

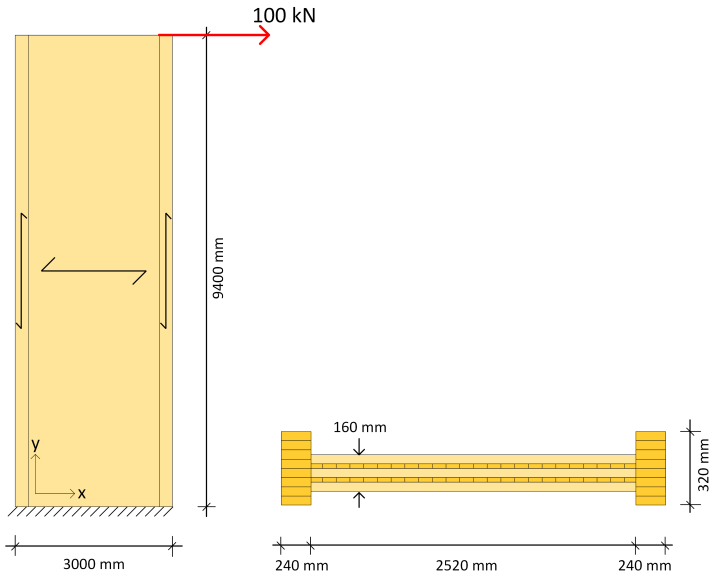

Figure 5.9: Validation model with a floor field clamped at the bottom and a 100 kN force on the top right.

The load causes the floor to deform due to shear and bending stresses. The maximum deflection due to these stresses can be calculated separately by Equations 5.15 and 5.16 respectively. Added up, they determine the total deflection as described in Equation 5.17 [51].

$$\delta_{shear} = \frac{F * h}{b * t * G_{mean}} \tag{5.15}$$

$$\delta_{bend} = \frac{F * h^3}{3 * E_{mean} * I} \tag{5.16}$$

$$\delta_{total} = \delta_{shear} + \delta_{bend} \tag{5.17}$$

The analytically calculated deflections for shear, bending, and the total deflection are given in Table 5.9 and are illustrated in Figure 5.10.

Table 5.9: Analytically calculated maximum deflections of a simple clamped floor field with a 100 kN load.

Shear deflection	2.84 mm
Bending deflection	6.99 mm
Total deflection	9.83 mm

In order to determine the maximum deflection in the numerical model due to bending stresses only, elements in the stiffness matrices corresponding to shear are increased to an approximately infinite number. This makes the shear stiffness of the CLT panel and GLT beams infinitely high, and ensures no deformation due to shear can occur. In order to determine the deflection due to shear stresses only, elements in the stiffness matrices corresponding to shear are increased to an approximately infinite number. For both situations the input for the stiffness matrices is given in Table 5.10 and Table 5.11.

Table 5.10: Stiffness matrix input for exclusive shear in the CLT panel and GLT beams

Stiffness Matrix CLT		Stiffness Matrix GLT		
Stiffness component	**Value [N/m]**	**Engineering constant**	**Value**	**Unit**
D_{1111}	$1e+12$	E_1	$1e+14$	[N/m]
D_{2211} = D_{1122}	0	E_2	$1e+12$	[N/m]
D_{2222}	$1e+12$	E_3	$1e+12$	[N/m]
D_{1133} = D_{3311}	0	ν_{12}	0.359	
D_{2233} = D_{3322}	0	ν_{13}	0	
D_{3333}	0	ν_{23}	0	
D_{1212}	$9.19e+7$	G_{12}	$6.50e+8$	[N/m]
D_{1313}	$1e+12$	G_{13}	$1e+12$	[N/m]
D_{2323}	$1e+12$	G_{23}	$1e+12$	[N/m]

Table 5.11: Stiffness matrix input for exclusive bending in the CLT panel and GLT beams

Stiffness Matrix CLT		Stiffness Matrix GLT		
Stiffness component	**Value [N/m]**	**Engineering constant**	**Value**	**Unit**
D_{1111}	$1.32e+9$	E_1	$1.15e+10$	[N/m]
D_{2211} = D_{1122}	0	E_2	$3.00e+8$	[N/m]
D_{2222}	$4.40e+8$	E_3	$1e+12$	[N/m]
D_{1133} = D_{3311}	0	ν_{12}	0.359	
D_{2233} = D_{3322}	0	ν_{13}	0	
D_{3333}	0	ν_{23}	0	
D_{1212}	$1e+12$	G_{12}	$1e+12$	[N/m]
D_{1313}	$1e+12$	G_{13}	$1e+12$	[N/m]
D_{2323}	$1e+12$	G_{23}	$1e+12$	[N/m]

The maximum deflections due to exclusive bending, exclusive shear, and the total deflection, from the analytical calculations and the numerical model are shown in Figure 5.10 and Figure 5.11 respectively. It can be seen that the results align with each other, indicating that the material input has been verified against the anticipated outcomes.

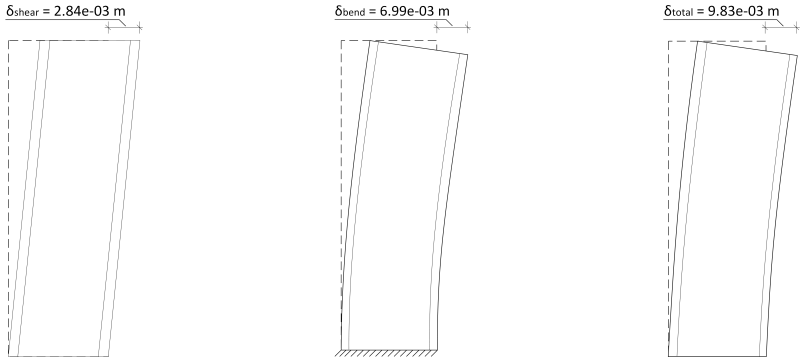

(a) Deflection due to shear **(b)** Deflection due to bending **(c)** Total deflection

Figure 5.10: Analytically calculated maximum deflection and the deformed shape of the validation model

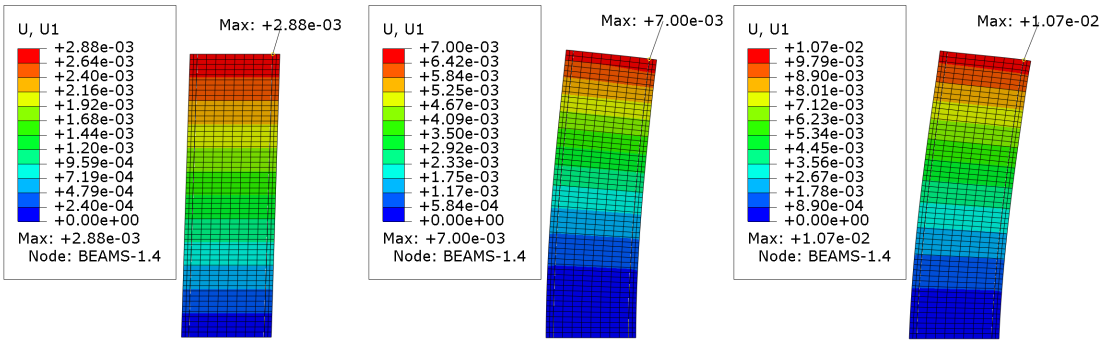

(a) Deflection due to shear **(b)** Deflection due to bending **(c)** Total deflection

Figure 5.11: Numerically determined maximum deflection and the deformed shape of the validation model

5.9.2. Shear and normal behaviour validation of screw connection

Having validated the model for the material properties, now the model input for the connections are validated. The screwed fasteners pairs are placed at a 150 mm interval. This is larger than the approximate 300x300 mm mesh size used in the floor model. It is therefore impractical to model the connections as individual springs between the nodes of the beams and the CLT panels. Instead, the connection properties are incorporated as surface-to-surface contact interactions with the corresponding constitutive properties per running meter. No literature, or examples were found where a similar approach was applied. Therefore the model parameters had to be validated.

In Section 5.7 and Annex C the shear and normal slip modulus and maximum resistance are determined for the crosswise inclined screw connections. In order to assess if these input values for the slip and opening moduli and maximum resistance can correctly be modelled, the maximum slip and opening will be analytically calculated and subsequently numerically validated. As the connection properties are assumed linear elastic, with no plastic damage behaviour, the maximum slip and opening can be determined by dividing the slip and opening modulus per running meter by the maximum resistances. The resulting slip and opening values are presented in Table 5.12.

Table 5.12: Analytically calculated maximum slip and opening values for the screwed connection between the GLT beam and CLT panel.

Load direction	**Max slip/opening [m]**
Parallel to contact surface (shear)	$9.72e-3$
Perpendicular to contact surface (normal)	$1.70e-3$

To test if the properties can correctly be modelled, two distinct linear elastic Abaqus models are created. Both models are showed in Figure 5.12 and test the maximum slip or opening in the corresponding directions. The two bodies which have to shear along, or be pulled apart from each other, are modelled as rigid. The sliding boundaries are positioned perpendicular to the contact surface and parallel to the load, so only displacements in either the transverse or normal direction is possible.

The surface-to-surface interaction was modelled with cohesive mechanical contact properties, damage evolution behaviour based on the maximum nominal stresses, and hard contact normal behaviour. The cohesive mechanical property option allows for specific, uncoupled, traction-separation behaviour to be used as input. In Abaqus, the traction-separation model is based on the assumption of linear elastic behaviour, followed by the initiation and evolution of damage. This elastic response is expressed through an elastic constitutive matrix that correlates normal and shear stresses to the respective normal and shear separations along the interface [58]. For the uncoupled stiffness coefficients from the constitutive matrix, the stiffness values from Table 5.8 are used. Regarding the damage initiation, it is important to note that the maximum nominal stresses refer to the stress level where degradation of the cohesive response starts. In this case these stress values coincide with the maximum resistance val-

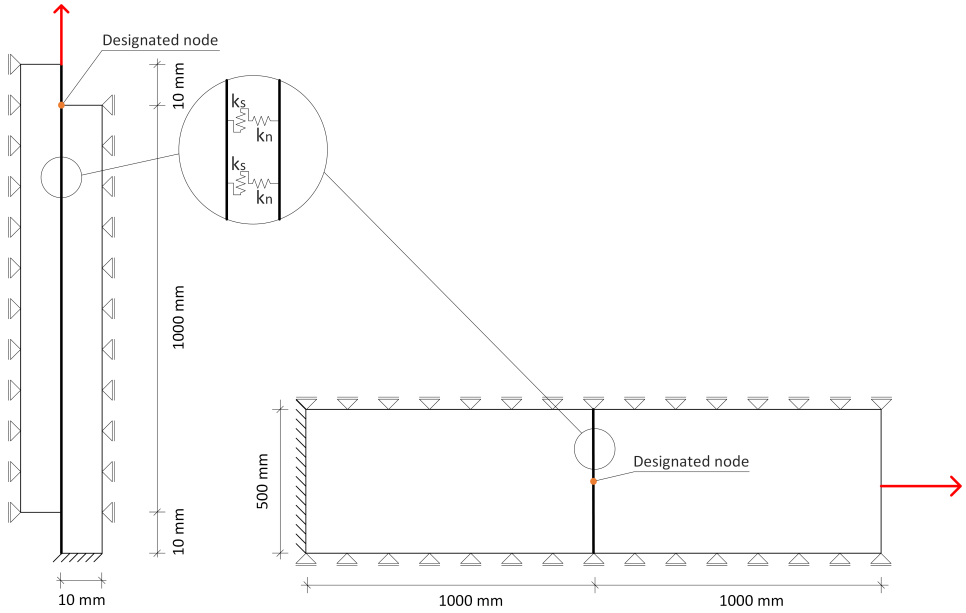

Figure 5.12: Validation models for the shear and normal tension stiffness and maximum resistance of the screw connection between the GLT beam and CLT panel

ues presented in Table 5.8. The damage evolution is set to have zero plastic displacement, simulating absolute brittle behaviour.

Running the models with a sufficiently high load causes the model to abort when the maximum stress is reached. The slip and opening values in the designated nodes are plotted against the stresses and displayed in Figure 5.13b. The maximum stress and slip values from the numerical model are presented in Table 5.13 and resemble the analytically calculated slip and opening values from Table 5.12. The model parameters are therefore valid.

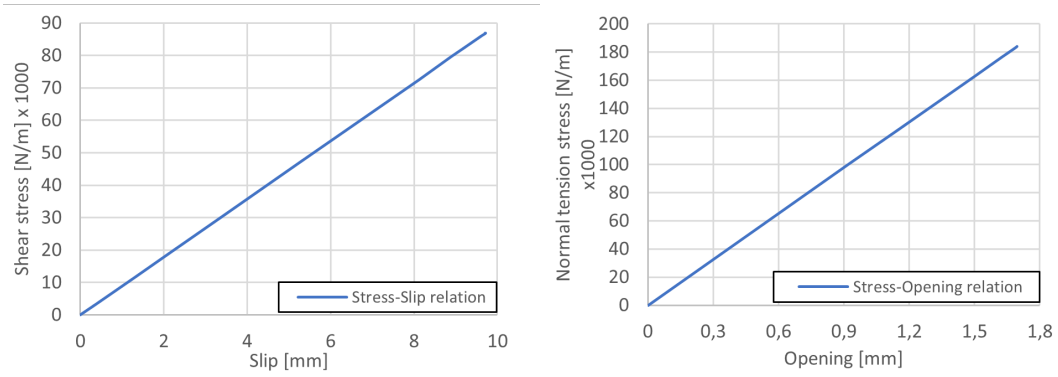

(a) Shear stress - slip relation

(b) Normal tension stress - opening relation

Figure 5.13: Constitutive behaviour of the screw connection, showing the stress against the slip/opening relations from the Abaqus environment.

Load direction	Maximum stress [N/m]	Maximum slip/opening [m]
Parallel to contact surface (shear)	$8.69e+4$	$9.72e-3$
Perpendicular to contact surface (normal)	$1.84e+5$	$1.70e-3$

Table 5.13: Connection properties per meter of screw connection between GLT beams and CLT panels from the Abaqus environment.

5.10. Discrete timber floor analysis results

This section presents the results of the numerical analyses on discrete timber floor systems subjected to catenary loads. The obtained results display the in-plane deformation, maximum resistance, and load redistributive behaviour of the four distinct floor models.

Numerical analyses were conducted on models featuring one, tow, three, and six consecutive discrete floor fields. The objective was to investigate variations in results when catenary loads have the potential to redistribute across multiple floor fields and stability systems. For each analysis, the deformation is plotted against the catenary load, specifically at the location where the catenary load is applied. Additionally, for each model, a detailed examination of the failure mode at the initiation of progressive damage is undertaken.

5.10.1. Load-displacement

Model 1

In plane stiffness development

In model 1, representing one floor field, the catenary force acts directly on the outer side of the intact beam, as indicated by the black arrow in Figure 5.14. Figure 5.14 shows the displaced situation of the floor at onset of progressive failure. The relation between the catenary load and the displacement in x-direction is given in Figure 5.15. The location where the displacement data is collected is the same node as where the load is positioned on the floor.

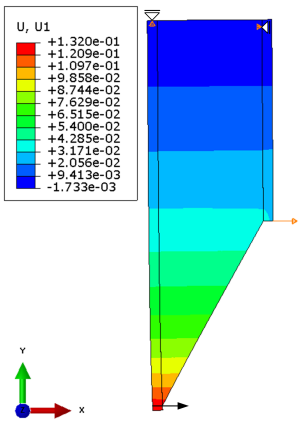

Figure 5.14: Deformed state at onset of failure of model 1

From the force-displacement data it can be seen that the first 58 mm of displacement is met with zero stiffness. In other words, no resistance through catenary action is activated and the structure is unstable. The free displacement occurs, because initially the floor does not have sufficient boundary conditions to create a stable structure. Only after the floor makes contact with a consecutive floor, and when the cavity between two modules is closed, catenary loads can be redistributed.

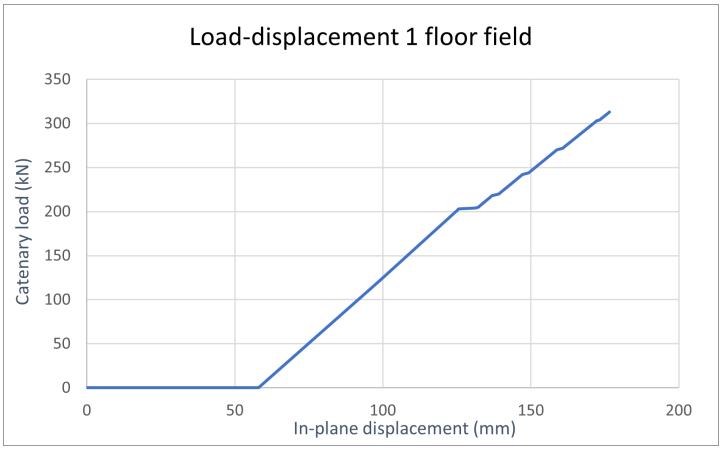

Figure 5.15: Catenary load against the deformation in x-direction of model 1

From the moment the cavity is closed, the resistance against the catenary force increases linearly with the displacement. This is because all elements and materials in the model are still in their linear elastic phase. The stiffness value corresponding to the slope of the load displacement curve is 2985 kN/m. The linear behaviour goes on until a sudden jump in the load displacement curve at 203 kN. The corresponding displacement at that point is 126 mm.

Onset of progressive failure
The sudden increase in displacement at 203 kN indicates that local failure or plastic deformation has occurred. Upon further investigation it turns out that the connection between the GLT beam and the CLT panel starts to fail at the point where the CLT panel tapers to a point. At a load of 203 kN, the shear force between the beam and the panel reaches its maximum resistance of 86.9 kN/m. Because the connection fails only locally and the analysis is only 2D, more resistance is found further along the beam-to-panel interface. At larger loads, an increasing number of sections along the interface reach the maximum shear resistance. This can also be seen by the consecutive jumps in the load-displacement graph of Figure 5.15. The analysis stops when the entire beam is disconnected from the panel.

Despite the potential existence of further in-plane resistance elsewhere in the structure, upon the onset of failure in the beam-to-panel connection, it is assumed that a point of progressive failure has been reached. This because vertical loads on the CLT panel cannot be resisted any longer when the connection with the beam has failed and further out-of-plane behaviour cannot be assessed in the 2D analysis. It is therefore assumed that after the initial beam-to-panel connection failure, progressive collapse becomes inevitable, marking the point at which the maximum catenary load is achieved

Model 2
In plane stiffness development
In model 2, with two consecutive floor fields, the catenary load is positioned at the same location as for the model with one floor panel. The same point is also the starting point of the connection with the consecutive floor field. Figure 5.16 shows the displaced situation of the two floor fields at the point of progressive failure.

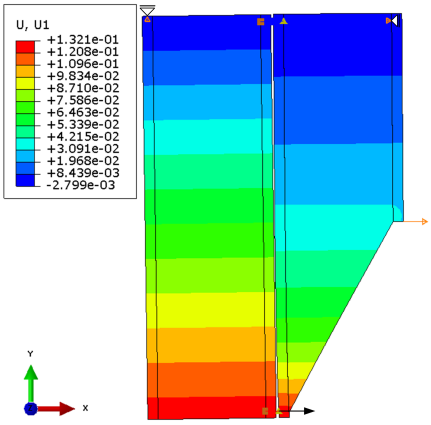

Figure 5.16: Deformed state at onset of failure of model 2

Figure 5.17 presents the load displacement graph of the two floor field model. Similar to the results of the single floor field model, the first 58 mm displacement are met with zero resistance from the system. This should come as no surprise as the boundary conditions are identical and an initial non-resisted displacement occurs until the cavity with the subsequent module is closed. From there the resisted catenary load increases linearly to the displacement with a stiffness of 2985 kN/m until a catenary load of 203 kN is reached. The behaviour of the model with two floor fields is identical to the model with one floor field.

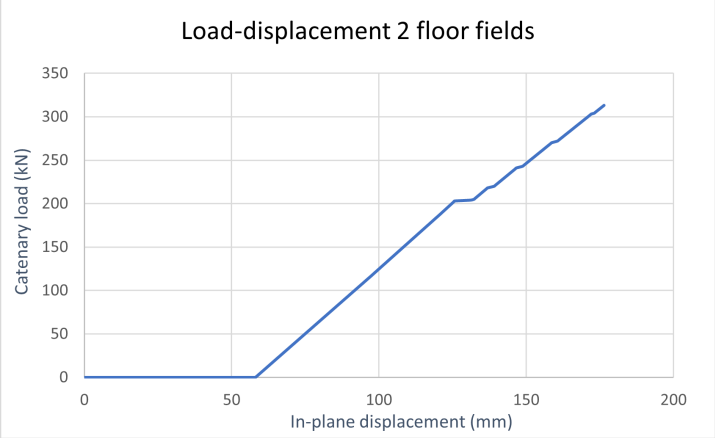

Figure 5.17: Catenary load against the deformation in x-direction of model 2

Onset of progressive failure

Similar to the model with one floor field, a sudden jump in displacement occurs. Upon further analysis it was determined that a similar failure occurred in the beam-to-panel connection, at the location where the panel tapers to a point. Further progression of failure and possible collapse is assumed to takes place from then on. The jump in displacement at 203 kN indicates the maximum resistance of the two modular floor fields against in plane catenary loads.

Model 3

In plane stiffness development

Model 3, with three floor fields, is very similar to the previous two models. Figures 5.18 and 5.18 show the deformed state and the load displacement graph at the same location of load ingress as for the previous models. The behaviour is again identical, with an initial unrestrained displacement of 58 mm followed by a linear load-displacement response. Onset of failure occurs again at 203 kN of catenary load and 126 mm displacement.

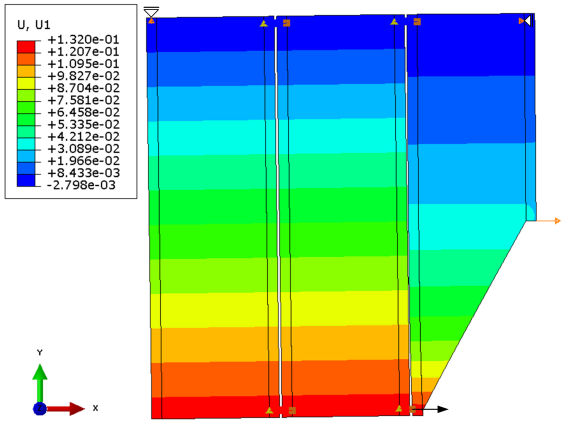

Figure 5.18: Deformed state at onset of failure of model 3

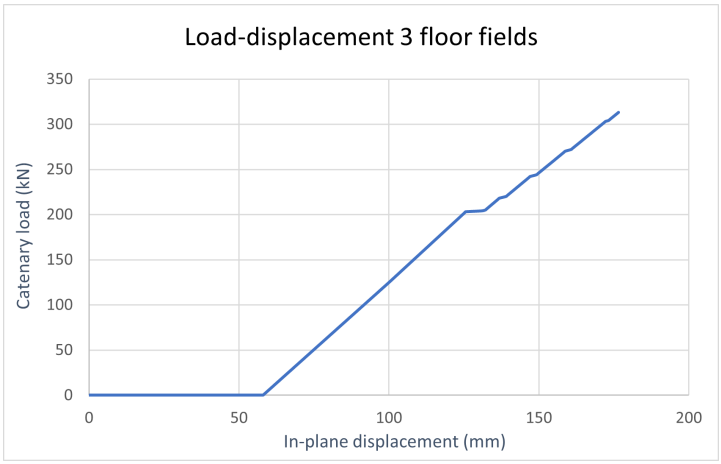

Figure 5.19: Catenary load against the deformation in x-direction of model 3

Model 4

In plane stiffness development

In model 4, representing six consecutive floor fields, the catenary load has the same point of ingress. Figure 5.20 displays the deformation in x direction at the maximum resistance of the floor system.

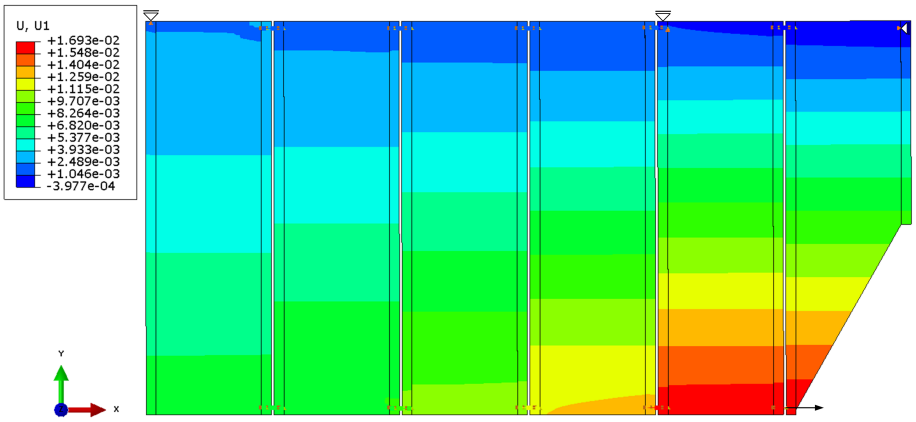

Figure 5.20: Deformed state at onset of failure of model 4

The load displacement graph of Figure 5.21 shows a linear behaviour without any initial free movement. The stiffness value equals 7403 kN/m and the maximum resistance of the floor system is 110 kN. The total elastic displacement is equal to 15 mm.

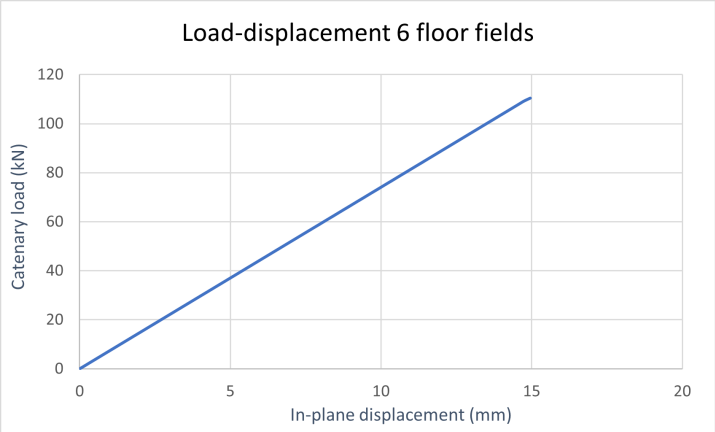

Figure 5.21: Catenary load against the deformation in x-direction of model 4

Onset of progressive failure
The analysis is stopped at the moment the first non-rigid connector reached its maximum resistance. Failure occurs due to the limited tension resistance of the net cross section area of the tie plate. Once the connection fails, catenary action becomes impossible, resulting in structural failure.

5.10.2. Load transfer

Looking at the distribution of in-plane principal stresses provides a better understanding of the load transfer mechanism. Figures 5.22 and 5.23 project the in-plane principal stress distribution in model 2 and 4. Both projections are made at the moment of failure. Models 1 and 3 are not assesses as they exhibit an identical behavior to that of Model 2.

Model 2

In Figure 5.22 it can be seen that almost all catenary loads are directly transferred along two paths. The first is in compression along the diagonal failure line to the contact point between the two damaged modules. The compression stress is met with a reaction force of 406 kN at the point of contact in the x direction. This is twice the value of the catenary load. The second path is in tension through the floor beam and panel, to the boundary condition at the other side of the module. Here the tension stress makes equilibrium with a tensile reaction force of 203 kN in x direction. From Figure 5.22 it can also be seen that almost no load is transferred to the left consecutive floor field. The only load transfer results from small shear stresses in the inter-module connection. The reaction force in the boundary condition in y-direction is 25 N. The catenary loads are thus in equilibrium through a compressive strut which makes contact with the consecutive module in the symmetric plane. Identical behaviours occur in the models with one and three floor fields.

Model 4

Upon inspection of the in-plane principal stresses of the model with six floor fields in Figure 5.23, a distinct area of tension stresses is identified along the short side of the modules from where the catenary load is applied. The observed tension stresses diminish over distance, indicating a portion of the load is transferred in shear. This distribution of stresses through shear is indicative of the diaphragm action in the floor fields. A continuous floor system would be more efficient in distributing the catenary load through shear forces to the set boundary conditions. However, in this discrete floor system, the distribution of all forces requires transmission through the inter-module connections. Since these connections are located at the corners of the floor panels, tensile stresses stay predominantly concentrated in the proximity of the shorter side of the panels.

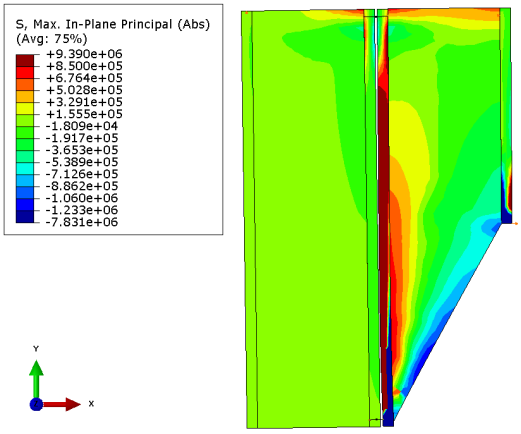

Figure 5.22: In-plane principal stresses in model 2

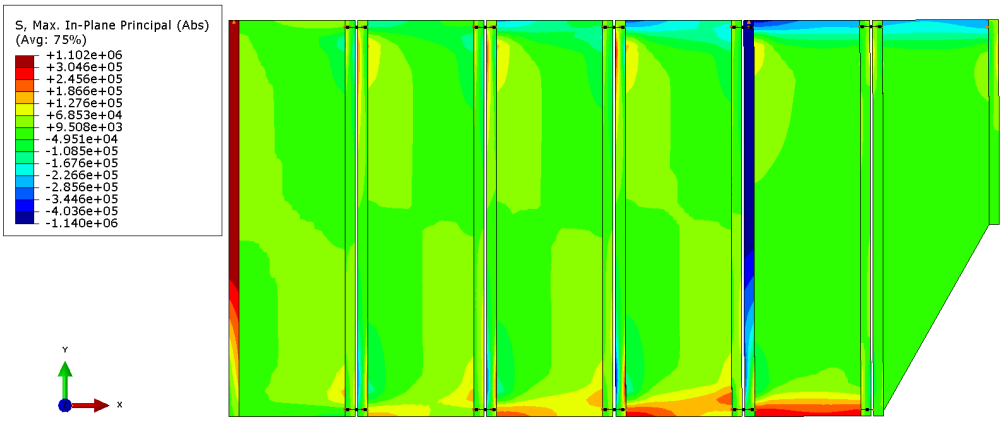

Figure 5.23: In-plane principal stresses in model 4

5.10.3. Axial force and elongation in the connections

Upon analysing the stress distribution in Figure 5.22, it becomes clear that for models 2 and 3 no tension forces are transferred through the inter-module connections to consecutive floor fields, and that an equilibrium is created with a compressive strut in the damaged floor field. For the model 4, tensile stresses are transferred to the consecutive floor fields through the connections. Figure 5.24 displays the accompanying axial forces in the inter-module connections and Table 5.14 presents the tension forces and axial elongations in the connections 1 to 5, as indicated in Figure 5.24. The connectors in compression mirror the exact force values as the connectors in tension. It is interesting to see that for the connections 2 till 5, the tension forces are reduced with a near constant value of 27.2 kN. It should be noted that connection 1 experiences a larger tension force than its determined ultimate resistance and zero elongation. This is because the connector is modelled as rigid. Furthermore, connection 2 experiences a tensile force equal to its ultimate resistance.

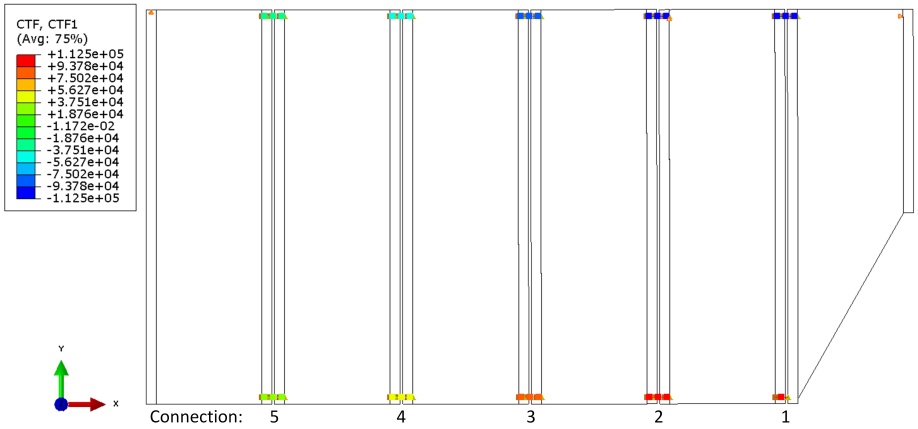

Figure 5.24: Forces in the connectors in x-direction. The connections in tension are indicated with numbers 1 to 5.

Connection	Connection Tension force [kN]	Force difference with the following connection [kN]	Axial elongation [mm]
1	110.0	2.1	0
2	108.9	26.5	1.58
3	82.4	27.5	2.40
4	54.6	27.8	1.58
5	26.9	26.9	0.78

Table 5.14: Tension force and elongation in the inter-module connections in the facade.

6

Integration of floor response

6.1. Introduction

In Chapter 3, the ALPA of Knuppe on a timber modular building is extensively described. One of the investigated scenarios involved the removal of a double intermediate facade column. It was observed that catenary action served as a potential ALP. However, the formation of a robust catenary was constrained by the low resistance and elongation capacity of the catenary. Knuppe used a 2D frame model for his ALPAs, which excluded the formation of out-of-plane ALPs. Chapter 5 showed that for the same column removal scenario, an additional ALP exists in the floors, in the form of diaphragm action. Incorporating the diaphragm action in the 2D frame model of a structure should introduce an additional deformation which is beneficial for the formation of catenary action.

This chapter assesses the influence of integrating the in-plane load-deformation behaviour, of the floor systems of a timber modular building, into a 2D frame model of the structure. Hereby, specifically examining its effect on the capability to establish robust catenary action.

6.2. Analysis model

In order to incorporate the behaviour of floors in a 2D frame model that does not allow for the direct modelling of floors, reference is made to the findings in Annex A. It was established in Annex A that the location of where elongation occurs within the catenary has a negligible impact on the equilibrium state. Building upon this conclusion, it is determined that the additional deformation in the floors due to catenary forces, obtained through a separate analysis, can be effectively incorporated into a 2D frame model by introducing spring boundary constraints at the ends of the catenaries. These spring boundary constraints should represent the load-deformation behaviour of the floors at the intersection between the floor plane and the 2D frame model plane.

Two of the three modelling scenarios are designed to analyse the global response following a double intermediate façade column removal in the case study building with three distinct assumptions. Scenario 1 serves as the base model and assumes that the discrete timber floor systems are perfectly rigid and catenary loads are transferred directly through the facade elements to auxiliary stability systems. In this case, the two outer building sections form rigid boundary constraints to the middle section. Scenario 2 assumes that the floor systems of all modules in the case study building contribute in distributing the additional gravity loads through diaphragm action and allow for a more ductile global response. For this scenario also the middle building section is modelled. However this time with boundary condition springs containing the in-plane load-displacement stiffness from model 4 (Chapter 5) with the six floor fields. Scenario 3 simulates the global response of a standalone single timber modular building section with the incorporated floor behaviour of the two floor fields from model 2 (Chapter 5). This scenario represents a façade column removal in a building where the stability system configuration does not allow for an instant redistribution of loads. Catenary loads cannot be transferred directly to a stability frame and have to make equilibrium through diaphragm action in the floors. This scenario is added to analyse the ability of forming catenary action in a building which produces an unstable initial response.

The three modelling scenarios use the same single timber modular building section, but with different boundary constraints. A schematising of the three modelling scenarios is depicted in Figure 4.6 in Chapter 4.

6.3. Model input

In order to quantify the effect of applying different boundary constraints on the ability to develop catenary action, a similar 2D quasi-static ALPA is performed as performed by Knuppe and described in Chapter 3. This is done because it is an eligible method which produces results that can clearly distinguish the conduct of different ALPs in the post removal behaviour of the structure. To simulate the case study buildings, a comparable frontal view 2D frame model is employed. However, for this study, the model incorporates the updated connector layout and eliminated maximum rotation, as introduced in Chapter4. These modifications are made to enhance the model's representation of the actual behaviour of both inter- and intra-module connections.

For the input values on material properties, connection idealisation and properties, and further specifics on the finite elements the reader is referred to Chapter 3, 4, or Knuppe's research [1]. The stiffness input values of the boundary condition springs, for the two floor fields model and the six floor fields model, are represented in Figures 5.17 and 5.21 respectively in Chapter 5.

6.4. Analysis procedure

The alternative load path analysis is performed as a force controlled, non-linear, quasi-static analysis, performed with the finite element software from Abaqus. The loading procedure follows the push-down method principles. A load is applied on every module column, representing the gravity loads on the floors, the self-weight of the longitudinal floor beams, and the self-weight of façade elements. In Annex A it was determined that the load on each column for the accidental limit state is 14.06 kN. When including the self-weight of the floor beams and the façade, an unamplified vertical load of 22 kN should be assumed per column. The push-down method dictates that the analysis has to take place in two steps. In the first step, all columns are quasi-statically loaded with unamplified load of 22 kN. In the second step, only the parts of the building above the damaged area are quasi-statically loaded with an additional amplified gravity loads. As the assumed DAF is set on 2.0, the columns above the damaged area are loaded with an additional 22 kN [59].

6.5. Results

6.5.1. Load-displacement

Scenario 1

For scenario 1 the deformed structure at the moment of failure is presented in Figure 6.1. Figure 6.2a and 6.2b show the response curves of the analysis. The x-axis of both figures display the vertical displacement of the location directly above the left removed column. The y-axis in Figure 6.2a displays the applied load on the columns above the damaged area, and in Figure 6.2b it represents the load factor. The load factor is determined as the ratio between the applied load and the design load. A load factor of 1.0 is equal to the standard unamplified gravity load. In order to resist the dynamically amplified load, the structure should be able to reach a load factor of 2.0, corresponding to the dynamic amplification factor of 2.0. From Figures 2a and 2b it can be seen that the timber modular structure with rigid boundary conditions only has the capacity to reach a load factor of 0.39. This corresponds with an applied load of 8.65 kN, and a vertical displacement of 0.20 meter.

When taking a further look at the response curves, the following behaviour can be identified. Initially, the system has almost zero resistance against the vertical displacement of the module floors. In this model that is due to the zero rotational stiffness of the inter-module connections. Furthermore, the response shows a nonlinear relation between the applied load and the vertical displacement, typical for the formation of catenary action. The load increases non-linearly till 8.65 kN is applied and a vertical displacement of 0.20 meters is reached. At that moment the analysis is stopped and the structure has

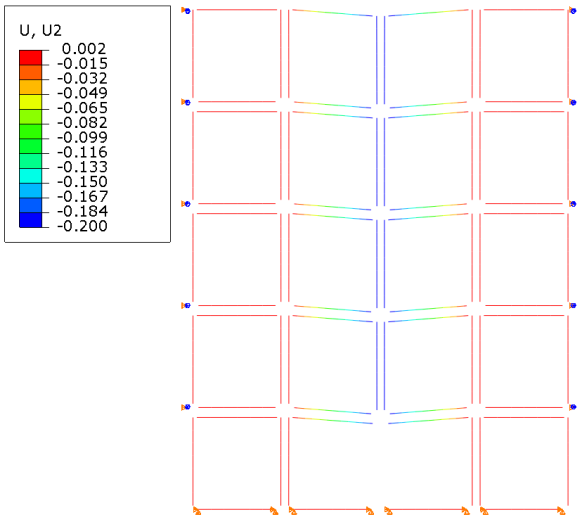

Figure 6.1: Vertical displacement [m] at failure of scenario 1

failed. The reason for failure is the insufficient axial resistance and elongation capacity of the inter-module connection. Figure 6.3 shows that at the horizontal displacement of 0.20 meters, the force in the catenary reaches the maximum capacity of the inter-module connection.

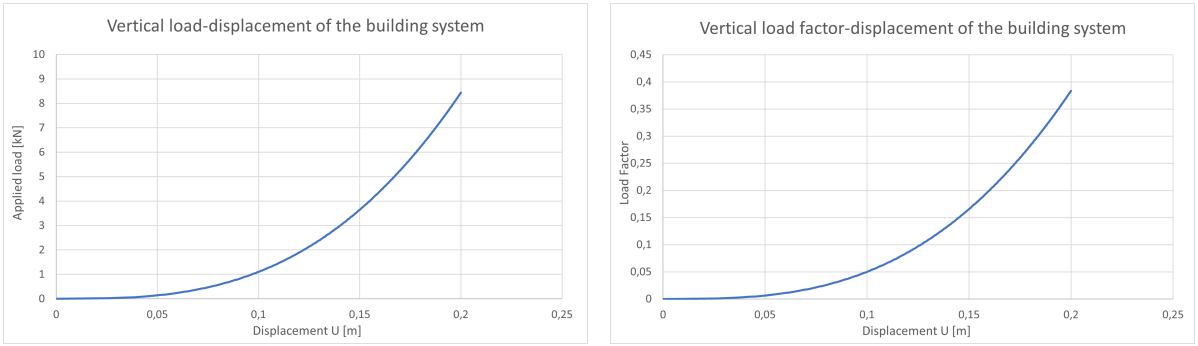

(a) Load-displacement **(b)** Load factor

Figure 6.2: Response curves for scenario 1

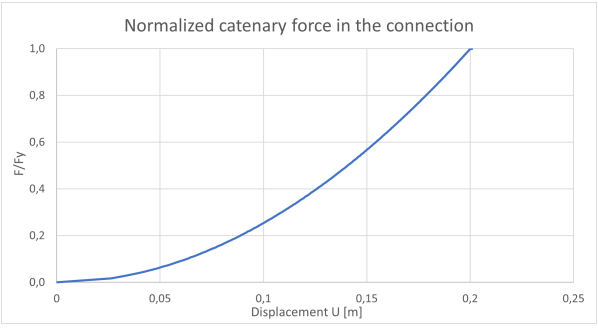

Figure 6.3: Normalised catenary force in the inter-module connection.

Scenario 2

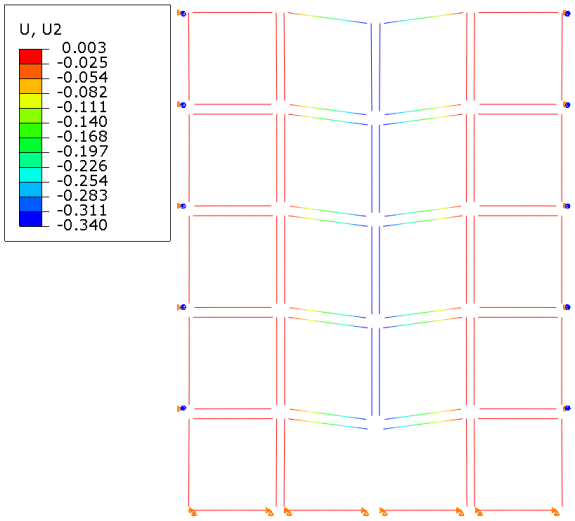

Figure 6.4: Vertical displacement [m] at failure of the building model, including spring boundary conditions of the model with six floor fields

For Scenario 2, the final deformed state of the structure at the moment of failure is presented in Figure 6.4. Figure 6.5 shows the associated vertical load-displacement and load factor-displacement curves. It can immediately be seen that scenario 2 shows a comparable, but more ductile, response than scenario 1. The initial response has zero stiffness, but increases in a nonlinear manner till a final vertical displacement of 0.34 m is achieved in the floor above the left removed column. The maximum vertical load that can be resisted is 14.29 kN and corresponds to a load factor of 0.65. Despite the system being more ductile and the maximum applied load is 65% higher compared to the base model of scenario 1, a robust catenary response can still not be formed. Failure occurs again due to the forces in the catenary reaching the maximum axial resistance of the inter-module connection.

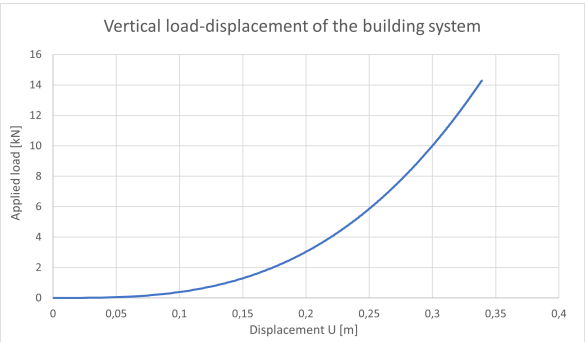

(a) Load-displacement

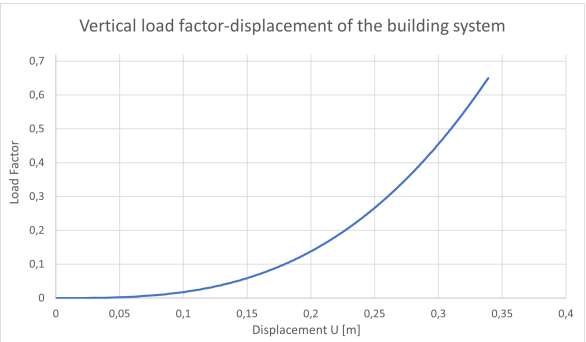

(b) Load factor

Figure 6.5: Response curves scenario 3

Scenario 3

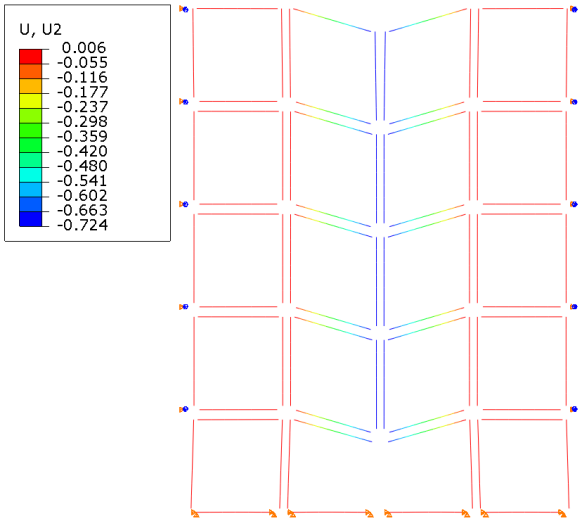

Figure 6.6: Vertical displacement [m] at failure of the standalone single building section, including spring boundary conditions of the two floor field model

Figure 6.6 and Figure 6.7 show the response of the building in scenario 3. From both figures it can immediately be seen that scenario 2 reaches a larger vertical displacement and can resist more vertical loads than scenario 1 and 2. Similar to the previous scenarios, the data for the response curves is attained from the location directly above the left removed column. Figure 6.7 shows that the system is able to resist the applied loads only after the floor displaced 0.54 meters vertically. This is in line with the expected behaviour. The boundary condition springs have zero stiffness until the structure moves 58 millimetres inward on both sides of the removed column. Until that moment, the structure is practically unstable. After the initial 0.54 meters of vertical displacement, the system develops a stiffness and the load increases in a nonlinear manner until a 31.04 kN is reached. This coincides with a load factor of 1.39. At failure the floors has deflected 0.72 meter. The load factor of 1.41 indicates that the system is able to form catenary action for an unamplified loading situation. However not for a loading situation including the dynamically amplified load.

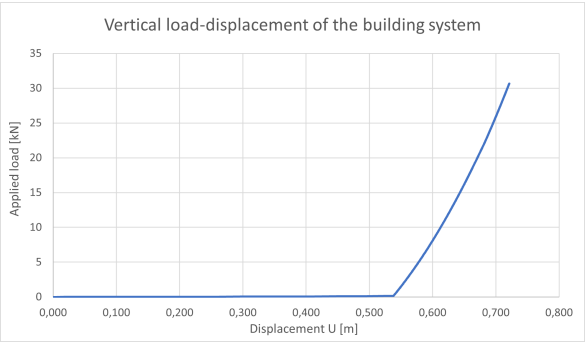

(a) Load-displacement

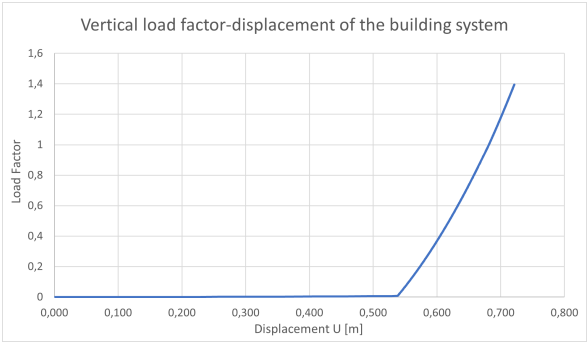

(b) Load factor

Figure 6.7: Response curves scenario 3

6.5.2. Ductility

Another method of analysing the response of the different scenarios is by assessing the relation between the force in the catenary and the total elongation throughout the catenary. In other words the ductility of the system. As should be well established by now, the ability to deform and elongate is very important in a catenary. Assessing the elongation in each scenario can provide valuable insight on the ability to reach a stable catenary. This can be done by including the catenary equation from Section 2.5 and Annex A (Equation A.6). Implementing the correct parameters for the vertical load and the length of the horizontal catenary elements gives a boundary for ductility requirements for the catenary system. The system will only be able to find an equilibrium and form a stable catenary if the resistance in the catenary is higher than the required force in the catenary at the elongation at moment of failure.

The elongation in this analysis is represented by the combined displacement and deformation of all elements which are situated in the plane of the 2D frame analysis and in the plane of a floor field, see Figure 6.8. The elongation data is gathered by summarizing the elongation of all connectors in the catenary, and the elongations of the floor beams in the 2D frame models. The relative in-plane displacement of the floors, at the location of the façade of the building, adds to the deformation capacity of the catenary. It is therefore also accounted for when determining the total elongation of the system by including the elongation of the boundary conditions springs. The catenary force is taken from the section forces in the middle node of one of the floors above the removed columns. Given the absence of vertical ties in the building, each floor must be capable of developing catenary action to achieve a robust global response. Since there are no variations in the floor fields and facade elements across the floors, the responses are essentially identical. Consequently, the decision is made to present only the force-elongation response of the second floor directly above the removed columns.

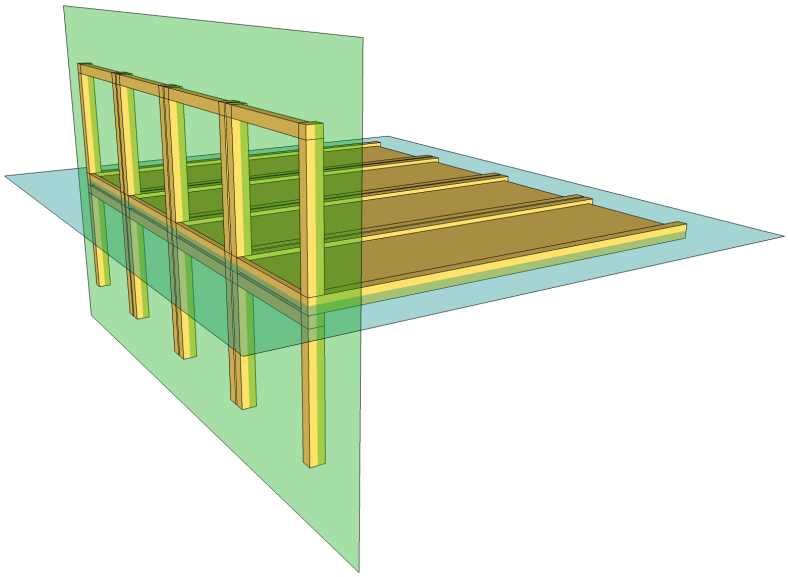

Figure 6.8: The total elongation in a catenary is determined as the total deformation and displacement of all elements on the line where the 2D frame structure (green plane) and the floor (blue plane) intersect.

Figure 6.9 presents the catenary force and elongation present in the catenary systems of scenario 1, 2, and 3. Furthermore, it displays the resulting catenary requirement boundary from the catenary equation. The vertical load on the catenary (F) is determined as two times the amplified load on a single column above the damaged area. This results in a total vertical load of 44 kN. The original length of the horizontal catenary elements (L_1) is 2.52 meter, which is determined by the width of the CLT floor panels.

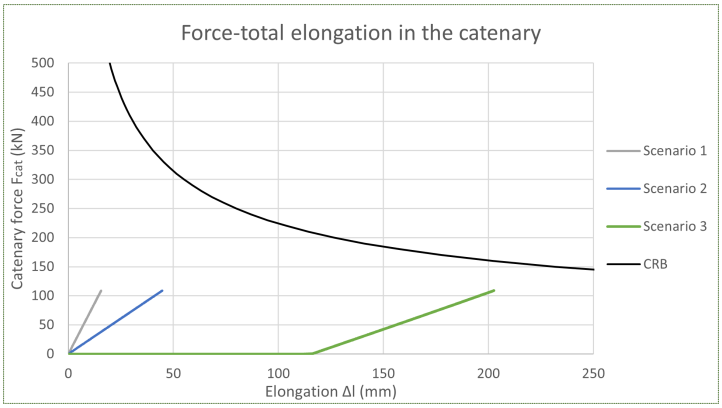

Figure 6.9: Response graph showing the elongation versus the total elongation in the catenary systems of scenario 1, 2, and 3. The catenary equation line represents the minimum required properties for the formation of catenary action in the assumed building.

In scenario 1, the base model exhibits the least elongation capacity with 15.4 mm. This is followed by scenario 2 which only allows for a total elongation in the catenary of 44.8 mm. Conversely, scenario 3 manifests the greatest elongation among the three scenarios. The responses of the catenary systems in scenarios 1 and 2 are characterised by a linear behaviour. This is because the failure modes in the catenaries are governed by the brittle failure mode of the inter-module connections. The overall behaviour is dictated by the collective stiffness of all elements in the catenaries. Scenario 2 presents a bi-linear behaviour, where the initial response is again distinguished by having zero stiffness. The catenary of scenario 3 undergoes an initial elongation of 116 mm, attributed to the boundary condition springs with zero initial stiffness up to 58 mm of deformation. Subsequently, the response evolves linearly, similar to scenarios 1 and 3. The peak force observed in the catenary amounts to 108.9 kN across all three scenarios. This aligns with the net tensile resistance of the tie plate in the inter-module connection, as given in Table 3.4. This indicates once again that the inter-module connection represents the limiting factor in the formation of a stable catenary.

7

Connection optimisation

7.1. Introduction

In chapter 6 it was established that the case study building lacks the capacity for robust catenary action in a double intermediate column removal scenario. Figure 6.9 illustrates that the force-elongation response in the catenary systems fails before surpassing the catenary requirement boundary. This is due to the inadequate resistance and elongation capacity within the system of floor fields and inter-module connections, preventing tension forces in the catenary from attaining equilibrium with additional gravity loads post-removal. The previous research by Knuppe explored the influence of enhancing the rotational resistance and stiffness of intra-module connections on the overall performance of the building model. However, enhancing the rotational properties alone proved insufficient for achieving a robust catenary [1].

Building upon the preceding chapter's findings, a more effective strategy for structural optimisation involves increasing the resistance or elongation capacity of the building elements forming the catenaries. The connections between the modules are a central item of attention because of their maximum resistance of 108.9 kN, which is the weakest link in the catenaries and determines the overall performance. This chapter addresses this limitation by proposing an optimised connection design, aimed at enabling the case study building to develop robust catenary action. For reference, the key parameters of the original connection are provided in Figure 7.1.

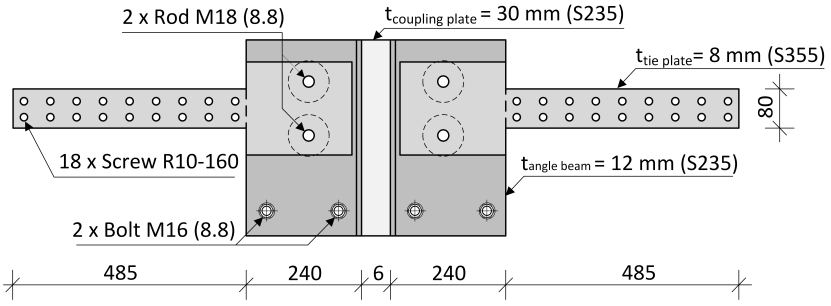

Figure 7.1: Original inter-module connection layout

7.2. Optimisation methods

The optimisation objective is to design an inter-module connection that enables a force-elongation response of the building, which meets the "catenary requirement boundary" dictated by the catenary equation. The catenary equation determines every combination of minimum required resistance and corresponding elongation capacity of a catenary to make equilibrium with the vertical point load on the catenary. The optimisation can be achieved by either increasing the resistance capacity or by improving

the ductility of the connection, by increasing its elongation capacity. In this study, both methods are applied to determine two optimised connection designs. The operational procedures of these methods are shortly explained in the subsequent section.

7.2.1. Method 1

Method 1 retains the standard design of the original inter-module connection, enhancing its resistance capacity by increasing the cross sections of the steel plates, the strength of the steel, and the dimensions and quantity of bolts, rods, and screws in the CLT. This method does not contribute to improved ductility. It rather increases the overall stiffness of the connection. The load distribution through the building system changes with a change in stiffness in certain components. It is therefore difficult to predict the resulting load-elongation response based on a set of connection properties. The best way of creating the connection design which will result in the required force-elongation response of the building system, is by means of iteration.

The iteration process starts with the original inter-module connection design with an insufficient tensile strength capacity. Following this, a new connection design is introduced, incorporating improved characteristics. Subsequent, the mechanical properties are determined using the component method, a methodology outlined in Chapter 3 and further expounded upon in Chapter 4.

To assess the impact of the new connection design on the overall performance of the building structure, the new connection properties are integrated into an ALPA model for the studied structure. This integration begins with implementing the connection properties in a floor model, evaluating whether the maximum resistance of the floor is still governed by the connections or if other failure modes become governing, potentially influencing the maximum tensile resistance of the catenary.

The next step involves extracting the new in-plane load-displacement response from the floor model. Subsequently, the in-plane response characteristics of the floor and the mechanical properties of the connection are implemented into a 2D frame model of the building structure.

The process ends in the analysis of the force-elongation response of the structure with the modified connection properties. If the response falls short of meeting the CRB, it is concluded that a robust catenary cannot be formed, requiring an adjustment of the inter-module connection design. Conversely, if the force-elongation response significantly exceeds the catenary requirement boundary, indicating a conservative design, adjustments need to be made to achieve a balanced and optimal connection for robust catenary action. The iteration process is also illustrated in Figure 7.2

The ALPA used in the iteration process adheres to the floor analysis procedure outlined in Chapter 5, and the 2D frame analysis of Chapter 6. For the case study building, the relevant floor analysis model is model 4, which includes six consecutive floor fields. To assess the full potential of the new connection design in forming catenary action, a modification is introduced in the loading procedure of the 2D frame analysis. Originally the push-down method is employed, where the initial load step brings the structure to its unamplified design load and a subsequent step applies amplified loads above the damaged areas. In the current analysis, the structure is loaded until failure, progressively increasing the load in the second step until reaching an adequate level.

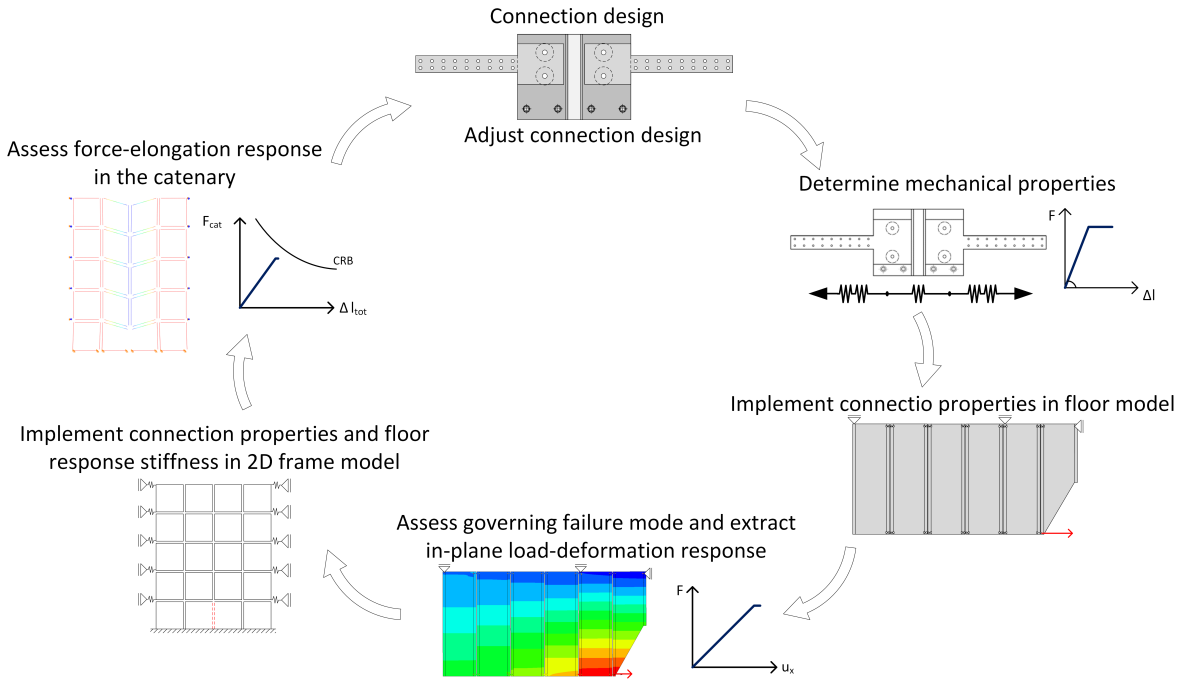

Figure 7.2: Iteration process

7.2.2. Method 2

In method 2, a modification is introduced to the original inter-module connection design to enhance its ductility. The specific modification in this case is the incorporation of a fuse. The objective of method 2 is to introduce more elongation capacity by making use of the plastic elongation characteristics of steel. While the ultimate resistance of S235 steel can theoretically reach values up to 40%, this is considered a best-case scenario. In practice, the ultimate strain is heavily influenced by the quality of the steel.

Kossakowski conducted multiple tensile tests on steel dog bones to establish the complete stress-strain curve of S235JR steel, which was subsequently numerically replicated [60]. Figure 7.3 illustrates a nominal stress-strain graph with both the experimental and numerical solutions. From the graph, it is evident that the ultimate strain from multiple experiments falls within the range of 22% to 26%. For the purposes of this study, a conservative lower limit of 20% is assumed for the ultimate strain of S235 steel.

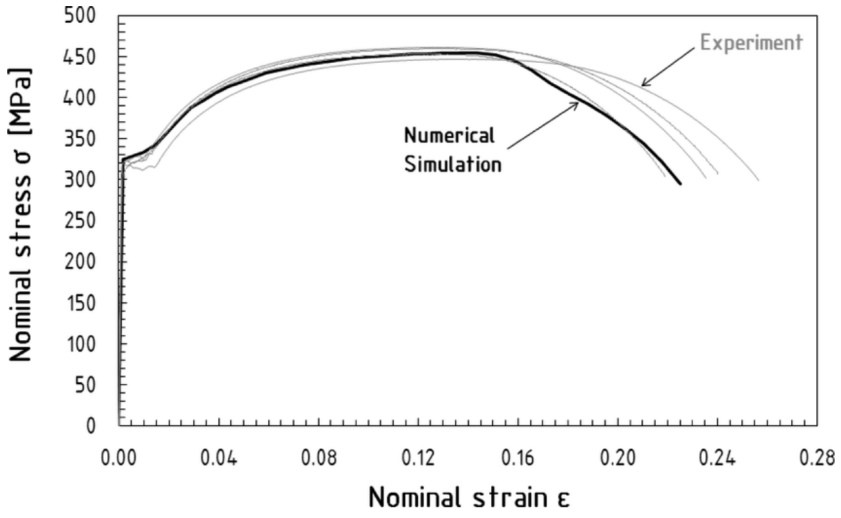

Figure 7.3: Nominal stress-strain curves for S235JR steel [60].

By introducing a fuse into the series of components and designing the ductile connection such that the fuse governs the maximum resistance, the fuse undergoes plastic deformation upon reaching the connection's yield resistance capacity. To ensure that the fuse governs the failure mode and utilises its full plastic potential, all other potential failure modes in the inter-module connection must possess a higher resistance than the maximum resistance of the fuse. Assuming S235 steel can achieve an ultimate strains of 20%, the fuse can extend 20% of its original length at the moment of failure.

The connection properties of the new design, incorporating the fuse, are recalculated using the component method and spring model detailed in Chapter 4. However, an additional spring is now incorporated into the spring model to account for the added fuse. While the numerical models still represent the inter-module connection with three connectors, the stiffnesses of the two outer connectors are determined by multiplying the stiffness of the shear screw group (K_{ss}), the tensile stiffness of the tie plate at the location of the screw group ($K_{pt.1}$), and the tensile stiffness of the fuse in the tie plate (K_{fuse}) in series. The associated spring model of the inter-module connection is illustrated in Figure 7.4.

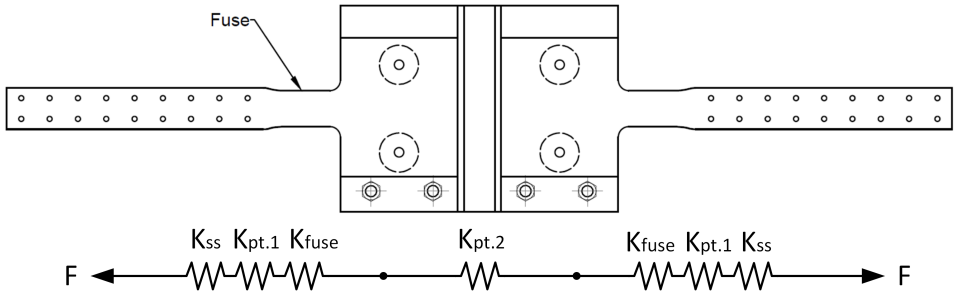

Figure 7.4: Spring model of the inter-module connection with a fuse [1].

Similar to method 1, the new force-elongation response in the catenary with the optimised ductile connection is compared to the CRB. Subsequently, the connection is iteratively optimised by adjusting the length of the fuse. The same optimisation process as illustrated in Figure 7.2 is used.

7.3. Optimised connection results

7.3.1. High-strength connection

Employing method 1 results in an optimised high-strength inter-module connection, as illustrated in Figure 7.5. Similar to the initial connection introduced in Chapter 3, the revised design comprises of three distinct components. The first component is the tie plate. This plate is fixed to the underside of the CLT panel through a set of screws. It is further connected to the floor beam and column of the module via a glued in rod. The second and third components consist of the angle beam and the coupling plate which are interconnected by a group of bolts. The tie plate and the angle beam are both connected by a bolted connection on the ends of the glued in rods. They are present at each module corner, while the coupling plate serves as the bridging element between two modules.

The new high-strength connection design exhibits an adequately high tensile resistance compared to the initial connection. This enhancement is due to the implementation of larger-diameter rods, bolts, and screws, alongside an increase in the number of screws from 18 to 39 per side of the connection, and an increase of bolts from two to three per side of the connection. Moreover, the steel strength of the tie plate and the angle beam is elevated through the utilisation of S355 steel instead of S235 steel, and the thickness of the tie plate is increased from 6 mm to 8 mm. These modifications elevate the tensile resistance of the new connection to 264.6 kN, with the tensile resistance still governed by the tensile resistance of the net cross section of the tie plate. The tensile properties of the high-strength connection, under tension, are presented in Table 7.1.

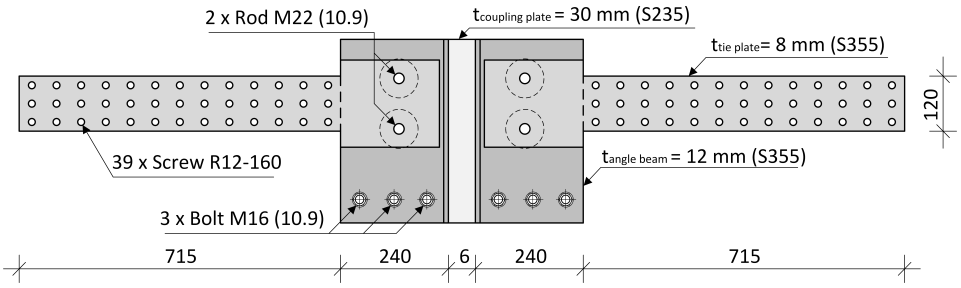

Figure 7.5: Optimised connection according to method 1

Property	Value	Unit
Shear resistance threaded rod M22	303.0	kN
Bearing resistance of tie plate with M22 threaded rod	431.2	kN
Shear resistance of bolt M16 with angle beam	282.6	kN
Bearing resistance of angle beam	601.4	kN
Tensile resistance of tie plate	264.6	kN
Yield shear resistance 12 mm screw (group)	265.0	kN
Maximum shear resistance 12 mm screw (group)	339.3	kN
Shear stiffness screw group K_{ss}	1.74E+05	kN/m
Stiffness tie plate $K_{pt.1}$	5.64E+05	kN/m
Stiffness coupling plate $K_{pt.2}$	6.30E+06	kN/m
Elastic stiffness of tie plate + screw group	1.33E+05	kN/m
Yield resistance of connection	264.6	kN
Elastic deformation of tie plate + screw group	1.99	mm
Plastic deformation of tie plate + screw group	0	mm

Table 7.1: Tensile properties of the high-strength connection

The performance of the building structure with the new high-strength connection design is computed by adjusting the inter-module connection properties in the 2D frame model of scenario 2, detailed in Section 6.2, with the specifications outlined in Table 7.1. The stiffness of the boundary condition spring, representing the in-plane load-displacement behaviour of the floor system with the new high-strength connection design, is determined by incorporating the same properties into the 6-field floor model introduced in Section 5.3.2. The resulting in-plane load-displacement response of the floor exhibits a linear progression with a stiffness of 9037 kN/m, as depicted in Figure 7.6.

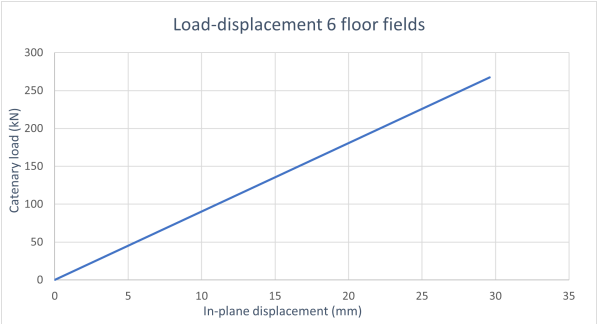

Figure 7.6: Load-displacement response of the 6 field floor analysis with the high-strength connection.

With the resulting boundary condition spring stiffness from Figure 7.6, the alternative load path analysis produces a vertical load-displacement curve and a load-elongation response in the catenary as shown in Figures 7.7 and 7.8 respectively. These figures illustrate that the newly designed high-resistance connection enables the building structure to establish a complete catenary in the event of a double intermediate column removal scenario. The vertical load-displacement response in Figure 7.7 indicates that the system can withstand 2.18 times the unamplified gravity load resulting from the removal scenario, indicating the building system has sufficient resistance to form a robust catenary. As well does the force-elongation response in the catenaries suggests the formation of a robust catenary. At the point of failure, the tensile resistance in the catenary surpasses the required tensile resistance at the same elongation. The red dot in Figure 7.8 marks the instance when the catenary response of the building withstands a load, equivalent to the amplified gravity load with the dynamic amplification factor of 2.0. The total response of the structure is mainly elastic with a plastic elongation of 1.99 mm. The response figures prove that improving the inter-module connection according to optimisation method 1 enhances the structural performance in the formation of catenary action.

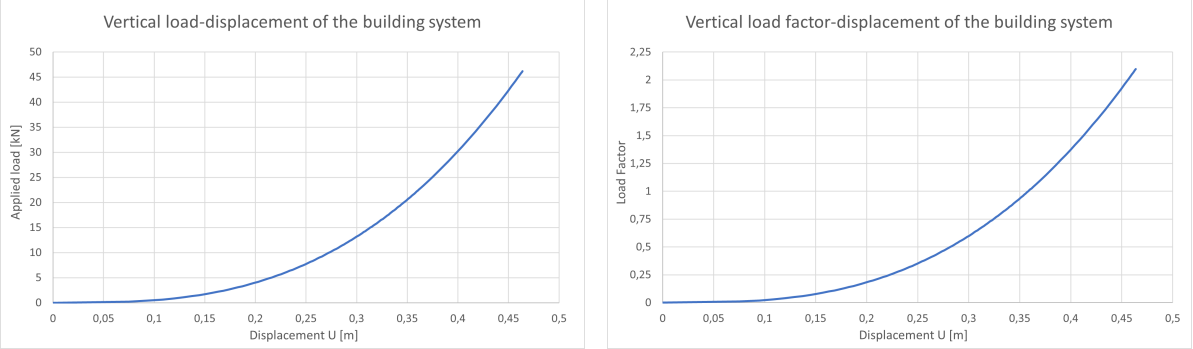

(a) Load-displacement

(b) Load factor

Figure 7.7: Vertical load-displacement response curves with the new high-strength inter-module connection

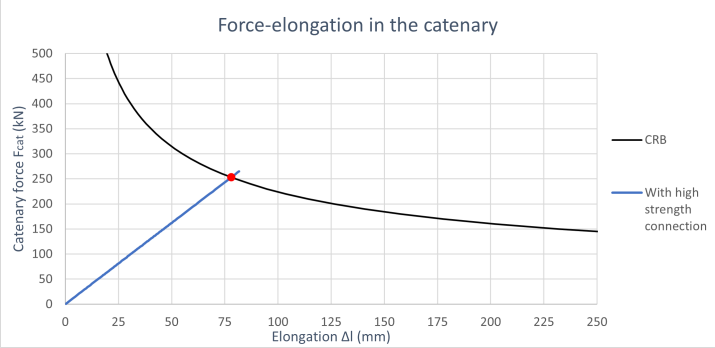

Figure 7.8: Force-elongation response in the catenary system of the first floor with the new high-strength inter-module connection.

7.3.2. Ductile connection

According to Figure 6.9, the original connection design in the case study building resulted in a total elongation in the catenary of 62 mm, which proved insufficient for a stable catenary response. To calculate the necessary elongation at a specific resistance, or force in the catenary, the catenary equation as given in Equation 2.3 can be rewritten in the form of Equation 7.1.

$$\Delta l = \frac{2L_1}{\sqrt{1 - \left(\frac{F}{F_{cat}}\right)^2}} - 2L_1 \tag{7.1}$$

Where:

Δl The total elongation in the catenary.

F_{cat} The tensile load in the catenary.

L_1 The original length of the horizontal catenary elements. In the case of the given building this is 2.52 meter.

F The vertical reaction force on the removed vertical element in the ALS load situation. In the case of the double intermediate façade column removal and a dynamic amplification factor of 2.0, this is 44 kN.

According to Equation 7.1, the required elongation at a maximum resistance of 108.9 kN is 470 mm. The difference between the elongation at failure, of catenary in the case study building with the original connection, and the required elongation, must be covered by the plastic elongation of a single fuse. In a catenary composed of multiple components in series with zero stiffness in the plastic response, only one component will reach its yielding point first and deform plastically. At a maximum resistance of 108.9 kN, the original connection design requires a fuse that can have a plastic elongation of 425 mm. Considering an ultimate strain rate of 20% for S235 steel, a fuse length of 2125 mm is needed, which implies an excessively large connection. Therefore, in addition to implementing a fuse, the resistance capacity also necessitates an increase in the new ductile connection design. Increasing the resistance capacity to 169.2 kN and applying method 2 results in a new ductile inter-module connection, as depicted in Figure 7.9. The design retains the same three distinct components; the relatively thin tie plate, the relatively thick coupling plate, and the angle beam. These components are connected in the same manner as the original and high-strength connections. However, in the ductile connection, each side features 30 screws of 12 mm diameter and three M18 bolts. The tie plate has a width of 150 mm at the location of the screw group and a width of 90 mm at the fuse. The thickness is 8 mm, and the steel type is S235 for a larger ultimate strain. The tensile properties of the ductile connection in tension are detailed in Table 7.2.

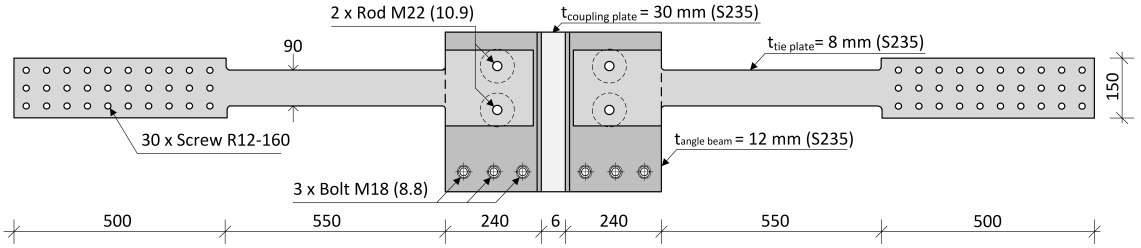

Figure 7.9: Optimised connection according to method 2

Property	Value	Unit
Shear resistance threaded rod M22	303.0	kN
Bearing resistance of tie plate with M22 threaded rod	316.8	kN
Shear resistance of bolt M18 with angle beam	276.5	kN
Bearing resistance of angle beam	308.6	kN
Net tensile resistance of tie plate at the screws	272.2	kN
Yield shear resistance 12 mm screw (group)	204.3	kN
Maximum shear resistance 12 mm screw (group)	261.6	kN
Yield tensile resistance of tie plate at the fuse	169.2	kN
Ultimate tensile resistance of tie plate at the fuse	259.2	kN
Shear stiffness screw group K_{ss}	1.34E+05	kN/m
Stiffness tie plate at the screw group $K_{pt.1}$	1.01E+06	kN/m
Stiffness tie plate at the fuse K_{fuse}	2.75E+05	kN/m
Stiffness coupling plate $K_{pt.2}$	6.30E+06	kN/m
Elastic stiffness of tie plate + screw group + fuse	8.28E+04	kN/m
Yield resistance of connection	169.2	kN
Elastic deformation of tie plate + screw group + fuse	2.05	mm
Plastic deformation of fuse	110	mm
Plastic deformation of tie plate + screw group + fuse	112.05	mm

Table 7.2: Tensile properties of the ductile connection

The 6-floor field model, incorporating the new ductile connection properties, provides the in-plane load-displacement response, as depicted in Figure 7.10. The initial elastic stiffness is 7859 kN/m, serving as the boundary condition spring stiffness in the 2D frame model.

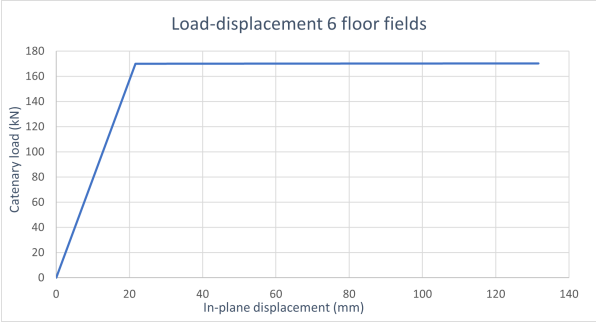

Figure 7.10: Load-displacement response of the 6 field floor analysis with the ductile connection.

The vertical load-displacement curve and load-elongation response for the building, featuring the new ductile connection, are presented in Figures 7.11 and 7.12 respectively. Similar to the high-strength connection derived from method 1, the new ductile connection guarantees the building structure's sufficient capacity for catenary action as an alternative load path in a double intermediate column removal scenario. The vertical load-displacement curve indicates ample resistance, withstanding 2.01 times the unamplified gravity loads resulting from a double intermediate façade column removal. Thus, indicating a robust catenary can be formed. The force-elongation response also indicates the formation of a robust catenary, with the red dot signifying the point where the applied load equals the amplified gravity load, aligning with the catenary requirement boundary. The total plastic elongation of the catenary from the force-elongation response is 110 mm, equivalent to the total plastic elongation of one fuse of 550 mm at an ultimate strain of 20%. The analysis results demonstrate that the new ductile

inter-module connection, resulting from optimisation method 2, enhances the robustness of the timber modular building by ensuring an alternative load path through catenary action.

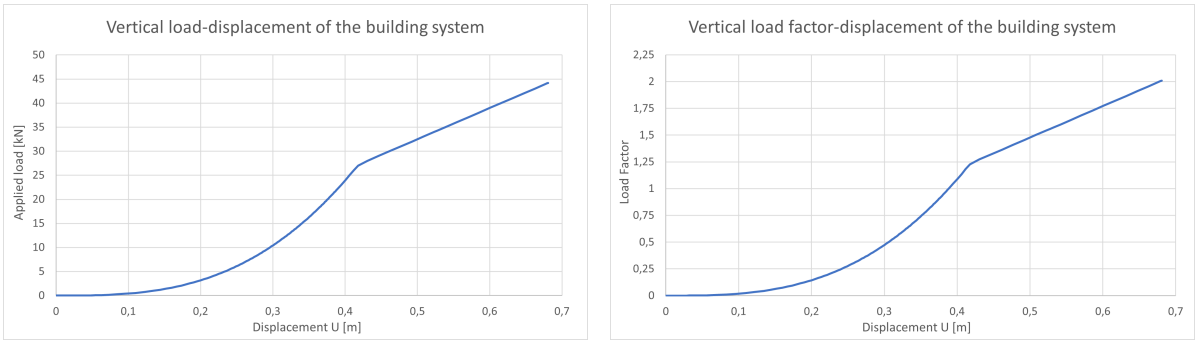

(a) Load-displacement

(b) Load factor

Figure 7.11: Vertical load-displacement response curves with the new high-strength inter-module connection

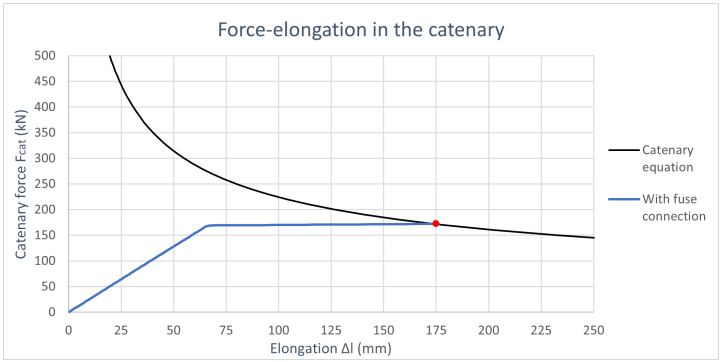

Figure 7.12: Force-elongation response in the catenary system of the first floor with the new ductile inter-module connection.

Part III

Research outcome

8

Discussion

In chapters 5, 6, and 7, three distinct studies are carried out, focusing on the in-plane behaviour of discrete timber floor systems, the incorporation of floor behaviour in a 2D frame model, and the optimisation of inter-module connections within a timber modular case study building. The results presented in the previous chapters offer valuable insights into the robustness criteria and the behaviour of timber modular buildings. In this discussion chapter, the key findings, their implications, and the implications of certain assumptions are explored.

8.1. Modelling approach and assumptions

Discrete floor modelling

Failure line assumption under large out-of-plane deformation

One of the first major assumptions involved the anticipated mode of failure for a CLT panel subjected to a substantial out-of-plane corner deflection. The assumption was that the failure would occur in a straight line, diagonally positioned over the module floor. When subjected to bending, CLT has multiple potential failure modes, such as tensile failure in the outer fibres, interlaminar shear failure, and rolling shear failure. The multiple failure modes cause CLT panels to fail in a splintered manner which is hard to replicate in a numerical model. The splintered pattern is mostly arbitrary in the plane of the panel, with different sections spalling out of plane. Even through the thickness of a panel, the outline of where material is detached exhibits variation. While determining a precise line of failure is virtually impossible due to this complexity, an average trajectory of the failure line can be assumed based on the location where bending stresses are expected to be the highest. In this case that is a straight line from the corner column (opposite to the removed column) to the middle column on the opposing longitudinal side of the module, as illustrated in Figure 5.4. The assumption of a straight failure line is a notable simplification and allows for an unobstructed load path without stress concentrations points. Section 5.10.2 shows that in models 1, 2, and 3, simulating a discrete floor system with one, two, and three floor fields respectively, relatively large and confined compressive stresses form part of an alternative load path along this failure line. The straight, unobstructed line does not take into account any possible damage or failure due to stress concentrations in the CLT panel. The resulting in-plane stress, which the damage CLT panel can resist, might therefore be conservative.

Stress based failure envelope

In order to model the orthotropic material properties of CLT and GLT, the maximum stress-based failure theory is applied. This choice was made because it was the only failure theory in Abaqus applicable with the current state of knowledge on in-plane shear failure of engineered timber elements. According to this theory, the strength capacities in any direction within a 2D planar element are determined by its components in the principal directions. For the CLT panel the maximum stress envelope is depicted in Figure 8.1. Applying the maximum stress theory entails that stresses in the non-principal directions have the same capacity as in the principal directions. This is however unlikely in engineered timber products, such as CLT. When depicting the load path of the compressive stresses along the diagonal

failure, stresses constantly have to weave through the glued interfaces of the panels in the 1 and 2 direction as illustrated in Figure 8.2. This is because the sides of the lamellas are not glued and cannot distribute stresses. The resulting stress load path is not an optimal path, as the strongest path would be parallel through a lamella, in the direction of the grain. The capacity in a non-principle direction of a CLT plate is therefore likely to be lower than modelled, which makes the material model non-conservative. Further research should give more insight in the exact stress capacities in all directions of cross laminated timber.

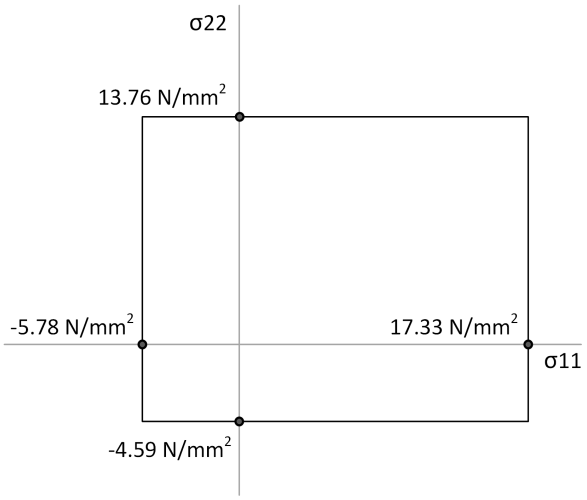

Figure 8.1: Stress based failure envelope for the CLT panel

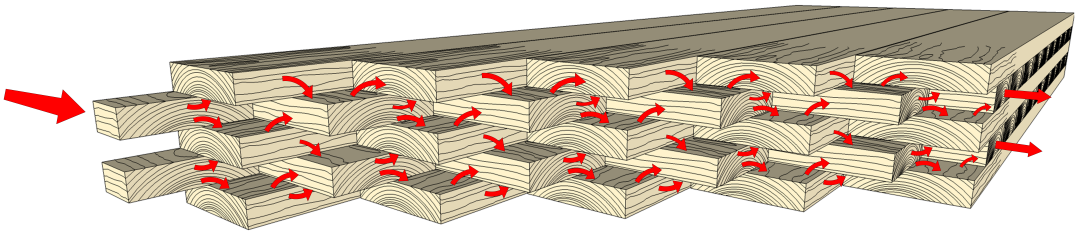

Figure 8.2: Compression force components weaving through the glued interfaces of the lamellas in a CLT panel.

Plasticity in the connector elements

In a series of steel connections, one connection is most likely to reach its yielding point first, show plastic deformation, and fail. For example, if a chain is loaded in tension till failure, only one link will actually fail. Strain hardening can allow multiple links to reach stresses above their yield strength and deform in a plastic manner, but due to imperfections and strain softening, only one link will reach its ultimate ductility. In the numerical models imperfections are not taken into account. Furthermore, the 2D frames are only loaded with vertical gravity loads in the models, inducing symmetric behavior. Consequently, equal catenary forces are generated in the two vertically displacing floor elements directly above the removed columns. Given their direct alignment above the removed column, these elements bear the most of the additional gravity loads, making them subjected to the highest catenary loads. Each floor element is connected to two identical connector elements with the same properties and failure mechanism. In order to prevent the four connectors in the catenary from reaching their full plastic potential and overestimating the ductility of the system, three connectors were given elastic properties only. As a result, only one connector can deform in a plastic manner. This approach has no effect on the 2D frame models with the original connection and the high-strength connection of optimisation method 1, as the connections show no plastic behaviour. However the approach does yield a conservative result for the optimised fuse connection of optimisation method 2. On the other hand, assuming one connec-

tion is allowed to behave in a ductile manner is more accurate than assuming that four connectors are able to reach their maximum elongation potential without failure. Moreover, implications such as the formation of prying forces are not taken into account which will also cause certain connections to reach their yielding strength prior to others.

The resulting elongation in the connectors of the catenary, with the optimised fuse connection, is presented in Figure 8.3. Only one connector reaches its full plastic potential. The other connectors at the ends of the diagonally displacing floor elements only elongate till their yield limit. Forces in the remaining connectors do not reach the yielding strength of the connectors.

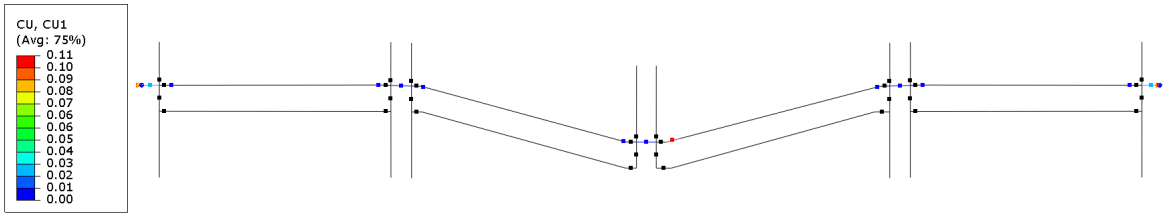

Figure 8.3: Total elongation at failure of the connectors in a catenary with the optimised fuse connection

Certain aspects such as the true plastic behaviour of all connection components and the formation of prying forces are not included in the connection models. Prying forces might occur with closing rotations the connection due to the timber floor and beam interacting in compression. This increases tensile forces in the steel plate, limiting its effective resistance. It is interesting to do further research on these effects, possibly by experimental testing or more detailed modelling of the entire connection. It is therefore recommended to test this unconventional connection for the maximum resistance and elongation capacity under catenary forces and the accompanying maximum rotation.

Dynamic amplification factor

In this thesis, a dynamic amplification factor of 2.0 was employed to determine the catenary requirement boundary for connection optimisations in Chapter 7. This value was adopted because Knuppe concluded in his research that a dynamic amplification factor for a timber modular building are very close to the suggested 2.0 in the new draft of Eurocode 5 [1]. However, it is crucial to note that the factor by which a quasi-static load should be increased to represent a dynamic loading scenario is not universally fixed for every structure. Instead, it depend son various factors, including the dimensions of the structure and its components, the dampening behavior of the material and structure, and the stiffness and energy dissipative capacity of the connections [61].

Structures responding to a column removal in an elastic manner with a brittle failure mode allow for minimal energy dissipation, making them more vulnerable to dynamic loading. Conversely, structures responding in a plastic manner do allow for energy dissipation and are less susceptible to dynamic loading. Both optimisation methods 1 and 2 assume the same vulnerability to dynamic loading, although they result in connections with significantly different structural behaviours. The high-strength connection from method 1 induces an elastic response in the catenary, while the connection from method 2 induces a response with substantial plastic deformation. Consequently, method 1 results in a structure which in reality is more susceptible to dynamic loading than method 2.

Optimising the connections in both methods, to a catenary requirement boundary based on a dynamic amplification factor of 2.0, ensures that one connection is not optimised to a fitting requirement. Hence, it is imperative to utilise appropriate dynamic amplification factors for alternative load path analyses and structural optimisations. For following analyses, using the optimisation method as presented in this thesis, it is recommended to employ dynamic amplification factors tailored to the structural response. As an alternative, or in order to perform a true optimisation, the suggestion is to perform a dynamic structural analysis as an additional step in the iteration process. By assessing the difference in response between dynamic and static analyses, an appropriate dynamic amplification factor can be determined for both optimisation methods.

Following the discussion on befitting dynamic amplification factors for the connection optimisations. An overview of different researches on dynamic amplification factors for the formation of catenary action in timber structures is given in Annex D.

Two-dimensionality

This thesis analyses the formation of catenary action in the timber modular building in a 2D frame. There are several reasons why a 2D frame approach was chosen. First of all, catenaries can essentially be created by 1D elements, which move in a 2D plane. The catenaries in the timber modular building only deflect vertically, so a 2D approach is sufficient to determine the forces and deformations in the catenary. Secondly, using a 2D approach allows to validate the model and results with simple analytical calculations and helps to determining a limit to which the catenaries have to be optimised. Using a 3D approach would complicate formulating an equation which can determine a catenary requirement boundary as simple trigonometry would not be applicable. Thirdly, formulating new methods for modelling connections in 3D was beyond the scope of this research.

As catenaries only need to elongate in their length, optimisation efforts can focus solely on the translational movement of inter-module connections. The use of a 2D frame approach allowed for the use of the already validated 2D frame model proposed by Knuppe [1]. The discussion point raised by Knuppe about potentially losing strength from additional resistance mechanisms in the out of plane direction is partly addressed by adding the in plane resistance of the floor systems.

Still, applying a 2D modelling approach does not take into account the initial bending resistance of the longitudinal floor and roof beams and the CLT floor plate before reaching a deflection at which failure occurs and catenary action takes over. Hypothetically, these components could mitigate the dynamic impact of column removal by prolonging the time during which additional gravity loads are applied to the catenary. Knuppe already demonstrated that a longer removal time of the column, or application time of the additional gravity load results in a reduction of the DAF.

Additionally, analysing the in-plane behaviour of discrete floor systems in separate models and applying this behaviour as spring boundary conditions to the 2D frame model proved to be a viable option for incorporating an out-of-plane resistance mechanism. However, this method overlooks the combined behaviour of the parallel systems. For example, in order for a fuse in the inter-module connection to reach a large plastic elongations, the intra-module screwed connection between the CLT panel and longitudinal floor beam needs to open same amount, leading to failure in the floor. This situation is illustrated in Figure 8.4. In reality, the inter-module connection and the CLT panel to floor beam connection provide a combined stiffness which is not taken into account by the 2D frame model. In order to include this effect, a 3D model is required. It would be good to analyse the parallel effect on the strength and stiffness of the inter-module connection and the intra-module floor panel to beam connection in a 3D model, as well as the impact of opening the floor panel-to-beam connection on the overall load-retaining capacity of the building structure.

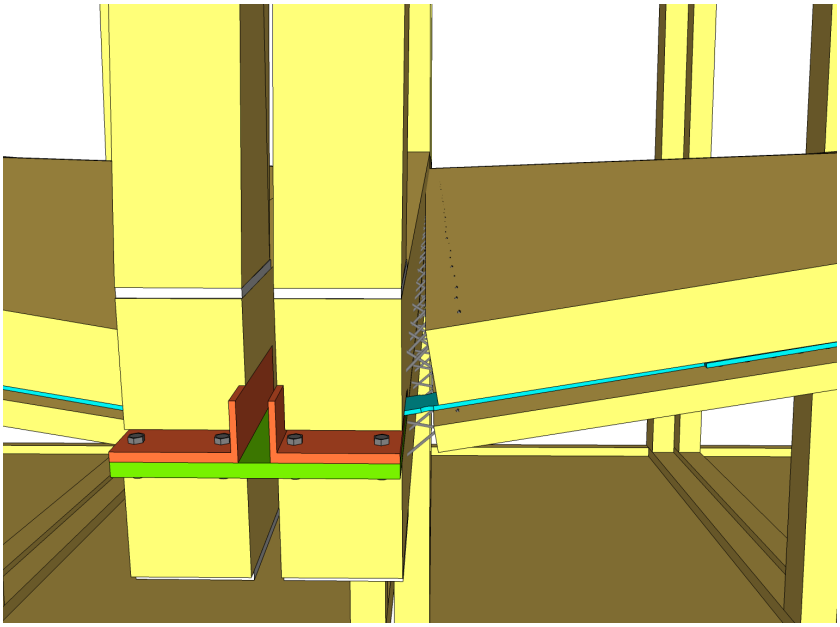

Figure 8.4: For elongation to occur in the tie plate of the inter module connection, the screwed connection between the floor panel and beam

8.2. Discussing the results

Discrete floor modelling

Stability frame configuration

Models 1, 2, and 3, with one, two, and three floor fields respectively, represent the behaviour of the floor system of a single standalone timber modular building section when loaded by catenary forces. Model 4, with six floor fields, analyses the same behaviour, but for the three-section case study building. Although the modules and connectors do not change, the difference in in-plane behaviour is tremendous. When overlaying the in-plane load-displacement graphs, the difference becomes especially clear, as shown in Figure 8.5. It can be seen that the results from models 1, 2, and 3 are identical, as the load-displacement lines are overlapping.

Figure 8.5: In-plane load displacement graphs of all floor models

The difference between the two behaviours is mainly due to the stability frame configuration in both situations. After a column is removed in a standalone building section, an initial large deformation occurs. This is because of the stability configuration. With two stability frames at the ends of the building,

one stability frames on one of the remaining sides, and a part of the floor system unable to transfer loads, an unstable system is created when subjected to catenary loads. A stable situation occurs when the two floor fields, which were unable to transfer loads, make contact. The system was previously not able to find and alternative load path in the floor system. However, after contact a pressure arc creates a situation in which equilibrium can be created. The large initial deformation is beneficial for forming catenary action. By adding a stability system, or changing the stability frame configuration an adverse effect on the in-plane deformation can be created. A comparable occurs in model 4. By adding a stability frame, catenary loads are able to find an alternative load path in the floor system from the beginning of the analysis. This is because after partial failure of the structure, a stable response is created. An alteration in stability system configuration in the model 4 will also trigger a different response. In the current situation, most of the tension forces are transferred to the furthest stability frame, passing through multiple elements which all deform slightly as a result. Adding a stability frame can alter the load path, making it shorter. Resulting in distributed forces to go through less elements, and create a stiffer response. In other words, the way the stability systems are incorporated in the building has an influence in the way catenary loads are transferred through the floor

Diaphragm action

The load transfer results show that diaphragm action occurs in all models. In models 1, 2, and 3, diaphragm action is the main mechanism of load transfer. Even though it occurs only in the first floor field where the catenary load is introduced. Model 4 introduces a more complex load distributing mechanism, involving both catenary action and diaphragm action. Directly after the load ingress point, 99% of the catenary load is transferred through the subsequent floor field to the next inter-module connection. Almost all of the load is therefore transferred directly through the cross-layered lamellas in the CLT floor. The cross-direction in the CLT panel is the strongest direction with most of the fibers oriented over the shorter span. Only 2.1 kN is distributed through diaphragm action. After the first two module floors, the load distributive mechanism is transitioned from a localised mechanism depending on direct transmittance of tension stresses through a local part of a floor panels, to a mechanism that distributes forces fully through diaphragm action. Table 5.14 presents the tension forces and elongation in the inter-module connections between the floor fields of model 4. The difference in tension force between two connections shows that from the second floor onward, each floor takes away, on average, 27.2 kN catenary loads in the connections. That means that per floor field, on average, 27.2 kN is distributed through diaphragm action. The catenary forces in the joints and shear forces in the floors yields a total deformation of 15 mm in the case model 4. The total elongation of all inter-modular connections is 6.4 mm. This means that 8.6 mm of deformation can be exclusively attributed to deformation of the floor fields alone.

Open cavity between the modules

In models 1, 2, and 3, a substantial part of the total in-plane deformation can be directly linked to the cavity between the modules. It allows the floor fields to have an inward movement of 30 mm, halfway the modules. This results in a significant deformation of 58 mm at the point of load ingress. If there were no cavity, or if an inter-module connection were to be placed halfway the length of the modules, the unrestrained deformation would not be allowed to occur. This results in a negative impact on the achievable elongation of the catenaries and a less favorable force-elongation response of the building structure. Furthermore, an additional connection along the longitudinal side of the modules would allow for more shear forces to be transferred between the modules and cause two consecutive floor beams react as composite beams in bending. This would result in an overall larger stiffness of the in-plane load-displacement behaviour of the floor system and a less favourable force-elongation response.

Addition of in-plane floor response into a 2D frame model

The impact of incorporating the in-plane behaviour of discrete timber floor systems in a 2D frame analysis, the catenary response, is quantified by comparing the load resistance of catenaries in scenarios 2 and 3 to the outcomes of scenario 1 from Chapter 6. In scenario 1, which represented the case study building without considering in-plane floor behavior, the catenary response was capable of resisting the gravity load with a load factor of 0.39. This is considered the baseline result. In scenario 2, rigid boundary constraints from scenario 1 were replaced with spring boundary constraints representing the in-plane floor stiffness of the case study building. This modification allowed the catenary response to

withstand a load factor of 0.65. Consequently, incorporating the stiffness and deformation capacity of the floor into the 2D frame analysis of the same structure increased the catenary's load resistance by 65%.

In order to create a stable 2D frame model of scenario 3, a form of constraint is required at the ends of the floors. This constraint can either be assumed rigid, resulting in the frame model of scenario 1, or employing spring boundary constraints to represent the floor stiffness of the individual building section, resulting in the frame model of scenario 3. When incorporating spring boundary constraints, the catenary response in scenario 3 was able to resist the gravity load to a load factor of 1.41. In this case, the 2D frame model of scenario 3 enables the structure to resist 259% more vertical gravity than the scenario 1 frame model. This underscores the significance of considering the in-plane behaviour of discrete floor systems when assessing the ability to form catenary action of modular building structures.

Connection optimisation

After the in-plane behavior of the floor systems into the 2D frame models, robust catenary action could not be established for both the building structures in scenarios 2 and 3. To achieve the necessary strength and elongation capacity, a connection optimisation was conducted on the case study building, employing two distinct methods. Method 1 resulted in a high-resistance connection with a stiff and brittle behaviour. The required resistance for the optimised connection, in order to allow the robust formation of catenary action, is 264.6 kN. This is an increase in resistance of 143% compared to the original connection which had a resistance of 108.9 kN. Method 2 resulted in a ductile connection with a large plastic elongation. The required resistance in the ductile connection is 169.2 kN. This is an increase of 55% compared to the original connection.

Preferred optimisation method

Both optimisation method 1 and method 2 result in a connection which allows the case study building structure to form a robust catenary. However, one cannot be preferred over the other when comparing the function of the connection in the scheme of robustness. According to the literature study, a building is robust when it can withstand propagation of damage to an extent which is disproportionate to the original damage. Both optimised connections successfully redistribute the additional gravity load resulting from the initial damage, namely the removal of a double intermediate façade column, and prevent the structure from undergoing partial collapse. In a deterministic quantification method for structural robustness, both connections reach the same goal and are therefore performed identically well. On the other hand, many building codes and design standards mandate the use of connections with ductile failure modes instead of connections with brittle failure modes. This is because they contain additional redundancy and present visible deformations as warning signs before failure. However, it is questionable whether these properties of ductile connections remain favorable in robustness scenarios. When optimising the connections, their redundancy in terms of post-yielding behavior is already taken into account. Furthermore, if a building does partially collapse due to a column removal event, the weakest connection in the catenary will transition from yielding to failing almost instantaneously, rendering the warning aspect ineffective.

Another way of determining a preferred optimisation method is to look at resulting material use. Excluding screws, bolts, and rods, the proposed optimised high-strength connection and fuse connection require 17.4 and 22.3 kg more steel than the original connection, respectively. As it stands, the fuse connection requires 4.9 kg more steel than the high-strength connection. However, in the current thesis, both connections are optimised with a DAF of 2.0. A benefit associated with the use of a ductile connection is that it dissipates more energy during deformation, thereby reducing the dynamic effects of sudden failure. A lower dynamic effect reduces the required resistance and elongation capacity of the connections. Consequently, less material is needed in the connection to meet the necessary capacity. Further research would have to determine the actual difference in required material use between the options, by taking into account befitting DAFs.

Catenary equation

The force-elongation graphs presented in Chapter 7 depict the catenary responses determined numerically for both the optimised high-strength connection and fuse connection. Additionally, these graphs illustrate the analytically determined catenary requirement boundary. When the loads in the numerical models are equal to the gravity loads used in the catenary equation, both the catenary responses and catenary requirement boundaries overlap. This implies that the catenary equation accurately predicts the necessary combination of total elongation in a catenary, maximum resistance, applied gravity load, and length of the floor elements. It is important to note that the moment of overlapping is not exact, as there is a small difference between the numerical and analytically determined catenary force, at the elongation where the numerical model resists the amplified gravity load. This difference is 1.2% for the high-strength connection and 0.5% for the fuse connection. However, these small differences are practically insignificant and can be attributed to inherent simplifications in the analytical formulation and discrepancies from the numerical analyses. Therefore, for practical purposes, the catenary equation can be considered a valid tool for determining the required resistance and elongation capacities of catenaries.

Even though load factor-displacement graphs can also show when a building can achieve a certain load factor corresponding to the maximum load in an accidental limit state, representing the formation of a robust catenary, the force-elongation response and the catenary requirement boundary can help better assess weather a catenary system requires more ductility or more resistance to enable a robust catenary response. Take for example Figure 6.9, showing the force-elongation responses of the 2D frame models of the case study building with rigid boundary constraints (scenario 1), spring boundary constraints of the full three section case study building (scenario 2), and spring boundary constraints of a single stand alone building section (scenario 3). For the latter, it becomes apparent that achieving a robust catenary response may be more attainable by increasing the resistance of the catenary by 50 kN, as opposed to increasing the total elongation by 266 mm. Such assessments are challenging with load factor-displacement response graphs alone.

It has to be mentioned that the catenary equation is particularly suited for timber modular buildings and the proposed connection type, as the inter-module connection has little to no rotational stiffness in the 2D frame. The equation as it is presented in this thesis is not accurate for modular buildings which, simultaneously with catenary action, rely on rotational strength in the connections to resist additional gravity loads. For instance, steel modules typically feature floor beam-to-column connections that are stiff to rigid. In the case of modular structures incorporating rotational stiffness in the connections between the floor and columns, the catenary equation would need to be adjusted to accommodate the extra load-carrying capacity resulting from moment-resisting flexural action in the connection.

9

Conclusion

This thesis was set out to providing an answer to the following research question:

What are the optimal mechanical properties of inter-module connections in timber modular buildings to facilitate structural robustness through catenary action and what method can be used to obtain these optimal properties?

In this chapter the concluding observations from the literature study and case study, and recommendations for further research, are presented.

9.1. Conclusions

Optimal mechanical properties

The main research question cannot be answered by giving an optimal pair of mechanical properties for inter-module connections which will allow the formation of catenary action in all timber modular buildings. From the literature review, the following two points regarding the required mechanical properties of catenaries and their connections can be concluded:

- The tensile resistance, required in the catenary elements to make equilibrium with the load on a catenary, reduce as the vertical deflection of the catenary increases. For a small vertical displacement elongation, a high tensile resistance in the catenary is required. If the catenary can elongate and deflect sufficiently, the required tensile resistance in the catenary can be reduced.
- The literature review points out that there are no specific requirements, such as a maximum deflection, for a structure to comply with for the formation of catenary action. It is up to the designer and engineer of a building to create a structure which can resist progressive collapse to an extend which is disproportionate to the of the initial damage. In the case of designing for catenary action, the designer must determine if an equilibrium state will be created at a large or small deflection.

Optimisation approach and catenary equation

Although no specific optimal mechanical properties can be appointed, this thesis does present an elaborate methodology which can be used to optimise an inter-module connection design to enable the robust formation of catenary action in a timber modular building. The optimisation method utilises an analytical optimisation tool, in the form of a catenary equation, to determine a bandwidth of befitting tensile resistance and elongation capacity combinations within a catenary which enable the robust formation of catenary action in timber modular buildings. Furthermore, the optimisation method relies on 2D quasi-static numerical analyses of the same building to determine the force-elongation response in catenary systems, following a column removal event.

The following can be concluded regarding the catenary equation:

- The catenary equation is a viable tool for determining a catenary requirement boundary (CRB). The catenary requirement boundary describes the required force-elongation relation in a catenary of a 2D frame, in order to find equilibrium with a central point load on the catenary. The input parameters of the equation are the point load on the catenary and the original length of the horizontal elements in the frame.
- The catenary equation and CRB are specifically helpful to engineers, because in combination with a force-elongation response of a catenary, they can visualise weather it is better to increase the resistance or the elongation capacity of the inter-module connection to enable a robust catenary response in a timber modular building.

In-plane floor behaviour

In order to conduct a numerical analysis which allows for the specific examination of catenary action in a timber modular building, a 2D frame model can be utilised. However, a limitation of the 2D approach is the exclusion of other alternative load paths in the analysis. In the context of timber modular buildings, the discrete floor systems represent one such alternative load path. Therefore, a distinct sub-goal was to determine the in-plane load-displacement and maximum resistance of discrete timber modular floor systems.

Key observations regarding the in-plane behaviour of discrete timber modular floor systems include:

- The in-plane load-deformation behaviour of timber discrete floor systems is heavily influenced by the stability system configuration and the accompanying boundary constraints.
- Smaller timber modular buildings with simple stability systems can lead to instable behaviours until the cavity between the two modules above the removed column is closed and catenary action can form. The extra deformation due to the instable response can be advantageous in forming catenary action an imposes a lower requirement on the resistance and elongation capacity of the inter-module connections.
- In large timber modular buildings with a more elaborate stability system configurations, the in-plane response of discrete timber floor system is shown to yield a stiffer response than for smaller timber modular buildings, therefore imposing a higher demand on the tension resistance and elongation capacity of the catenary.

Integration of floor behaviour in 2D frame model

Another sub goal was to develop an approach to integrate the in-plane behaviour of the timber modular floor systems into the 2D frame model of the building and determine the effects on the formation of catenary action.

- The case study showed that the in-plane behaviour of floors can seamlessly be integrated in the 2D frame model by implementing the stiffness of the floors in spring boundary constraints on the ends of the floors.
- The integration of in-plane behaviour from discrete floor systems into 2D frame models can substantially improve the elongation capacity of a catenary, and with that its load resistance, compared to a situation where the constraints are assumed rigid and in-plane behaviour of the floor systems is not incorporated. The actual increase of resistance is dependent on the building structure and its stability system configuration. In this study a building section of four modules wide and five modules high, with stability frames on the sides and back of the section, was analysed with a 2D frame model. Its ability to form catenary action was analysed with rigid boundary constraints at the ends of the floors, and spring boundary constraints. The spring boundary constraints represented the in plane floor stiffness of a standalone building section and a scenario where the building section has an accompanying building section on either side. For the stand alone building section, the vertical gravity load resistance increased by 259% when spring boundary constraints were applied, instead of rigid boundary conditions. For the building section enclosed by two other building sections, the load resistance increased by 65%.

Optimised connections

The case study ended by enhancing the performance of the timber modular case study building to enable robust catenary action by optimising the inter-module connections. Two distinct methods, focusing on either increasing the tensile resistance or overall ductility, were employed to create two optimised connection designs. Method 1 resulted in a high-strength with a brittle failure mode. Method 2 yielded a ductile connection by implementing a fuse and making use of the 20% plastic strain of S235 steel. The following conclusions can be drawn from the two optimised connections:

Method 1

- The inter-module connection from Method 1 facilitated robust catenary action by increasing its tensile resistance to 264.6 kN, a factor of 2.43 higher than the original connection's tension resistance.
- Despite a maximum elongation of only 1.99 mm and zero plastic elongation in the inter-module connection, the total elongation in the catenary reached 78 mm.

Method 2

- The inter-module connection design from Method 2 achieved a maximum tensile resistance of 169.2 kN, a factor 1.55 higher than the original connection.
- The inclusion of a fuse in the inter-module connection, with a length of 550 mm and a cross-section of 90 by 8 mm, allowed for a single fuse to undergo plastic deformation of 110 mm. During the alternative load path analysis, the catenary reached a total elongation of 169 mm at the moment of maximum loading.

General conclusions

- To fully utilise the plastic elongation of the fuse, it is crucial that the tensile resistance of the inter-module connection is governed by the maximum resistance of the fuse.
- A critical discussion highlighted the significance of using fitting dynamic amplification factors for determining the required load in the catenary equation. The discussion emphasised that for a true optimisation of the inter-module connection a dynamic structural analysis is required in the optimisation process, as adding plastic deformation increases the energy dissipation potential and decreases the dynamic effect on the load. This in turn decreases the resistance and elongation requirements for the catenary component. This is especially beneficial for the fuse connection as it allows for more ductility and energy dissipation.
- The optimisation methods are adaptable in their application for varying timber modular building configurations.

9.2. Recommendations

In light of the successful optimisation of inter-module connections in a timber modular building for achieving robustness through catenary action, the following recommendations provide compelling directions for further research.

- This thesis employed 2D models of the timber modular building to evaluate the in-plane floor behaviour and catenary action in the façade construction. Consequently, certain ALPs were omitted, leading to a conservative estimation of the load distribution in the catenaries. To obtain a more precise understanding of the loads in the catenaries, it is advisable to extend the study by implementing a 3D modelling approach, which would incorporate additional resistance mechanisms. In order to optimise the connections with a 3D approach, the catenary equation would likely necessitate an adjustment to take into account the influence of additional load paths on the required axial load in the catenary.
- This study employed a DAF of 2.0 to determine the CRB, which was subsequently utilised in the optimisation of the inter-module connections with both optimisation methods. For increased precision in determining the CRB, and achieving further optimisation in subsequent applications, it is advisable to conduct a detailed study on the energy dissipation capabilities of both optimised

connections and its correlated dynamic effect on the gravity loads. This provides more insights into the overall structural behaviour of the structure with the new connections and allows for further optimisation.

- The modelled behaviour of the inter- and intra-module connections are based on an assumed spring model, offering a reasonable estimation of overall connection performance. However, like any model, it remains a conceptual representation of reality. Certain factors and limitations that could impact connection performance, such as prying forces during closing rotations, maximum rotation limits, and accurate assessments of tensile resistance and elongation capacity in a rotated state, are not fully considered in the spring model. Further research, potentially through experimental testing, is essential to validate the proposed performance of the connections.
- The catenary equation in this research depicts a catenary requirement boundary for catenary action in the façades of structures with single span floors and lacking rotation stiffness in the connections between floors or beams and columns. Further research efforts should be directed towards adjusting the catenary equation to accommodate structures with rotational stiffness in their connections, thereby extending its applicability to a broader spectrum of building types.
- The goal of this thesis was to optimise connections to enable catenary action in timber modular buildings. The two proposed optimisation methods yield two different connection designs. However, as robustness is analysed in a deterministic analysis method with a binary valued result, robustness is achieved or not, neither optimisation methods can be labelled as best practice. To be able to appoint a better method, other assessment criteria need to be researched. Further study in adapting different steel strengths with different plastic elongations can for example point out a potential best method in terms of material use and production costs.
- Expanding on this connection optimisation study, future research should explore alternative connection types to unveil the adaptability and effectiveness of the methods across different structural configurations. Moreover, researching other connection types on the ability to provide robustness through catenary action can provide engineers with a broader toolkit for possible connection types to apply in other structural systems.

Part IV

References and Appendices

References

[1] J. Knuppe, "Robustness of Modular Timber Buildings: An investigation into alternative load paths in volumetric timber post and beam modules," Delft University of Technology, Delft, Tech. Rep., 2022. [Online]. Available: https://repository.tudelft.nl/islandora/object/uuid:f6bf1b27-322b-4f2c-9d15-d96604a2e946.

[2] M. Lawson, R. Ogden, and R. Bergin, "Application of Modular Construction in High-Rise Buildings," *Journal of Architectural Engineering*, vol. 18, no. 2, pp. 148–154, Jun. 2012, ISSN: 1076-0431. DOI: 10.1061/(asce)ae.1943-5568.0000057.

[3] H. T. Thai, Q. V. Ho, W. Li, and T. Ngo, "Progressive collapse and robustness of modular high-rise buildings," *Structure and Infrastructure Engineering*, vol. 19, no. 3, pp. 302–314, 2022, ISSN: 17448980. DOI: 10.1080/15732479.2021.1944226.

[4] F. E. Boafo, J. H. Kim, and J. T. Kim, "Performance of modular prefabricated architecture: Case study-based review and future pathways," *Sustainability (Switzerland)*, vol. 8, no. 6, Jun. 2016, ISSN: 20711050. DOI: 10.3390/su8060558.

[5] World Economic Form, "Industry Agenda Shaping the Future of Construction A Breakthrough in Mindset and Technology Prepared in collaboration with The Boston Consulting Group," Geneva, Tech. Rep., May 2016. [Online]. Available: https://www.weforum.org/reports/shaping-the-future-of-construction-a-breakthrough-in-mindset-and-technology/.

[6] V. Tavares, N. Lacerda, and F. Freire, "Embodied energy and greenhouse gas emissions analysis of a prefabricated modular house: The "Moby" case study," *Journal of Cleaner Production*, vol. 212, pp. 1044–1053, 2019, ISSN: 0959-6526. DOI: https://doi.org/10.1016/j.jclepro.2018.12.028. [Online]. Available: https://www.sciencedirect.com/science/article/pii/S0959652618337302.

[7] W. Pan, Y. Yang, and L. Yang, "High-Rise Modular Building: Ten-Year Journey and Future Development," in *Construction Research Congress 2018: Sustainable Design and Construction and Education - Selected Papers from the Construction Research Congress 2018*, vol. 2018-April, American Society of Civil Engineers (ASCE), 2018, pp. 523–532, ISBN: 9780784481301. DOI: 10.1061/9780784481301.052.

[8] S. Srisangeerthanan, M. J. Hashemi, P. Rajeev, E. Gad, and S. Fernando, "Review of performance requirements for inter-module connections in multi-story modular buildings," *Journal of Building Engineering*, vol. 28, Mar. 2020, ISSN: 23527102. DOI: 10.1016/j.jobe.2019.101087.

[9] CEN, "Eurocode 1: Actions on structures - Part 1-7: General actions - Accidental actions," Delft, Tech. Rep., 2015.

[10] J. A. J. Huber, M. Ekevad, U. A. Girhammar, and S. Berg, "A Review of Structural Robustness with Focus on Timber Buildings," in *40th IABSE Symposium*, Nantes: Tomorrow's Megastructures, Sep. 2018, pp. 17–25. DOI: 10.2749/nantes.2018.s32-17.

[11] F. J. Luo, Y. Bai, J. Hou, and Y. Huang, "Progressive collapse analysis and structural robustness of steel-framed modular buildings," *Engineering Failure Analysis*, vol. 104, pp. 643–656, Oct. 2019, ISSN: 13506307. DOI: 10.1016/j.engfailanal.2019.06.044.

[12] M. Alembagheri, P. Sharafi, R. Hajirezaei, and Z. Tao, "Anti-collapse resistance mechanisms in corner-supported modular steel buildings," *Journal of Constructional Steel Research*, vol. 170, Jul. 2020, ISSN: 0143974X. DOI: 10.1016/j.jcsr.2020.106083.

[13] H. T. Thai, T. Ngo, and B. Uy, "A review on modular construction for high-rise buildings," *Structures*, vol. 28, pp. 1265–1290, Dec. 2020, ISSN: 23520124. DOI: 10.1016/j.istruc.2020.09.070.

[14] Y. S. Chua, J. Y. Liew, and S. D. Pang, “Modelling of connections and lateral behavior of high-rise modular steel buildings,” *Journal of Constructional Steel Research*, vol. 166, Mar. 2020, ISSN: 0143974X. DOI: 10.1016/j.jcsr.2019.105901.

[15] Y. S. Chua, S. D. Pang, J. Y. Liew, and Z. Dai, “Robustness of inter-module connections and steel modular buildings under column loss scenarios,” *Journal of Building Engineering*, vol. 47, Apr. 2022, ISSN: 23527102. DOI: 10.1016/j.jobe.2021.103888.

[16] Institution of Structural Engineers, *Practical Guide to Structural Robustness and Disproportionate Collapse in Buildings*. London: Institution of Structural Engineers, 2010, ISBN: 978-1-906335-17-5.

[17] Arup Group, “Review of international research on structural robustness and disproportional collapse,” Department for Communities and Local Government, London, Tech. Rep., Oct. 2011.

[18] P. Palma and G. Fink, *Design for robustness, adaptability, disassembly and reuse, and repairability of taller timber buildings: a state of the art report*, Jan. 2022.

[19] J. A. Huber, M. Ekevad, U. A. Girhammar, and S. Berg, “Structural robustness and timber buildings–a review,” *Wood Material Science and Engineering*, vol. 14, no. 2, pp. 107–128, Mar. 2018, ISSN: 17480280. DOI: 10.1080/17480272.2018.1446052.

[20] K. Voulpiotis, “Robustness of Tall Timber Buildings,” Ph.D. dissertation, ETH Zurich, Zurich, Oct. 2021. DOI: 10.3929/ethz-b-000526211.

[21] J. A. Huber, “Numerical Modelling of Timber Building Components to Prevent Disproportionate Collapse,” Ph.D. dissertation, Luleå University of Technology, Skellefteå, 2021, ISBN: 978-91-7790-881-4.

[22] U. Starossek and M. Haberland, “Approaches to measures of structural robustness,” *Structure and Infrastructure Engineering*, vol. 7, no. 7-8, pp. 625–631, 2011. DOI: 10.1080/15732479.2010.501562. [Online]. Available: https://doi.org/10.1080/15732479.2010.501562.

[23] M. P. Byfield, “Behavior and Design of Commercial Multistory Buildings Subjected to Blast,” *Journal of Performance of Constructed Facilities*, vol. 20, no. 4, pp. 324–329, 2006. DOI: 10.1061/ASCE0887-3828200620:4324.

[24] P. Smith, “An Investigation into Tensile Membrane Action as a Means of Emergency Load Redistribution,” Ph.D. dissertation, University of Southampton, 2016. [Online]. Available: https://eprints.soton.ac.uk/418026/.

[25] H. Mpidi Bita, J. A. J. Huber, P. Palma, and T. Tannert, “Prevention of Disproportionate Collapse for Multistory Mass Timber Buildings: Review of Current Practices and Recent Research,” *Journal of Structural Engineering*, vol. 148, no. 7, Jul. 2022, ISSN: 0733-9445. DOI: 10.1061/(asce)st.1943-541x.0003377.

[26] K. Voulpiotis, S. Schär, and A. Frangi, “Quantifying robustness in tall timber buildings: A case study,” *Engineering Structures*, vol. 265, Aug. 2022, ISSN: 18737323. DOI: 10.1016/j.engstruct.2022.114427.

[27] H. Mpidi Bita and T. Tannert, “Experimental Study of Disproportionate Collapse Prevention Mechanisms for Mass-Timber Floor Systems,” *Journal of Structural Engineering*, vol. 146, no. 2, Feb. 2020, ISSN: 0733-9445. DOI: 10.1061/(asce)st.1943-541x.0002485.

[28] M. Byfield and S. Paramasivam, “Catenary action in steel-framed buildings,” *Proceedings of the Institution of Civil Engineers: Structures and Buildings*, vol. 160, no. 5, pp. 247–257, Oct. 2007, ISSN: 09650911. DOI: 10.1680/stbu.2007.160.5.247.

[29] FBI, *The Oaklahoma City Bombing: 20 Years Later*, Apr. 2015. [Online]. Available: https://www.fbi.gov/news/stories/the-oklahoma-city-bombing-20-years-later.

[30] NIST, “Global structural analysis of the response of the World Trade Center towers to impact damage and fire (Chapters 4- Appendix C),” National Institute of Standards and Technology, Gaithersburg, MD, Tech. Rep., 2005. DOI: 10.6028/NIST.NCSTAR.1-6dv2. [Online]. Available: https://nvlpubs.nist.gov/nistpubs/Legacy/NCSTAR/ncstar1-6dv2.pdf.

[31] M. T. Ahmadi, A. A. Aghakouchak, R. Mirghaderi, *et al.*, "Collapse of the 16-Story Plasco Building in Tehran due to Fire," *Fire Technology*, vol. 56, no. 2, pp. 769–799, Mar. 2020, ISSN: 15728099. DOI: 10.1007/s10694-019-00903-y.

[32] S. Epackachi, S. R. Mirghaderi, and P. Aghelizadeh, "Failure analysis of the 16-story Plasco building under re condition," *Scientia Iranica*, vol. 29, no. 3A, pp. 1107–1124, May 2022, ISSN: 23453605. DOI: 10.24200/SCI.2022.57903.5495.

[33] A. A. Aghakouchak, S. Garivani, A. Shahmari, and M. Heshmati, "Structural investigation of the collapse of the 16-story Plasco building due to fire," *Structural Design of Tall and Special Buildings*, vol. 30, no. 1, Jan. 2021, ISSN: 15417808. DOI: 10.1002/tal.1815.

[34] C. H. Lyu, B. P. Gilbert, H. Guan, *et al.*, "Experimental collapse response of post-and-beam mass timber frames under a quasi-static column removal scenario," *Engineering Structures*, vol. 213, p. 110 562, 2020, ISSN: 0141-0296. DOI: https://doi.org/10.1016/j.engstruct.2020.110562. [Online]. Available: https://www.sciencedirect.com/science/article/pii/S0141029619342178.

[35] H. Mpidi Bita and T. Tannert, "Disproportionate collapse prevention analysis for a mid-rise flat-plate cross-laminated timber building," *Engineering Structures*, vol. 178, pp. 460–471, 2019, ISSN: 0141-0296. DOI: https://doi.org/10.1016/j.engstruct.2018.10.048. [Online]. Available: https://www.sciencedirect.com/science/article/pii/S0141029618325719.

[36] A. Przystup, T. Reynolds, and T. Tannert, "Experimental and numerical analyses of full- span floors and component level subassem- blies for robust design of CLT floors," Jan. 2023.

[37] K. Voulpiotis, J. Köhler, R. Jockwer, and A. Frangi, "A holistic framework for designing for structural robustness in tall timber buildings," *Engineering Structures*, vol. 227, Jan. 2021, ISSN: 18737323. DOI: 10.1016/j.engstruct.2020.111432.

[38] J. A. J. Huber, Y. Huang, S. Knutsen, A. Przystup, T. Tannert, and S. Berg, "APPLICATION OF A TUBE CONNECTOR FOR CATENARY ACTION IN CLT FLOORS," in *World Conference on Timber Engineering*, Oslo, Feb. 2023, pp. 1216–1223. DOI: 10.52202/069179-0166.

[39] General Service Administration, "Alternate Path Analysis and Design Guidelines for Progressive Collapse Resistance," General Service Administration, Tech. Rep., Jan. 2016.

[40] Department of Defense, "Design of Buildings to Resist Progressive Collapse," Unified Facilities Criteria, Tech. Rep., Nov. 2016. [Online]. Available: http://dod.wbdg.org/..

[41] Stufib, "Constructieve samenhang van bouwconstructies Stufib-rapport 8," Bunschoten, Tech. Rep., Sep. 2006. [Online]. Available: https://stufib.nl/downloads/rapportenstufib/.

[42] P. M. Lawson, M. P. Byfield, S. O. Popo-Ola, and P. J. Grubb, "Robustness of light steel frames and modular construction," *Proceedings of the Institution of Civil Engineers: Structures and Buildings*, vol. 161, no. 1, pp. 3–16, 2008, ISSN: 09650911. DOI: 10.1680/stbu.2008.161.1.3.

[43] CEN, "Eurocode 5: Design of timber structures - Part 1-1: General-Common rules and rules for buildings," Nederlands Normalisatie-instituut, Delft, Tech. Rep., 2005.

[44] A. S. Rebouças, Z. Mehdipour, J. M. Branco, and P. B. Lourenço, "Ductile Moment-Resisting Timber Connections: A Review," *Buildings*, vol. 12, no. 2, 2022, ISSN: 2075-5309. DOI: 10.3390/buildings12020240. [Online]. Available: https://www.mdpi.com/2075-5309/12/2/240.

[45] CEN, "Eurocode 3: Design of steel structures - Part 1-1: General rules and rules for buildings," Tech. Rep., 2006.

[46] Stora Enso, *Cross-laminated timber (CLT)*, Oct. 2017. [Online]. Available: https://www.storaenso.com/en/products/mass-timber-construction/building-products/clt#T2c3af613-108a-4115-bf63-165f74694654.

[47] C. Johansson and E. Johansson, "Modeling of Cross Laminated Timber in FE Analysis A sensitivity study regarding different CLT modeling assump-tions and their influence on high-rise timber buildings (Master's Thesis)," Chalmers University of Technology, Gothenburg, Tech. Rep., 2021. [Online]. Available: www.chalmers.se.

[48] G. R. Liu and S. S. Quek, “Briefing on Mechanics for Solids and Structures,” in *The Finite Element Method*, Aug. 2014, pp. 13–41, ISBN: 9780080983561. DOI: 10.1016/B978-0-08-098356-1.00002-3.

[49] S. Ashtari, “In-plane Stiffness of Cross-laminated Timber Floors (Master’s Thesis),” University of British Columbia Library, Vancouver, Tech. Rep., 2012. DOI: 10.14288/1.0073342.

[50] E. Rizzi, M. Capovilla, M. Piazza, and I. Giongo, “In-Plane Behavior of Timber Diaphragms Retrofitted with CLT Panels: An Interdisciplinary Approach,” in Aug. 2019, pp. 1613–1622, ISBN: 978-3-319-99440-6. DOI: 10.1007/978-3-319-99441-3{_}173.

[51] Swedish Wood, *The CLT Handbook*, 1st ed., E. Borgström and J. Fröbel, Eds. Stockholm: Skogsindustrierna, 2019, ISBN: ISBN 978-91-983214-4-3. [Online]. Available: www.traguiden.se,.

[52] J. Sharifi, “In-Plane Shear Modulus of Cross-Laminated Timber,” Ph.D. dissertation, Luleå University of Technology, Wood Science and Engineering, 2021, ISBN: 978-91-7790-824-1.

[53] N. Khorsandnia, H. Valipour, and K. Crews, “Structural response of timber-concrete composite beams predicted by finite element models and manual calculations,” in *Advances in Structural Engineering*, vol. 17, Aug. 2013.

[54] M. Lavrenčič and B. Brank, “Failure analysis of ribbed cross-laminated timber plates,” *Coupled Systems Mechanics*, vol. 7, pp. 79–93, Aug. 2018. DOI: 10.12989/csm.2018.7.1.079.

[55] L. Ekhagen, “FE-Modelling of a Joint for Cross-Laminated Timber,” Ph.D. dissertation, Karlstad University, Karlstad, 2021.

[56] Dassault Systèmes, *Linear elastic behavior*, 2008. [Online]. Available: https://classes.engineering.wustl.edu/2009/spring/mase5513/abaqus/docs/v6.6/books/usb/default.htm?startat=pt05ch17s02abm02.html.

[57] CEN, “NEN-EN 14080 Timbe structures - Glued laminated timber and glued solid timber - Requirements 2013,” Nederlands Normalisatie-instituut, Delft, Tech. Rep., Jul. 2012.

[58] Dassault Systèmes, *Surface-based cohesive behavior*, 2008. [Online]. Available: http://130.149.89.49:2080/v6.8/books/usb/default.htm?startat=pt09ch31s01alm62.html.

[59] M. Ferraioli, “A modal pushdown procedure for progressive collapse analysis of steel frame structures,” *Journal of Constructional Steel Research*, vol. 156, pp. 227–241, 2019, ISSN: 0143-974X. DOI: https://doi.org/10.1016/j.jcsr.2019.02.003. [Online]. Available: https://www.sciencedirect.com/science/article/pii/S0143974X18309428.

[60] P. Kossakowski, “Influence of Initial Porosity on Strength Properties of S235JR Steel at Low Stress Triaxiality,” *Archives of Civil Engineering*, vol. 58, pp. 293–308, Jan. 2012. DOI: 10.2478/v.10169-012-0017-9.

[61] A. Cao, P. Palma, and A. Frangi, “Column removal analyses of timber structures - Framework to assess dynamic amplification factors for simplified structural design methods,” Dec. 2021.

[62] T. Bogensperger, T. Moosbrugger, and G. Silly, “Verification of CLT-plates under loads in plane,” in *11th World Conference on Timber Engineering, WCTE 2010*, 2010, pp. 1–9. [Online]. Available: https://www.researchgate.net/publication/265653209.

[63] Rothoblaas, *VGZ - Full threaded screw with cylindrical head*. [Online]. Available: https://www.rothoblaas.com/products/fastening/screws/screws-structures/vgz#technical-data-0.

[64] J. M. Biggs, *Introduction to Structural Dynamics*. 1964, ISBN: 0070052557.

[65] C. Zhang, H. Hong, K. Bi, and Y. Xueyuan, “Dynamic amplification factors for a system with multiple-degrees-of-freedom,” *Earthquake Engineering and Engineering Vibration*, vol. 19, pp. 363–375, Dec. 2020. DOI: 10.1007/s11803-020-0567-9.

[66] X. Cheng, B. P. Gilbert, I. Underhill, and H. Karampour, “Experimental dynamic collapse response of post-and-beam mass timber frames under a sudden column removal scenario,” *Engineering Structures*, vol. 233, p. 111 918, Dec. 2021. DOI: 10.1016/j.engstruct.2021.111918.

[67] P. Palma, R. Steiger, and R. Jockwer, “Addressing design for robustness in the 2nd□generation EN 1995 Eurocode 5,” Dec. 2019.

A

Hand calculations on catenary solutions and catenary equation

Annex A presents multiple hand calculations on a standard catenary system. For every calculation, different fixed parameters are assumed to asses at which deformations, loads, and elongations the system finds equilibrium. It is assumed that under normal use, the vertical floor loads are evenly distributed on the module floors, and when a column is removed, the reaction force on that column becomes the acting load.

Loading situation

Load combination

According to NEN-EN 1990 section 8.3.4.3 the accidental load combination is:

$$E_d = \sum G_{k,j} + \Psi_{2,1}\, Q_{k,1} + \sum \Psi_{2,i}\, Q_{k,i}$$

According to the Dutch national annex:

$$E_d = \sum G_{k,j} + 0.3\, Q_{k,1}$$

Loads

From Knuppe (2022) [1]:

Load	Symbol	Value	Unit
Self weight of the floor	$G_{k,floor}$	3.72	kN/m^2
Self weight of the ceiling	$G_{k,ceiling}$	0.7	kN/m^2
Live load floor (residential)	$Q_{k,floor}$	3.0	kN/m^2

Table A.1: Vertical loads on module

Total load on the floor

$$E_d = \sum (3.72 + 0.7)0.3 \cdot 3.0 = 5.32\, kN/m^2$$

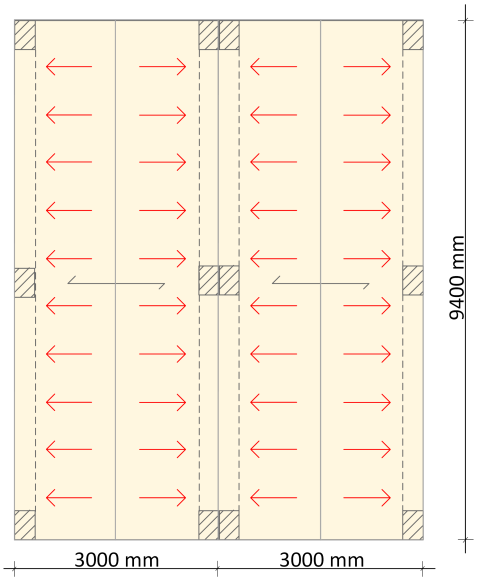

Figure A.1: Distribution of loads on floor and ceiling

Line load on two adjacent beams

$$q_d = 2 \cdot \frac{1}{2} \cdot b \cdot E_d = 2 \cdot \frac{1}{2} \cdot 3 \cdot 5.32 = 15.96\, kN/m$$

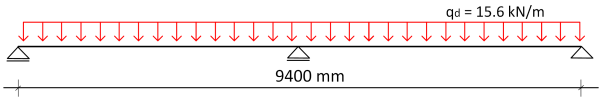

Figure A.2: Distribution of loads on two floor beams

Reaction force on the outer column

$$R_1 = \frac{3}{8}\, q\, l = \frac{3}{8} \cdot 15.96 \cdot 9.4 = 28.13 kN$$

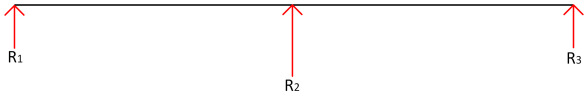

Figure A.3: Reaction forces of the two outer and middle columns

Accounting for Dynamic Amplification Factor

When taking dynamic amplification factor 2.0, the full catenary over 4 floor fields can be schematised as the following:

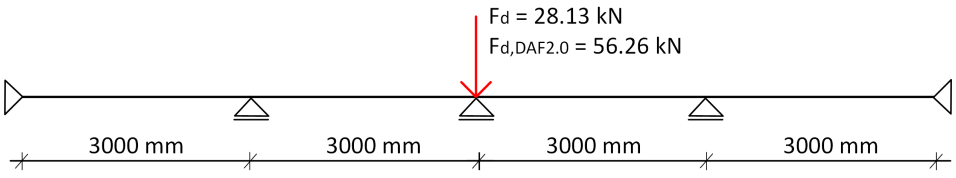

Figure A.4: Load on a facade column at accidental limit state due to intermediate facade column removal.

Equilibrium situations

Based on simple geometry and equilibrium of forces deflections, the elongations and catenary forces are calculated. Six situations are presented with different set parameters (indicated in red text in the figures below).

Assuming maximum rotation of 0.15 Rad as Knuppe proposed as maximum rotation in the inter-module connections.

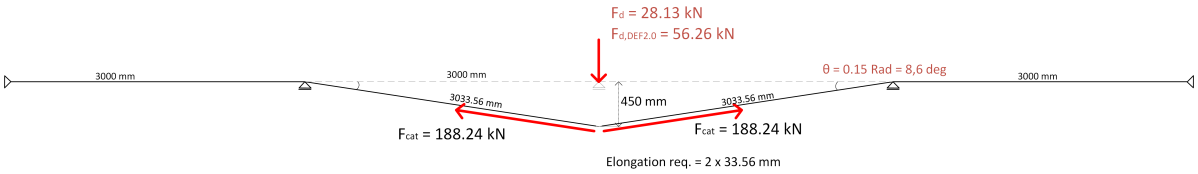

Assuming maximum catenary reaction force of 100 kN.

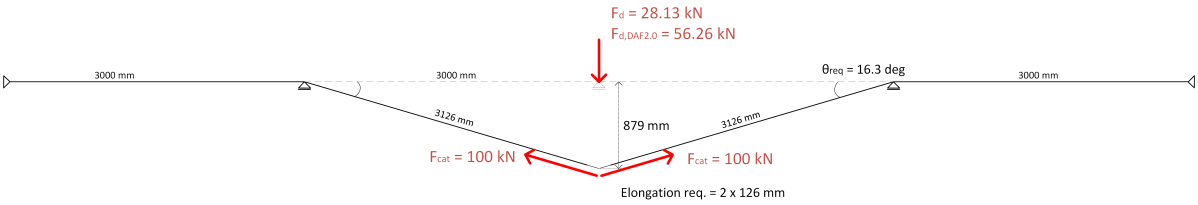

Assuming a Dynamic Amplification Factor of 1.5 and a maximum catenary force of 100 kN.

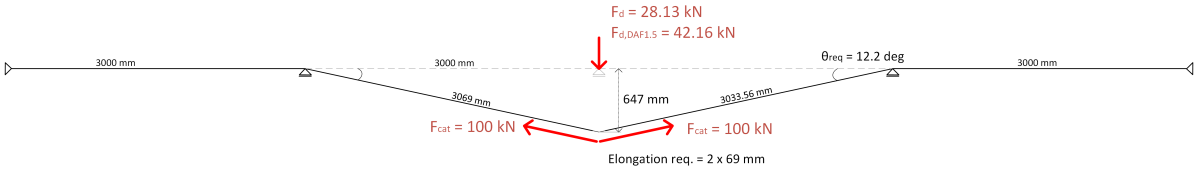

Assuming maximum axial elastic deformation of 3.36 mm (Knuppe, 2022) in all connections. E.I. a total elongation of 8 x 3.36 = 26.88 mm.

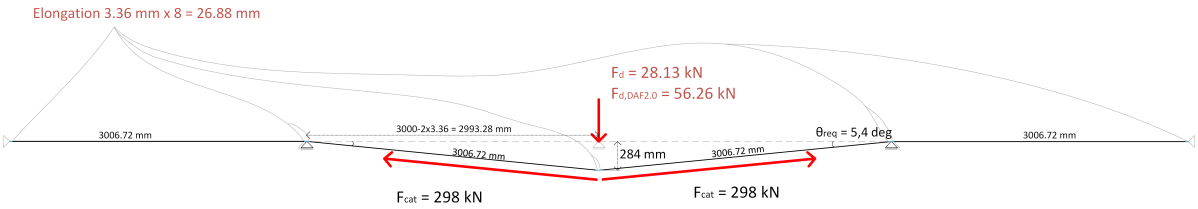

The situation with a maximum catenary force of 100 kN gave a required elongation of the system of 2 x 126 = 252 mm. Assuming a total elongation of 252 mm spread over different locations gives the following:

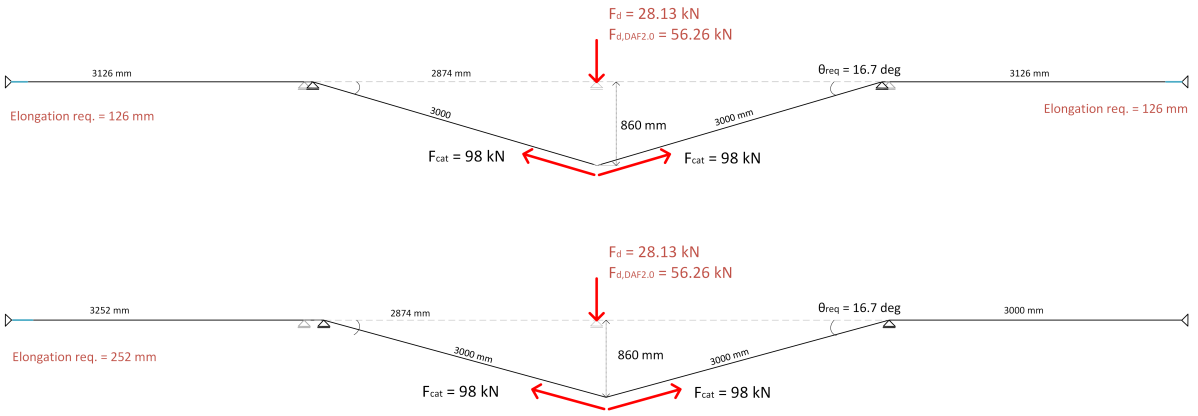

Conclusions from equilibrium situations

- If a maximum rotational deformation capacity of 0.15 Rad is to be assumed, the required capacity of the elements in the catenary is 188.24 kN. Furthermore, a total elongation of 33.56 mm is required (per side of the catenary) to facilitate the 450 mm deflection in the catenary.
- According to Knuppe, the yield resistance of the connection is 108.9 kN [1]. If a maximum catenary force of 100 kN is imposed, the catenary requires a vertical deflection of 879 mm. Corresponding to this deflection an elongation is required of 126 mm (per side of the catenary).
- If a DAF of 1.5 is used to decrease amplified gravity load, and the maximum tensile capacity in the catenary is kept at 100 kN, the required elongation in the catenary decreases by a factor 0.55. This indicates that the relation between the load on the catenary and the required elongation is nonlinear.
- For small elongations, the location of the elongation has an inconsiderable impact on the catenary force and the deflection. In the situation where all deformation originates in the deflecting elements, and where the maximum catenary force is set to 100 kN the required elongation is 126 mm per side of the catenary. If the same elongation is spread over all connections, or located at one end of the system, the deflection and catenary force are decreased by only 2%.
- As the location of the elongation in the catenary has a negligible effect on the forces in the catenary, it can be concluded that any additional deformation in the system, e.g. due to in-plane deformation of the modular floor system, can be inserted anywhere along the catenary by an additional spring.

Catenary equation

As concluded above, the location where the elongation occurs within the system has an inconsiderable impact on its equilibrium. This finding implies that the elongation required to support a 4-field catenary, is essentially the same as that needed for a 2-field catenary. It allows the establishment of an equation that quantifies the relationship between the catenary force and the corresponding elongation in the system. This equation serves as a fundamental tool in analysing and designing structures that rely on catenary action. The derivation of the equation is given below.

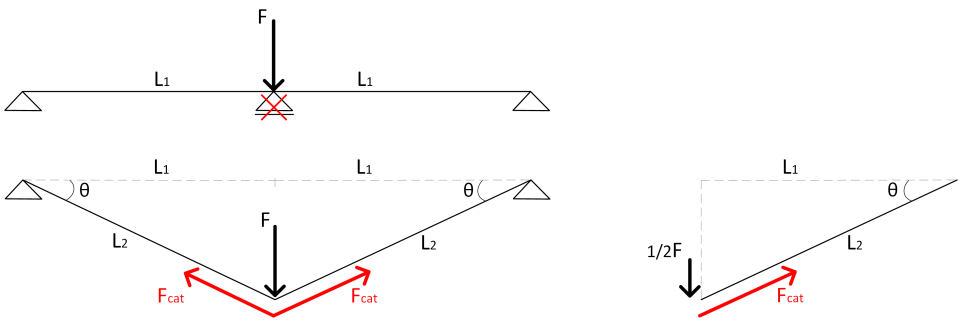

The following two equations apply:

$$\sin(\theta) = \frac{\frac{1}{2}F}{F_{cat}} \tag{A.1}$$

and

$$\cos(\theta) = \frac{L_1}{L_2} \tag{A.2}$$

Remember the Pythagorean identity: $\cos(\theta) = \sqrt{1 - \sin^2(\theta)}$

Combine the Pythagorean identity with Equation A.2 and rewrite:

$$\sqrt{1 - \sin^2(\theta)} = \frac{L_1}{L_2}$$

$$1 - \sin^2(\theta) = \left(\frac{L_1}{L_2}\right)^2$$

$$\sin(\theta) = \sqrt{1 - \left(\frac{L_1}{L_2}\right)^2} \tag{A.3}$$

Combine the Equation A.3 with Equation A.1: and rewrite:

$$\frac{F}{2F_{cat}} = \sqrt{1 - \left(\frac{L_1}{L_2}\right)^2}$$

$$\frac{1}{F_{cat}} = \frac{2\sqrt{1 - \left(\frac{L_1}{L_2}\right)^2}}{F}$$

$$F_{cat} = \frac{F}{2\sqrt{1 - \left(\frac{L_1}{L_2}\right)^2}} \tag{A.4}$$

The elongation of one side of the catenary is calculated as:

$$\Delta l = L_2 - L_1$$

And so the elongation of the total catenary is:

$$\Delta l = 2(L_2 - L_1)$$

Rewrite to:

$$L_2 = \frac{1}{2}\Delta l + L_1 \tag{A.5}$$

Now combine Equation A.5 with Equation A.4 to describe the relation between the force in the catenary and the total elongation of the catenary.

$$F_{cat} = \frac{F}{2\sqrt{1 - \left(\frac{L_1}{\frac{1}{2}\Delta l + L_1}\right)^2}} \tag{A.6}$$

Where:

L_1	Length of a module floor in the direction of the catenary
F	Load on the removed column which has to be taken up by the catenary

B

Mean shear modulus of CLT panel

When the edges of the boards in a CLT panel are not glued, the shear modulus of the whole cross section, G¬s,mean, differs from the shear modulus of a single board, G¬0,mean. Due to the gap between the boards, no interaction takes place between the boards in a single lamella. This effect, together with the effect of having different thicknesses of lamellas in uneven layups, causes a different shear modulus of a CLT panel, compared to a single board. Bogensperger et al. [62] described the relation between the shear modulus of a CLT panel and a timber board as:

$$\frac{G_{s,mean}}{G_{0,mean}} = \frac{1}{1 + 6 * \alpha_{FE-FIT,ortho} * \left(\frac{t}{a}\right)^2} \tag{B.1}$$

With:

$$\alpha_{FE-FIT,ortho} = 0.32 * \left(\frac{t}{a}\right)^2 \tag{B.2}$$

Where:

t Mean thickness of boards

a Mean board width

$G_{0,mean}$ Mean shear modulus of a timber board

The mean thickness of the boards in the CLT floor (t) is 32 mm, and average widths of the boards (a) are 200 mm [46]. The mean shear modulus of the CLT panel can therefore be calculated as:

$$G_{s,mean} = 0.832 * G_{0,mean} \tag{B.3}$$

C

Calculations of the connection properties

The connection between the CLT panel and the GLT beams is designed with crosswise inclined dowel type fasteners pairs. The design is determined by the idea that the fasteners entering from the bottom of the CLT panel provides the shear resistance to the vertical floor load and the fasteners entering from the top of the CLT panel provides rotational restraint to the eccentrically connected beam. The module floor is engineered to have sufficient capacity in the Ultimate Limit State. The fasteners in this study are VGZ screws from Rothoblaas with a diameter of 7 mm and a length of 260 mm [63]. The ULS design of the connection determined that sufficient capacity is included when the spacing of the fastener pairs is 150 mm as shown in figure C.1. As the fasteners are distributed over a total length of 9.4 meters (the length of the module) the stiffness and strength of the connection can best be described as a value per running meter. This is also the value which is required as input in Abaqus for the surface-to-surface interaction properties.

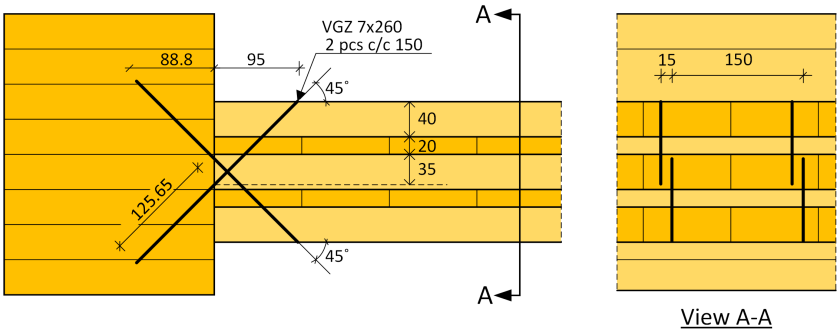

Figure C.1: Intra module connection between CLT panel and GLT beams

Properties
The resistance and stiffness of the screw connection are calculated, for the accidental limit state, according to Eurocode 5 and the Johansen model. As a result, most safety factors are omitted from the equations and the partial factors are as given in table C.2.

Number of effective fasteners:

$$n_{ef} = \frac{1000}{150} = 6.7$$

Table C.1: Properties of a VGZ 7x260 screw [63]

VGZ 7x260	Symbol	Value	Unit
Outer thread diameter of screw	d	7	mm
Inner thread diameter of screw	d_1	7	mm
Condition	d_1/d	0.71	
Head diameter	d_h	9.5	mm
Length	L	260	mm
Thread length	L_{thr}	250	mm
Angle between screw axis and timber grain (beam)	α_{beam}	90	°
Angle between screw axis and timber grain (panel)	$\alpha_{beam,1}$	45	°
	$\alpha_{beam,2}$	90	°
Effective contact length at the screw head	$l_{eff,beam}$	124.35	mm
Effective contact length at the screw tip	$l_{eff,panel}$	115.65	mm
Characteristic wood density	ρ_k	350	kg/m^3
Mean wood density	ρ_{mean}	420	kg/m^3
Yield strength of screw	$f_{y,k}$	1000	N/mm^2
Characteristic ultimate strength of screw	$f_{u,k}$	1240	N/mm^2

Table C.2: Partial factors and modification factor for accidental limit state

Parameter	Symbol	Value	Comment
Partial factor for timber	γ_M	1	
Modification factor	k_{mod}	1.1	
Partial factor for steel	γ_{M2}	1	
Partial factor shear strength	k_{shear}	1.2	According to EC5 9.2.4.2 [43]

Shear strength

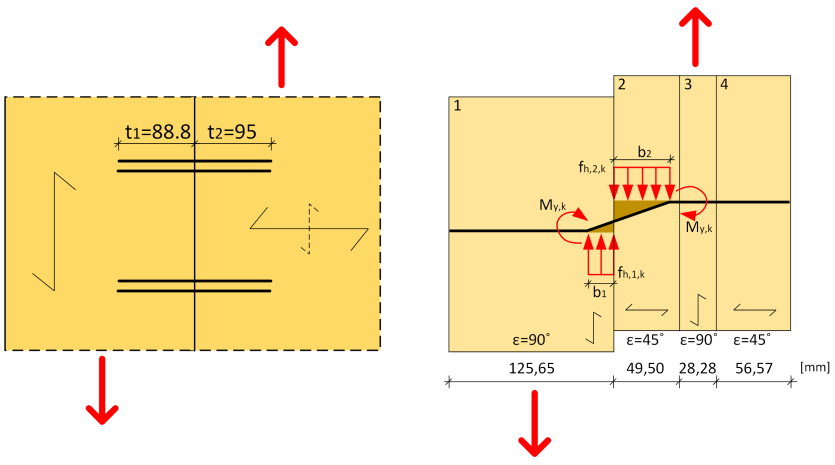

Figure C.2: Situation of connection in shear and failure mode f of the Johansen model

The strength of the connection in shear is determined according to the Johansen model and is determined by the embedment strength, the yield moment of the fastener and the joint geometry. For dowel type fasteners with one shear plane, 6 failure modes can occur. The different characteristic value of the dowel-effect contribution per shear plane $F_{D,k}$ are described by the Equation C.1:

$$F_{D,k} = min\begin{cases} f_{h,1,k}\, t_{h,1}\, d & (a) \\ f_{h,2,k}\, t_{h,2}\, d & (b) \\ \frac{f_{h,1,k}\, t_{h,1}\, d}{1+\beta}\left[\sqrt{\beta + 2\,\beta^2\left[1+\frac{t_{h,2}}{t_{h,1}}+(\frac{t_{h,2}}{t_{h,1}})^2\right]} - \beta\,(1+\frac{t_{h,2}}{t_{h,1}})\right] & (c) \\ \frac{f_{h,1,k}\, t_{h,1}\, d}{2+\beta}\left[\sqrt{2\beta\,(1+\beta)+\frac{4\,\beta\,(2+\beta)\,M_{y,k}}{f_{h,1,k}\, d\, t_{h,1}^2}} - \beta\right] & (d) \\ \frac{f_{h,1,k}\, t_{h,2}\, d}{1+2\beta}\left[\sqrt{2\,\beta^2\,(1+\beta)+\frac{4\,\beta\,(1+2\beta)\,M_{y,k}}{f_{h,1,k}\, d\, t_{h,2}^2}} - \beta\right] & (e) \\ \sqrt{\frac{2\,\beta}{1+\beta}}\sqrt{2 M_{y,k}\, f_{h,1,k}\, d} & (f) \end{cases} \tag{C.1}$$

With:

$\beta = \frac{f_{h,2,k}}{f_{h,1,k}}$

Where:

$f_{h,1,k}$, $f_{h,2,k}$	The characteristic embedment strengths of members 1 and 2
$t_{h,1}$, $t_{h,2}$	The embedment depths of members 1 and 2
$M_{y,k}$	The characteristic yield moment of the fastener
d	The diameter of the fastener

The embedment strengths, used in Equations C.1(a) to C.1(f), are of one value. However, as the fasteners in the CLT panels pass through multiple layers with different fiber orientations and embedment strengths, multiple embedment strengths can act on one fastener. For equation C.1(f) for example, first a check has to be done to determine in which layer of the CLT a possible plastic hinge in the fasteners may occur. This will determine the effective embedment depth and embedment strength. Table C.3 shows the embedment lengths of parts of the fasteners in the different layers, and the angles between the fastener axis, grain, and force orientation.

Table C.3: Embedment depth of the fastener and the angles between the force, grain, and fasteners axis, in the GLT beam and the different layers of the CLT panel.

Layer	$t_{h,i}$**[mm]**	α **[°]**	β **[°]**	ϵ **[°]**
GLT beam (1)	125.65	0	45	90
CLT panel (1)	49.50	90	45	45
CLT panel (2)	28.28	0	45	90
CLT panel (3)	56.75	90	45	45

Where:

$t_{h,i}$	Embedment length through each layer
α	Angle between the direction of the acting force and the grain
β	Angle between the fastener axis and the surface of the wide face
ϵ	Angle between the direction of the grain

The embedment strength of a screw in the GLT beam, according to the new draft EC5:

$$f_{h,1,k} = \frac{0.019 \cdot \rho_k \cdot d^{-0.3}}{2.5 \cdot \cos^2(\epsilon) + \sin\epsilon} = \frac{0.019 \cdot 350 \cdot 7^{-0.3}}{2.5 \cdot \cos^2(90) + \sin(90)} = 15.13 N/mm^2 \tag{C.2}$$

The embedment strength of a screw in the middle layer of the CLT panel (layer 2):

$$f_{h,2,k} = \frac{0.019 \cdot \rho_k \cdot d^{-0.3}}{2.5 \cdot \cos^2(\epsilon) + \sin\epsilon} = \frac{0.019 \cdot 350 \cdot 7^{-0.3}}{2.5 \cdot \cos^2(45) + \sin(45)} = 8.65 N/mm^2 \tag{C.3}$$

The ratio between the embedment strengths of the beam and panel layer (2):

$$\beta = \frac{f_{h,2,k}}{f_{h,1,k}} = \frac{8.65}{15.13} = 0.57 \tag{C.4}$$

The characteristic yield moment of the screw, according to the new draft EC5:

$$M_{y,k} = 0.3 \cdot f_{u,k} \cdot d^{2.6} \tag{C.5}$$

With:

$d = 0.86 \cdot d$

$$M_{y,k} = 0.3 \cdot 1240 \cdot (0.86 \cdot 7)^{2.6} = 39582 Nmm$$

In the case that in both members the maximum embedment strength is reached and two plastic hinges form in the fastener (as displayed in Figure C.2, the following steps should be taken to derived for the effective embedment length b1:

$$\beta = \frac{f_{h,2,k}}{f_{h,1,k}} \rightarrow \beta \cdot b_2 = b_1$$

$$\Sigma M_A = 0$$

$$2\, M_{y,k} = -\frac{1}{2} \cdot f_{h,2,k} \cdot b_2^2 \cdot d + f_{h,1,k} \cdot d \cdot b_1 \cdot \left(b_2 + \frac{1}{2} \cdot b_1\right)$$

Substitute $f_{h,2,k} = \beta \cdot f_{h,1,k}$ and $b_2 = \frac{b1}{\beta}$:

$$2\, M_{y,k} = -\frac{1}{2} \cdot \beta \cdot f_{h,1,k} \cdot \left(\frac{b_1}{\beta}\right)^2 \cdot d + f_{h,1,k} \cdot d \cdot b_1 \cdot \left(\frac{b_1}{\beta} + \frac{1}{2} \cdot b_1\right)$$

Solving for b_1 gives:

$$b_1 = \sqrt{\frac{2 \cdot M_{y,k}}{f_{h,1,k} \cdot d}} \cdot \sqrt{\frac{2 \cdot \beta}{1 + \beta}} = \sqrt{\frac{2 \cdot 39582}{15.13 \cdot 7}} \cdot \sqrt{\frac{2 \cdot 0.57}{1 + 0.57}} = 23.3 mm \tag{C.6}$$

The effective embedment depth in the CLT panel (also the depth at which a plastic hinge will occur) is:

$$b_2 = \frac{b_1}{\beta} = \frac{23.3}{0.57} = 40.8 mm \tag{C.7}$$

The calculated effective embedment depth is smaller than the passing length of the fasteners through the middle layer. 40.8 mm < 49.5 mm. Therefore, the embedment strength $f_{h,2,k}$, as calculated before is the correct value for the embedment strength of the CLT in equation C.1(f) of the Johansen model. The same value will also be used for determining the shear resistances of failure modes (a) to (e). This will slightly underestimate the embedment strength of the entire CLT plate, but it is for now assumed that failure mode (f) will be governing anyways.

The maximum characteristic strength value of the dowel-effect for failure modes (a) to (e) are:

Table C.4: Characteristic strengths of different dowel effects, in the dowel type connection, according to the Johansen model.

Failure mode	Characteristic strength [kN]
(a)	$F_{D,k} = 13.41$
(b)	$F_{D,k} = 8.14$
(c)	$F_{D,k} = 15.02$
(d)	$F_{D,k} = 7.42$
(e)	$F_{D,k} = 3.26$
(f)	$F_{D,k} = 2.47$

The final characteristic strength for the dowel-effect is determined by the lowest characteristic strength from table C.4. As it turns out, the assumption of failure mode (f) being governing is correct.

Even whilst using a decreased embedment strength of the CLT panel. The characteristic dowel-effect strength of a single fastener in the connection $F_{D,k} = 2.47\,kN$.

Next to the dowel-effect strength, the rope effect plays an important part in the final shear strength of the connection. According to the Eurocode, the characteristic strength of the rope effect $F_{rp,k}$ for connections with screws is the same as the characteristic value of the dowel-effect strength.

$$F_{rp,k} = 2.47\,kN$$

This is lower than the characteristic withdrawal strength, see the calculation for the withdrawal strength below.

The total characteristic shear strength per fastener:

$$F_{V,i,k} = F_{D,k} + F_{rp,k} = 2.47 + 2.47 = 4.49\,kN$$

Total characteristic shear strength per meter:

$$F_{V,k} = F_{V,i,k} \cdot 2 \cdot n_{ef} = 4.94 \cdot 2 \cdot 6.7 = 65.85\,kN \cdot \left(\frac{1}{m}\right)$$

Design value of the shear strength per meter:

$$F_{V,d} = k_{mod} \cdot k_{shear} \cdot \frac{F_{V,k}}{\gamma_M} = 1.1 \cdot 1.2 \cdot \frac{65.85}{1.0} = 86.92\,kN \cdot \left(\frac{1}{m}\right)$$

Shear stiffness

The shear stiffness is determined by the lateral slip modulus $K_{SLS,v,mean}$ per plane per fastener, multiplied by the number of fasteners. According to the draft of the new Eurocode 5, the lateral slip modulus for screws is calculated as:

$$K_{SLS,v,mean} = 60 \cdot (0.7 \cdot d)^{1.7} \tag{C.8}$$

For shear plane on the beam side ($\alpha = 0°$), the stiffness modulus is:

$$K_{SLS,v,beam} = 60 \cdot (0.7 \cdot 7)^{1.7} = 894\,N/mm$$

The shear plane on the CLT panel side has a different grain orientation ($\alpha = 90°$). According to the draft of the new Eurocode 5, for connection members loaded perpendicular to the grain, the mean lateral slip modulus $K_{SLS,v,mean}$ should be reduced by 50%.

$$K_{SLS,v,panel} = 0.5 \cdot K_{SLS,v,beam} = 0.5 \cdot 894 = 447\,N/mm$$

The actual mean lateral slip modulus of the shear plane is determined by taking the mean of the two values.

$$K_{SLS,v,mean} = 671\,N/mm$$

As 6.7 fastener pairs work parallel to each other per running meter, the final stiffness modulus per meter can be multiplied by the number of fasteners:

$$K_{SLS,v} = K_{SLS,v,mean} \cdot 2 \cdot n_{ef} = 671 \cdot 2 \cdot 6.7 = 8942\,N/mm \cdot \left(\frac{1}{m}\right)$$

Normal tension strength

According to the draft version of the new Eurocode 5, the design tension resistance $F_{t,Rd}$ of connections with slanted fasteners is determined by the normal tension resistance per fastener, accounted for by the angle between the fastener and the force. A visual representation of how the force components act in the connection is given in figure C.3.

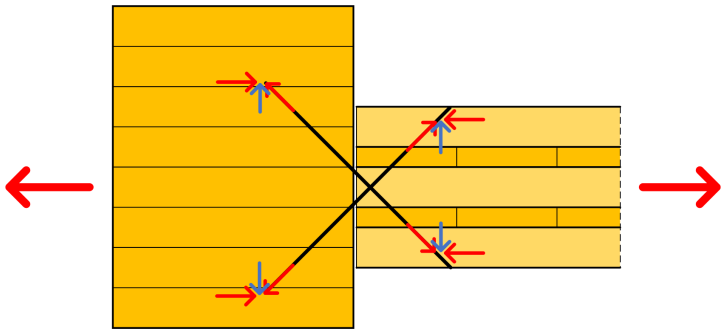

Figure C.3: Force components in the dowel type connection, exerted on by a normal tension force.

In order to determine the normal tension strength of the connections, first the characteristic withdrawal capacity of a single fastener has to be determined. According to EN 1995-1-1 8.7.2 the characteristic withdrawal strength at an angle α to the grain should be taken as:

$$f_{ax,\alpha,k} = \frac{3.6 \cdot 10^{-3} \cdot \rho_k^{1.5}}{\sin^2(\alpha) + \cos^2(\alpha)} \tag{C.9}$$

For α = 0°:

$$f_{ax,0,k} = \frac{3.6 \cdot 10^{-3} \cdot 350^{1.5}}{\sin^2(0) + \cos^2(0)} = 35.36\,N/mm^2$$

For α = 90°:

$$f_{ax,90,k} = \frac{3.6 \cdot 10^{-3} \cdot 350^{1.5}}{\sin^2(90) + \cos^2(90)} = 23.57\,N/mm^2$$

The characteristic withdrawal capacity for the screw in the beam and the CLT panel are:

$$F_{ax,k,beam} = (\pi \cdot d \cdot l_w)^{0.8} \cdot f_{ax,0,k} = (\pi \cdot 7 \cdot 125.65)^{0.8} \cdot 35.36 = 198.86\,kN$$

$$\begin{aligned} F_{ax,k,panel} &= (\pi \cdot d \cdot l_{w,\alpha=90})^{0.8} \cdot f_{ax,90,k} + (\pi \cdot d \cdot l_{w,\alpha=0})^{0.8} \cdot f_{ax,0,k} \\ &= (\pi \cdot 7 \cdot (49.50 + 56.57))^{0.8} \cdot 23.57 + (\pi \cdot 7 \cdot 23.23)^{0.8} \cdot 35.36 = 17.75\,kN \end{aligned}$$

The characteristic withdrawal capacity of a single fastener is determined by the minimum value of the two.

$$F_{ax,k} = min\left\{F_{ax,k,beam}; F_{ax,k,floor}\right\} = min\left\{18.86\,;\,17.75\right\} = 17.75\,kN$$

The design value of the withdrawal capacity of a single fastener is:

$$F_{ax,d} = k_{mod} \cdot \frac{F_{ax,k}}{\gamma_M} = 1.1 \cdot \frac{17.75}{1.0} = 19.53\,kN$$

The load carrying capacity in normal direction of per meter is determined as:

$$F_{n,d} = 2 \cdot F_{ax,d} \cdot \mathsf{cos}(45) \cdot n_{ef} = 2 \cdot 19.53 \cdot \mathsf{cos}(45) \cdot 6.7 = 184.06\,kN \cdot \left(\frac{1}{m}\right)$$

Normal tension stiffness

The formulation of the axial slip modulus $K_{SLS,ax}$ for a screw or bonded-in rod is not dependant on the angle between the fastener axis or force and the grain direction. The parameters which make up the axial slip modulus are the mean density of the wood, the fastener diameter, and the embedment length.

$$K_{SLS,ax,mean} = 160 \cdot \left(\frac{\rho_{mean}}{420}\right)^{0.85} \cdot d^{0.9} \cdot l_w^{0.6} \tag{C.10}$$

The effective embedment length of the fasteners in the beam is 115,65 mm. The axial slip modulus of the part of the screw in the beam is:

$$K_{SLS,ax,beam} = 160 \cdot \left(\frac{420}{420}\right)^{0.85} \cdot 7^{0.9} \cdot 115.65^{0.6} = 15944\,N/mm$$

The effective embedment length of the fasteners in the CLT panel is 124,35 mm. The axial slip modulus of the part of the screw in the CLT panel is:

$$K_{SLS,ax,panel} = 160 \cdot \left(\frac{420}{420}\right)^{0.85} \cdot 7^{0.9} \cdot 154.35^{0.6} = 16653\,N/mm$$

The axial slip modulus in the beam and the CLT panel act simultaneous and thus in series. The total axial slip modulus of one screw is therefore calculated as:

$$K_{SLS,ax,i} = \frac{K_{SLS,ax,beam} \cdot K_{SLS,ax,panel}}{K_{SLS,ax,beam} + K_{SLS,ax,panel}} = \frac{15944 \cdot 16653}{15944 + 16653} = 8145\,N/mm$$

The axial slip modulus acts in the direction of the fastener. However, as there are two fasteners at an angle of 45 degrees, the normal tension stiffness value of one fastener pair, in the direction of the load, is $2xK_{SLS,ax,i}$. All fasteners in a running meter act simultaneously in the normal direction. Their stiffnesses can therefore be multiplied by the effective number of fasteners per meter.

$$K_{SLS,n} = 2 \cdot K_{SLS,ax,i} \cdot n_{ef} = 2 \cdot 8145 \cdot 6.7 = 108605\,N/mm \cdot \left(\frac{1}{m}\right)$$

D

Literature review on the dynamic amplification factor in timber frames

The draft of the new Eurocode 5 prescribes that the performance of a structure under a sudden column removal should be verified either by a dynamic analysis, or a quasi-static analysis in which the dynamic effects are accounted for with appropriate DAFs. It goes on to say that for instantaneous loading scenarios, when no other accurate information is available, a DAF of 2.0 may be used. This value is based on the theoretical maximum dynamic amplification factor of 2.0 for elastic single-degree-of-freedom systems as described by JM Biggs in his book 'Introduction to structural dynamics' [64][65]. However, for purely elastic multiple-degrees-of-freedom systems the dynamic amplification factor may exceed 2.0. This effect is also seen in the results of Knuppe, where the ratio between the maximum static and dynamic push-down load, on a double intermediate façade column removal scenario, yields a value of 2.6 [1]. In Knuppe's analysis, the rotational response in the connections stays elastic, while the axial resistance in the forming catenary has a bi-linear elastoplastic response with little ductility. Knuppe's 2D models did not incorporate material dampening, neither did it take into account other load distribution paths in the out-of-plane direction. Furthermore, an instantaneous element removal speed was assumed, aiding to the higher dynamic amplification value.

Cheng et al. performed experimental drop-down tests on LVL post-and-beam mass timber frames, to study the dynamic behaviour after sudden column removal scenarios. They performed 25 tests with three different beam-column connections. It was concluded that the dynamic amplification factor is dependent on the type of connection and failure mode. When ductile failure occurred in the connections, a DAF of 1.5 was deemed reasonable. However, when brittle failure modes occurred, the DAF sometimes exceeded the theoretical value of 2.0 [66]. Also Cao et al. proposed a DAF of 2.0, based on a parameter study of 216 nonlinear dynamic analyses on a theoretical 2D timber framework. Their goal was to investigate the relation between the dynamic amplification factor, the damping ratio, and the connection stiffnesses. Results showed that models without material dampening could yield dynamic amplification factors larger than 2.0, but when 3% material dampening was added, all analyses results yielded DAFs lower than 2.0. Their 2D frame models contained connections with high stiffnesses, representing dowel type joints with linear elastic stiffness properties and brittle failure modes [61]. These results are in line with the results of Cheng et al. for brittle system failures in experimental results.

Palma et al. discuss the robustness design provisions in the new draft Eurocode, stating that the proposed dynamic amplification factor in the draft Eurocode 5 should be chosen dependent on the type of structure [67]. This is in line with the findings of Cheng et al. and Cao et al. which determined different DAFs for different structures.

The catenary in a modular timber building can be seen as a multiple-degree-of-freedom system. One degree of freedom is the rotation of the connections, while the second degree of freedom is the axial translation in the catenary components such as the floors and connections. When both the rotational and translational resistance in the connections behave elastic, dynamic amplification factors larger than

2.0 can occur. However, for the updated 2D frame model, as introduced in Chapter 6, and used for the connection optimisations in Chapter 7, the rotational stiffness in the newly assumed location of rotation is zero. Furthermore, the translational force-elongation response in the catenary, with the high-strength connection from optimisation method 1, does show a mainly elastic force-elongation response with only 1.99 mm of plastic elongation. Because the catenaries, in the 2D frame model with the high-strength connection only have translational elastic properties, they represent a single-degree-of-freedom system with a brittle failure mode. For quasi-static structural performance analyses, a DAF of 2.0 is appropriate.

Based on the findings of Cheng et al. [66], in order to analyse the structural performance of a timber modular building with the ductile connections, a DAF of 1.5 may be deemed more suitable for subsequent research. However, the test setup of Cheng et al. was relatively small compared to the timber modular building system, with a MEGANT type connector, which could only reach tensile loads of 10 kN [66]. In order to accurately determine an appropriate DAF for the timber system with the newly proposed fuse connection, a dynamic analysis of the connection should be performed.